

RELATIVE FISSION PRODUCT YIELD DETERMINATION  
IN THE USGS TRIGA MARK I REACTOR

by  
Michael A. Koehl

**© Copyright by Michael A. Koehl, 2016**

All Rights Reserved

A thesis submitted to the Faculty and the Board of Trustees of the Colorado School of Mines in partial fulfillment of the requirements for the degree of Doctor of Philosophy (Nuclear Engineering).

Golden, Colorado

Date: \_\_\_\_\_

Signed: \_\_\_\_\_

Michael A. Koehl

Signed: \_\_\_\_\_

Dr. Jenifer C. Braley

Thesis Advisor

Golden, Colorado

Date: \_\_\_\_\_

Signed: \_\_\_\_\_

Dr. Mark P. Jensen

Professor and Director

Nuclear Science and Engineering Program

## ABSTRACT

Fission product yield data sets are one of the most important and fundamental compilations of basic information in the nuclear industry. This data has a wide range of applications which include nuclear fuel burnup and nonproliferation safeguards. Relative fission yields constitute a major fraction of the reported yield data and reduce the number of required absolute measurements. Radiochemical separations of fission products reduce interferences, facilitate the measurement of low level radionuclides, and are instrumental in the analysis of low-yielding symmetrical fission products. It is especially useful in the measurement of the valley nuclides and those on the extreme wings of the mass yield curve, including lanthanides, where absolute yields have high errors.

This overall project was conducted in three stages: characterization of the neutron flux in irradiation positions within the U.S. Geological Survey TRIGA Mark I Reactor (GSTR), determining the mass attenuation coefficients of precipitates used in radiochemical separations, and measuring the relative fission products in the GSTR. Using the Westcott convention, the Westcott flux,  $\phi_w$ ; modified spectral index,  $r\sqrt{T_n/T_0}$ ; neutron temperature,  $T_n$ ; and gold-based cadmium ratios were determined for various sampling positions in the USGS TRIGA Mark I reactor. The differential neutron energy spectrum measurement was obtained using the computer iterative code SAND-II-SNL. The mass attenuation coefficients for molecular precipitates were determined through experiment and compared to results using the EGS5 Monte Carlo computer code. Difficulties associated with sufficient production of fission product isotopes in research reactors limits the ability to complete a direct, experimental assessment of mass attenuation coefficients for these isotopes. Experimental attenuation coefficients of radioisotopes produced through neutron activation agree well with the EGS5 calculated results. This suggests mass attenuation coefficients of molecular precipitates can be approximated using EGS5, especially in the instance of radioisotopes produced predominantly through uranium fission.

Relative fission product yields were determined for three sampling positions in the USGS TRIGA Mark I reactor through radiochemical analysis. The relative mass yield distribution for valley nuclides decreases with epithermal neutrons compared to thermal neutrons. Additionally, a proportionality constant which related the measured beta activity of a fission product to the number of fissions that occur in a sample of irradiated uranium was determined for the detector

used in this study and used to determine the thermal and epithermal flux. These values agree well with a previous study which used activation foils to determine the flux. The results of this project clearly demonstrate that R-values can be measured in the GSTR.

## TABLE OF CONTENTS

ABSTRACT .....	iii
LIST OF FIGURES .....	viii
LIST OF TABLES .....	x
ACKNOWLEDGMENTS .....	xi
DEDICATION .....	xii
CHAPTER 1 INTRODUCTION .....	1
1.1 Executive Summary: .....	1
1.2 Motivation .....	2
1.3 Thesis Organization.....	3
CHAPTER 2 BACKGROUND AND RATIONAL FOR STUDIES.....	4
2.1 K-value method fission basis and the R-value .....	4
2.2 Previous Efforts using R-values .....	7
2.3 Fission Product Yield Energy Dependence of Epithermal Neutrons .....	8
2.4 Water Boiler & Omega West Reactor Thermal Calibrations.....	12
2.4 References Cited.....	13
CHAPTER 3 MEASURED NEUTRON FLUX PARAMETERS IN THE USGS TRIGA MARK I REACTOR.....	16
3.1 Abstract .....	16
3.2 Introduction .....	16
3.3 Experimental .....	18
3.3.1 Foil Irradiations.....	18
3.3.2 Application of Westcott Convention .....	21
3.3.3 SAND-II-SNL Code Operations.....	23
3.4 Results .....	23
3.4.1 Westcott Convention.....	23
3.4.2 SAND-II-SNL Code .....	25
3.4.2 Comparison to Similar TRIGA Reactors.....	27
3.5 Discussion .....	29
3.5.1 Westcott Convention.....	29
3.5.2 SAND-II-SNL Code .....	29
3.5.3 Comparison to Similar TRIGA Reactors.....	30

3.6	Conclusion.....	31
3.7	Acknowledgements .....	31
3.8	References Cited.....	31
CHAPTER 4	EXPERIMENTAL AND MONTE CARLO INVESTIGATION OF MASS ATTENUATION COEFFICIENTS OF FISSION PRODUCT ISOTOPES IN MOLECULAR PRECIPITATES .....	33
4.1	Introduction .....	33
4.2	Experimental .....	35
	4.2.1 Gas Proportional Counting System.....	35
	4.2.2 Source Preparation .....	35
	4.2.3 Gas Proportional Counter Efficiency.....	37
	4.2.4 EGS5 Monte Carlo Simulation .....	37
	4.2.5 Empirical Mass Attenuation Formula.....	38
4.3	Results .....	39
	4.3.1 Detector Resolution .....	39
	4.3.2 Mass Attenuation Coefficients.....	39
4.4	Discussion .....	42
	4.4.1 Detector Resolution .....	42
	4.4.2 Mass Attenuation Coefficients.....	43
4.5	Conclusions .....	44
4.6	Acknowledgements .....	44
4.7	References Cited.....	44
CHAPTER 5	RELATIVE FISSION PRODUCT YIELDS IN THE USGS TRIGA MARK I REACTOR.....	46
5.1	Introduction .....	46
5.2	Experimental .....	49
	5.2.1 General Laboratory practices.....	49
	5.2.2 HPLC System.....	52
	5.2.3 Electroplating system.....	52
	5.2.4 Gas Proportional Counting System.....	53
	5.2.5 Preparation of uranium targets.....	53
5.3	Results .....	54
	5.3.1 Determination of the number of fissions .....	55

	5.3.2	Relative fission product yields.....	56
5.4		Discussion .....	57
5.5		Conclusions .....	58
5.6		Acknowledgements .....	60
5.7		References Cited.....	60
CHAPTER 6		GENERAL CONCLUSIONS.....	61
APPENDIX A		RADIOCHEMICAL PROCEDURES .....	65
A.1		General Instructions Applicable to All Procedures .....	65
A.2.		Preparation and Standardization of Carrier Solutions .....	65
	A.2.1.	Cadmium.....	65
	A.2.2.	Cesium .....	66
	A.2.3.	Silver .....	66
	A.2.4.	Zirconium.....	66
	A.2.5.	Molybdenum .....	67
	A.2.6.	Lanthanides .....	67
A.3.		Radiochemical Separations .....	67
	A.3.1	Cadmium.....	67
	A.3.2	Cesium .....	70
	A.3.3	Silver .....	71
	A.3.4	Zirconium-95 and Zirconium-97 .....	73
	A.3.5.	Molybdenum .....	76
	A.3.6.	Separation of the Lanthanides by HPLC.....	79
APPENDIX B		EGS5 SIMULATION.....	85

## LIST OF FIGURES

Figure 2.1.	Effect of shell corrections within a fissioning nucleus showing the tendency to form a $^{132}\text{Sn}$ core heavy fragment (left) and a lighter fragment. Nucleons in the neck are distributed between the two fragments.....	6
Figure 2.2.	Product yield curves for neutron fission of $^{235}\text{U}$ , $^{238}\text{U}$ and $^{239}\text{Pu}$ at thermal, fission and 14 MeV energies.....	6
Figure 2.3.	Epithermal $^{115}\text{Cd}$ R-values for $^{239}\text{Pu}$ relative to the thermal value. R-values use $^{99}\text{Mo}$ as the reference nuclide and thermal $^{235}\text{U}$ fission. The line at R=1 is the thermal measurement ratio.....	9
Figure 2.4.	Epithermal $^{115}\text{Cd}$ R-values (R-115) for $^{235}\text{U}$ relative to the thermal value. R-values use $^{99}\text{Mo}$ as the reference nuclide and thermal $^{235}\text{U}$ fission. The line at R=1 is the thermal measurement ratio. ....	10
Figure 2.5.	Absolute fission fragment yield differences with respect to thermal values (a). Fission fragment yield ratios with respect to thermal values. Note: the values in (b) are not R-values, but rather show a ratio of one pair of absolute yields. .	11
Figure 2.6.	SUPU Water Boiler flux and cadmium ratio distributions in the central position (i.e. “glory hole”) and tangent hole.....	12
Figure 3.1	Schematic of the U.S. Geological Survey TRIGA Mark I Reactor core showing location of central thimble, lazy susan, and dry tube irradiation positions .....	17
Figure 3.2	A plot of $s_0 G_{epi}/G_{thg}$ vs $R_s/\sigma_0 G_{thg}$ for Mn, Au, and Mo foils. The intercept is the Westcott flux, $\phi_w$ . The modified spectral index, $r\sqrt{T_n/T_0}$ is calculated by dividing the slope by the intercept .....	24
Figure 3.3	SAND-II-SNL differential neutron energy spectrum for various positions within the GSTR .....	26
Figure 4.1.	Experimental Setup and Monte Carlo Simulation: 1. P-10 gas, 2. Precipitate or electroplated metal, 3. Filter Paper or Stainless Steel planchette, 4. Double-sided Tape, 5. Aluminum, 6. DURAL window, 7. Air, 8. Mylar cover, 9. Aluminum plate.....	36
Figure 4.2.	Comparison of EGS5 calculated detector resolution vs measured detector resolution from the decay of $^{42}\text{K}$ . ....	40
Figure 4.3.	EGS5 calculated efficiencies of fission product nuclides over various areal thicknesses. ....	42
Figure 5.1.	(a) Calculated R-values from ENDF-B/VII cumulative fission yields for $^{235}\text{U}$ and (b) the asymmetric mass distribution yields from fission of $^{235}\text{U}$ by thermal neutrons.....	48

Figure 5.2. Comparison of (a) the differential neutron energy spectrum for sampling positions within the GSTR [19], (b) the  $^{235}\text{U}$  fission cross section from ENDF-B/VII Reich Moore resonance parameters calculated using NJOY 2012, and (c)  $R_{115}$ -values from incident neutrons of 0.002 to 35 eV[25,27]. The thermal  $R_{115}$ -value is designated by a horizontal dashed line and the cadmium cut-off energy of 0.55 eV is designated by a horizontal line..... 59

## LIST OF TABLES

Table 2.1.	Ratios of activity of various fission products to that of <sup>99</sup> Mo for thermal neutrons and epithermal neutrons (resonance fission).....	9
Table 3.1	Characteristics of the Mn, Au, Mo, and Lu activation foils/wire, and their nuclear data .....	20
Table 3.2	Calculated neutron flux distribution parameters within the GSTR .....	24
Table 3.3	Measured vs calculated cadmium ratio for gold in various sampling positions within the GSTR .....	25
Table 3.4	Measured saturated activities for foils in various sampling positions in the GSTR used in the SAND-II-SNL spectrum unfolding code .....	26
Table 3.5	Saturated thermal activities in various sampling positions within the GSTR calculated with the SAND-II-SNL spectrum unfolding code.....	27
Table 3.6	Comparison of published neutron flux values at facilities with similar cores to the GSTR .....	28
Table 3.7	Calculated approximate Westcott flux, spectral index, and cadmium ratio (Au) for TRIGA reactors with cores similar to the GSTR. Calculations based on reported thermal and epithermal flux.....	29
Table 4.1.	Average measured density of precipitates used in this study. ....	37
Table 4.2.	Experimental, calculated, and theoretical values of mass attenuation coefficients. ....	41
Table 5.1.	Carrier Standardization. ....	50
Table 5.2.	Characteristics of the U <sub>3</sub> O <sub>8</sub> irradiation targets and nuclear data.....	54
Table 5.3.	Calculated neutron flux based on K-factor method. ....	55
Table 5.4.	Relative fission product yields.....	57

## ACKNOWLEDGMENTS

I would like to thank my advisor, Dr. Jenifer C. Braley, whose knowledge and support made this work possible. I thank her for her support, guidance and for giving me the opportunity to do this research. I would also like to thank the support from the USGS TRIGA reactor staff without whose sage wisdom this project would not have gone as smoothly: Tim Debey, Alex Buehrle, Brycen Roy, and Christopher Farwell. The knowledge received from the Los Alamos Nuclear and Radiochemistry Group was critical to the success of this project. I would like to thank the following for taking the time out of their busy day to explain the nuances of their work: Scott Bowen, Susan Pacheco, Rowena Gibson, Ann Shocke. As with any project that uses electronic equipment, there inevitably seems to be one person that can fix it all. For this project it was Ed Dempsy.

I would like to thank my thesis committee for their support and advisement: Dr. Uwe Greife, Dr. Mark P. Jensen, Dr. Mark R. Deinert, and Dr. Robert S. Rundberg. I would also like to extend my thanks to the United States Army Advanced Civil Schooling program who provided tuition for this program. Finally, this project would never have succeeded without the support of my colleagues in the Braley research group.

## DEDICATION

I would like to dedicate this work to my wife, Kathleen, and my four children, Desiree, Grayson, Drake, and Griffin who have lovingly supported me throughout this research.

## CHAPTER 1

### GENERAL INTRODUCTION

This project studied relative fission product yields for  $^{235}\text{U}$  for sampling positions within the US Geological Survey TRIGA Reactor (GSTR) at the Denver Federal Center in Lakewood, CO using radiochemical methods to separate individual fission products and evaluate their beta activity using a gas proportional counter. This work is separated into three sections: characterizing sampling positions within the GSTR, determining mass attenuation coefficients of molecular precipitates, and finally determining the relative fission product yield within those sampling positions.

#### **1.1 Executive Summary**

The use of beta spectrometry instead of gamma spectrometry removes uncertainties of branching values associated with gamma decay modes. Initial studies focused on characterizing the sampling positions within the GSTR and compared the results to historical data from the Los Alamos SUPO Homogeneous Water Boiler reactor. The results of the characterization of the reactor indicated that the cadmium ratios available within sampling positions of the reactor were comparable to those of the now deactivated SUPO reactor. The mathematical construction of a ratios of fission product yields removes the difficulty of making absolute measurements but corrections need to be applied for the chemical yield of samples. The largest correction is from the self-attenuation of the precipitates. In general, due to the nature of beta decay, experimentally determined mass attenuation coefficients are required to make these corrections. Difficulties associated with sufficient production of fission product isotopes in research reactors limits the ability to complete a direct, experimental assessment of mass attenuation coefficients for these isotopes. Therefore a multi-purpose Monte Carlo code, EGS5 was used to simulate the gas proportional counter and then compared to experimentally determined mass attenuation coefficients of isotopes that were readily produced in a thermal reactor. When compared to experimental values, the simulated results were found to have good agreement.

Finally samples of enriched uranium were irradiated in the GSTR and the relative yields were calculated from the activity of radiochemically separated fission products measured with a gas proportional counter. Additionally, a detector specific proportionality constant was determined

from a sample supplied by Los Alamos National Laboratory which relates the activity of  $^{99}\text{Mo}$  samples to the total number of fissions in a sample. This factor was used to determine the thermal and epithermal flux in three irradiation positions within the GSTR. Results show good agreement with the previous characterization of those sampling positions.

## 1.2 Motivation

Fission product yield data sets are one of the most important and fundamental compilations of basic information in the nuclear industry. Fission yield data are important in the measurement of nuclear fuel burnup, nonproliferation safeguards, reactor design and operation, nuclear physics calculations, decay heat studies, shielding calculations, fuel handling and reprocessing, neutron dosimetry and flux measurements, and environmental studies – all of these factors feed into stockpile stewardship. Current data sets present a wide range of uncertainty and demands for improved accuracy of fission product data are prevalent throughout the industry.

Relative fission yields, which constitute a major fraction of the reported yield data, are yields which have been measured relative to some other nuclide or normalized to some value. The basic premise in relative measurements is to reduce the number of absolute measurements, normally to one or possibly a few. Once the absolute yield of one fission product is accurately known, relative measurements can be used as monitors of the total number of fissions. Additionally, other absolute yields can be calculated relative to the singular fission product yield. R-values are relative fission product yields based on thermal neutron measurements ( $r^*$ -values) relative to a standard isotope. R-values are sensitive to the neutron environment of the fissile fuel.

While a few viable non-destructive techniques exist, the majority of relative yield data is collected through radiochemical techniques. It is especially useful in the measurement of the valley nuclides and those on the extreme wings of the mass yield curve, including lanthanides, where absolute yields have high errors. Radiochemical separations reduce interferences, facilitate the measurement of low level radionuclides and are instrumental in the analysis of low-yielding symmetrical fission products. This makes the use of such separations an important skill set to maintain, despite the increase in non-destructive techniques.

The following objectives have been developed for this project:

- Characterize sampling positions within the USGS TRIGA Mark I reactor by determining the neutron flux, cadmium ratios, and neutron temperature
- Improve and modify experimental techniques to accurately measure the relative fission product yield thermal calibration of a TRIGA reactor ( $r^*$ -value)
- Study the various energy dependence of fission yield ratios based on the extended R-value database using models from the literature or developed during this work

### **1.3 Thesis Organization**

To put this proposed effort in context, Chapter 2 will describe the mathematical framework used in this project to determine ratios of relative fission product yields. Additionally, the current understanding the incident neutron energy dependence and its relationship to these measurements will be discussed. Chapter 3 contains the characterization of the USGS TRIGA research reactor. Data from the activation of thin foils is presented and compared to historic measurements in order to demonstrate the feasibility of the thermal calibration fission yield ratios. Chapter 4 presents an Electron Gamma Shower Monte Carlo code, EGS5 simulation of the gas proportional counter used in this project. Mass attenuation coefficients for various precipitates are calculated using this code and compared to experimental values and empirical formulas. Chapter 5 contains the determination of relative fission yields from the fission of  $^{235}\text{U}$  in sampling positions within the GSTR. Chemical separations procedures used in this project are presented in Appendix A. Finally, the EGS5 code used in the calculation of the mass attenuation coefficients is presented in Appendix B.

## CHAPTER 2

### BACKGROUND AND RATIONAL FOR STUDIES

As discussed in the introduction, one of the most important parameters required for studies of nuclear fuel and viability of the nuclear stockpile is burnup. Various methods have been developed to measure burnup by destructive and non-destructive means. The destructive method, which is based on the determination of specific nuclides by radiochemical analysis after appropriate chemical separation, is widely used as a reference method to measure burnup of spent fuel [1-3] and can be used to directly determine the number of fissions that occurred within the fuel.

#### 2.1 K-value method fission basis and the R-value

To experimentally determine the number of fissions occurring in a fissionable material after irradiation, there are two equally valid fission basis [4]. The first is based on a direct measured ratio of the standard fission isotope to the independently measured number of fissions in a fission chamber. The second is based on gamma spectroscopy and evaluated nuclear data. Both require measuring the activity of a given fission product, however the second relies on absolute nuclear data while the first method, the K-factor method, relies on values which ratio out systemic errors.

The activity of a fission product ( $j$ ) of a fissioning isotope ( $f$ ) in a given neutron environment ( $e$ ) is given by:

$$A_j^{f,e} = \varepsilon_j \lambda_j Y_j^{f,e} F \quad (2.1)$$

where:  $\varepsilon$  is the detector efficiency,  $\lambda$  is the decay constant,  $Y$  is the independent fission yield, and  $F$  is the number of fissions. Defining the quantity  $K$  as the inverse of the product of the efficiency the decay constant and the yield gives the following, after rearranging:

$$K_j^{f,e} = \frac{F}{A_j^{f,e}} \quad (2.2)$$

This K-factor is a detector dependent value, hence it cannot be shared among laboratories. It is based on maintaining a highly calibrated and consistent set of procedures to determine the fission product nuclide activity [5]. A suite of K-values for various fissioning isotopes and fission products is of limited value, but the introduction of a mathematical framework based on ratios (Q-value and R-value) enables data that is detector independent and usable by other laboratories.

These ratios provide the ability to assess relative fission product content. This framework requires a reference isotope ( $^{99}\text{Mo}$  or  $^{147}\text{Nd}$ ), fission material ( $^{235}\text{U}$ ), and neutron environment (thermal neutrons) [5].

The Q-value is defined as a ratio of K-values in different fuel and energy conditions to the K-value of the reference fission material and neutron environment, thermal fission of  $^{235}\text{U}$ , denoted by (\*):

$$Q_j^{f,e} = \frac{K_j^*}{K_j^{f,e}} = \frac{Y_j^{f,e}}{Y_j^*} \quad (2.3)$$

An R-value is defined as a double ratio of fission product count rates:

$$R_j^{f,e} = \frac{A_j^{f,e} / A_{99}^{f,e}}{A_j^* / A_{99}^*} = \frac{r_j^{f,e}}{r_j^*} \quad (2.4)$$

where the numerator ( $r_j^{f,e}$ ) is the activity ratio of a given fission product to the standard isotope ( $^{99}\text{Mo}$ ) in a given fissioning isotope and neutron energy and the denominator is the ratio of the same two fission products in the thermal fission of  $^{235}\text{U}$  ( $r_j^*$ ). Using the two-mode of fission hypothesis, Q-values for a given fissioning isotope in a wide energy range, up to 14.3 MeV [6], is a linear function of any R-value in the same neutron environment (e.g. for  $^{235}\text{U}$ ,  $1/Q_{99}^{U235,e} = 1.87 \times 10^{-3} R_{111}^{U235,e} + 9.98 \times 10^{-3}$ ) [5].

These ratios and relations are useful in scaling and reducing the number of directly measured K-values to a singular thermal value [7].

$$K_j^{f,e} = \frac{K_{99}^{f,e}}{r_j^* R_j^{f,e}} = \frac{K_{99}^*}{r_j^* Q_j^{f,e}} \quad \text{and} \quad Q_j^{f,e} = R_j^{f,e} \frac{K_{99}^*}{K_{99}^{f,e}} = R_j^{f,e} Q_{99}^{f,e} \quad (2.5a, 2.5b)$$

This framework then relies on one detector dependent direct thermal K-value measurement and a self-consistent data set that includes thermal  $r^*$ -value calibrations; a suite of R-values that are detector independent; and a handful of fuel dependent Q-values, which can be determined from R-values;. The only measurement that requires direct fission counting is the thermal K-value. Radiochemically determined thermal  $r^*$ -value calibrations and accurate R-value measurements are the cornerstone of this project.

In addition to being a scalar in the K-value method, R-values are a sensitive determination of the neutron energy. The fission reaction involves the break-up of an unstable, heavy nucleus into two, or rarely, three fission fragments (FP) as shown in Equation 2.6 with  $^{235}\text{U}$  fuel.

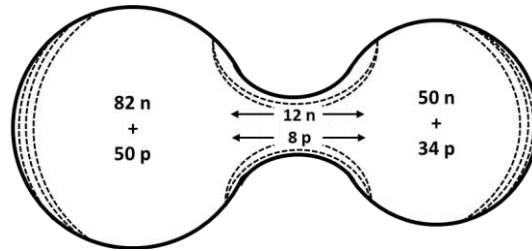
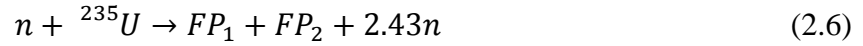


Figure 2.2. Effect of shell corrections within a fissioning nucleus showing the tendency to form a  $^{132}\text{Sn}$  core heavy fragment (left) and a lighter fragment. Nucleons in the neck are distributed between the two fragments.

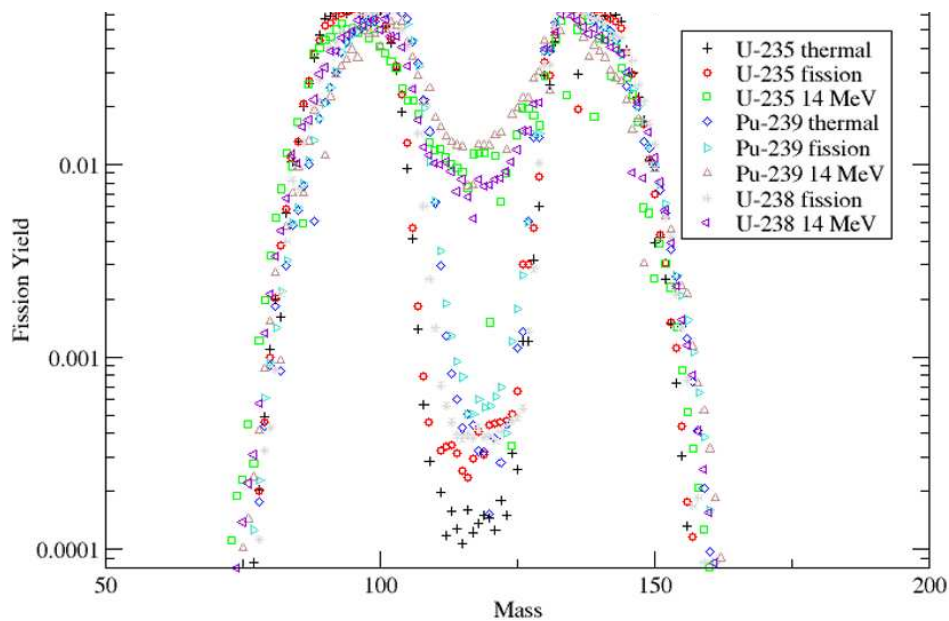


Figure 2.1. Product yield curves for neutron fission of  $^{235}\text{U}$ ,  $^{238}\text{U}$  and  $^{239}\text{Pu}$  at thermal, fission and 14 MeV energies.

According to the liquid drop model with shell corrections, a random sharing of the excitation energy is considered to occur among all of the nucleons until that energy is distributed in such a way as to partially overcome the nuclear binding force of one part from the other part. This causes

a distortion from an original spherical shape that increases the separation of the nucleons along the long axis of the distorted nucleus. The shell corrections include energy fluctuations from the average due to the inhomogeneous distribution of energy and explain asymmetric fission [8, 9], or the tendency in fission of uranium and heavier actinides to form a  $^{132}\text{Sn}$  heavy fragment and a lighter fragment. The heavy fission fragment  $^{132}\text{Sn}$  core forms due to the double-magic nucleus with completely occupied neutron ( $N=82$ ) and proton ( $Z=50$ ) shells (Figure 2.1). The “neck” between the two fragments contains, on average 12 neutron and 8 protons [10, 11]. Eventually the two parts separate due to the columbic repulsion between protons and the nucleons in the neck are distributed among the two fragments.

Figure 2.2 shows the familiar asymmetric double peaked mass distribution [12] which is a result of this phenomenon. As the mass of the fissioning isotope increases, the average mid-point of the light peak shifts towards heavier fragments. As the energy of the incident neutron increases, symmetric fission increases, and the probability of “valley” yield increases and probability of yield in the “wings” increases. Current theoretical reactor codes based on the liquid drop model, which describes the potential energy surface of fission and the systematics of energy dependence of yields, provide accurate and reliable nuclear reactor codes that are in reasonable agreement with reality. Nevertheless, more accurate nuclear data would improve the predictions of fuel composition models and hence overall stockpile stewardship [13]. In addition, variations in relative amounts of symmetric and asymmetric fission are sensitively observed by radiochemical determination of changes in peak-to-valley fission-product mass-yield ratios inherent in R-value measurements. More experimental data are required for improvement of these models.

## 2.2 Previous Efforts using R-values

In 1975, F.P. Ford and Norris, in a seminal report entitled, “A compilation of yields from neutron-induced fission of  $^{232}\text{Th}$ ,  $^{235}\text{U}$ ,  $^{236}\text{U}$ ,  $^{237}\text{Np}$ ,  $^{238}\text{U}$ , and  $^{239}\text{Pu}$ ” described a basis for fission product measurements (K-factor method) [5]. This work was an extrapolation of measurements of many scientists within the Los Alamos Radiochemistry Group extending over multiple decades. The cornerstone of this basis is relative fission product yields (R-values). The mathematical framework and experimental methods are described in this paper as well as a description on error analysis. While this was a thorough effort, the wide variety of measurements collected from internal documents resulted in a percent standard deviation of R-value uncertainty ranging from

approximately 1% to nearly 7% with 3% assigned to values that were not able to be calculated. Most errors were approximately 2.5% standard deviation. This work was published as a Los Alamos Scientific Laboratory internal report and, while unclassified, was initially not widely circulated.

H.D. Selby, et al, published a meta-data analysis in 2010 in a widely-available publication that further described the K-factor method, thermal calibration measurements ( $r^*$ -values), and the resolution of a previously unknown energy dependence of fission yields for reference nuclides in R-value measurements [7]. The data were again collected from experiments completed several decades previously and relied heavily on the Ford and Norris report. This meta-analysis provided valuable insight for evaluating the sparse data sets involved in this assessment. Errors in measurement in this paper are an improvement of the 1975 report, however they remain as high as 2%-3% with  $^{95}\text{Zr}$  as high as 6.9%.

Improvements remain to be made in reporting full uncertainty calculations, particularly in the propagation of uncertainties in the derived fission product yield results, with attention to major correlations and separate reporting of statistical and systematic uncertainty components, as well as the combined uncertainties.

### **2.3 Fission Product Yield Energy Dependence of Epithermal Neutrons**

Due to the complexity of the fission process, the precise dependence of fission yields on energy is still an open question and further experimental studies and theory are needed. In general, as stated in the previous section, the valley and wing fission product yield increase with increasing neutron energy. There are, however, some anomalies which have been pointed out by a number of experiments. These anomalies show a trend in the variation of mass asymmetry for resonances of epithermal neutron energies that is exactly opposite to the trend shown in Figure 2.1.

A compilation of the experimentally determined energy dependence is given by R.W Mills [14] and in IAEA-TECDOC-1168 [15]. The Los Alamos Radiochemistry Group measured R-values for values of  $^{235}\text{U}$  in thermal and epithermal neutron fission relative to  $^{99}\text{Mo}$  for  $^{97}\text{Zr}$ ,  $^{109}\text{Pd}$ ,  $^{111}\text{Ag}$ ,  $^{112}\text{Pd}$ ,  $^{115}\text{Cd}$ , and  $^{136}\text{Cs}$  in the Los Alamos Water Boiler reactor shown in Table 2.1. The thermal measurements (right column, Table 2.1) are taken from the Omega West reactor. The data show that R-values are less than one for all fission product nuclides in the valley region which

means the valley, in the mass yield curve, for epithermal neutrons is lower than that of thermal neutrons. This apparently contradicts the trend of the yield of valley mass chains to increase with increasing neutron energies.

Table 2.1. Ratios of activity of various fission products to that of  $^{99}\text{Mo}$  for thermal neutrons and epithermal neutrons (resonance fission) [16].

Thermal fission			Resonance fission			Resonance fission		
Cd ratio=1000			(Cd-wrapped) Cd ratio=8			(Cd-wrapped) Cd ratio=30		
Activity/ $(^{98}\text{Mo activity})$			Activity/ $(^{98}\text{Mo activity})$			Activity/ $(^{98}\text{Mo activity})$		
Fission Product	Average	Std. Dev.	Average	Std. Dev.	R	Average	Std. Dev.	R
$^{97}\text{Zr}$	2.88	2.3%	2.88	3.5%	1.00	2.82	2.7%	0.98
$^{109}\text{Pd}$	5.99E-03	1.3%	5.89E-03	1.8%	0.98	5.97E-03	1.8%	1.00
$^{111}\text{Ag}$	9.80E-04	1.8%	8.70E-04	0.9%	0.89	9.00E-04	2.4%	0.92
$^{112}\text{Pd}$	1.07E-03	0.6%	9.08E-04	0.6%	0.85	9.20E-04	0.9%	0.86
$^{115}\text{Cd}$	3.73E-03	0.7%	3.14E-03	2.8%	0.84	3.10E-03	1.8%	0.83
$^{136}\text{Cs}$	1.72E-04	0.8%	1.69E-04	0.7%	0.98	1.65E-04	1.1%	0.96

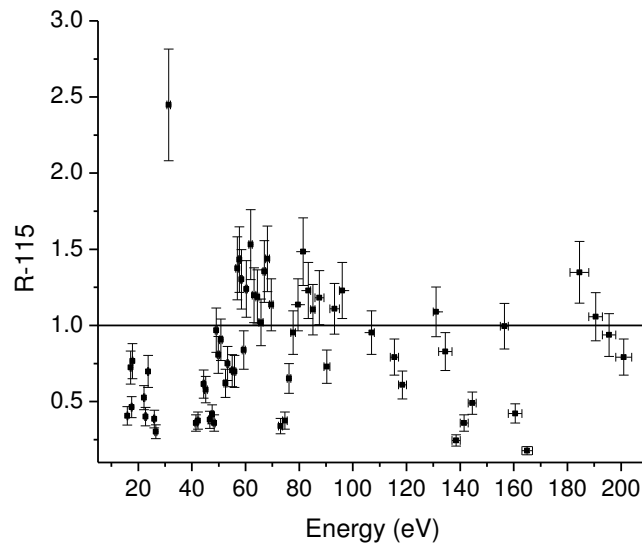


Figure 2.3. Epithermal  $^{115}\text{Cd}$  R-values for  $^{239}\text{Pu}$  relative to the thermal value. R-values use  $^{99}\text{Mo}$  as the reference nuclide and thermal  $^{235}\text{U}$  fission. The line at  $R=1$  is the thermal measurement ratio.

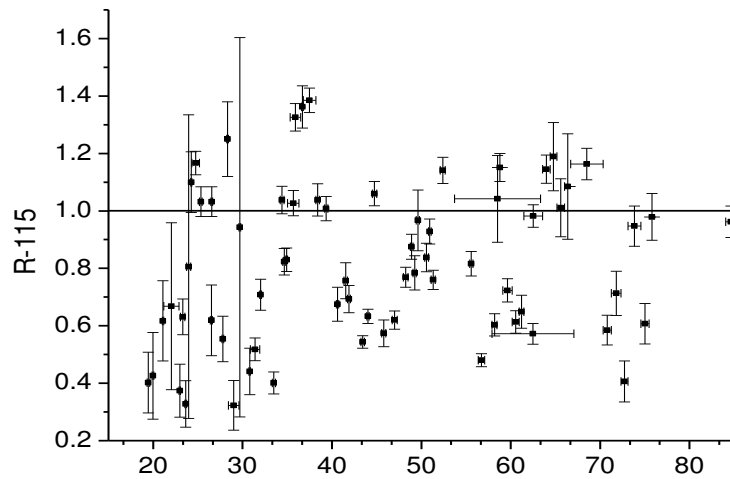


Figure 2.4. Epithermal  $^{115}\text{Cd}$  R-values (R-115) for  $^{235}\text{U}$  relative to the thermal value. R-values use  $^{99}\text{Mo}$  as the reference nuclide and thermal  $^{235}\text{U}$  fission. The line at  $R=1$  is the thermal measurement

Using a neutron source from a nuclear explosion and the time of flight to determine the neutron spectra on a spinning wheel of fissile material, G.A. Cowan et al. measured R-values of epithermal neutron fission relative to  $^{99}\text{Mo}$  for  $^{235}\text{U}$ , ( $E_n = 19.3\text{--}86.3$  eV) [17-19] and for  $^{239}\text{Pu}$  ( $E_n = 15.8\text{--}204$  eV) [20]. Figures 2.3 and 2.4 show some of those results. Their papers document variations in the yields of symmetric or near-symmetric fission products at resonances in  $^{235}\text{U}$  and  $^{239}\text{Pu}$  neutron induced fission. It can be seen that the variation of fission yields at different energy points relative to the thermal yield is significant (assuming that the yield of  $^{99}\text{Mo}$ , a fission product in the light mass peak, is constant), exhibiting a resonance like structure around the thermal yield value. F.J. Hamsch et al. measured the fission fragment yield versus mass and total kinetic energy versus incident neutron energy in the energy range 0.006–130 eV at the Geel Electron Linear Accelerator (GELINA) using a Frisch-gridded ionization chamber [21]. The results are shown in Figures 2.5a and 2.5b. It can be seen from Figure 2.5a that the mass distributions for neutron energies between the resonances are almost the same as for thermal neutrons. The asymmetric peaks of mass distributions change their shape with the resonances or resonance groups. The yield differences,  $\text{YIELD}(E_n) - \text{YIELD}(\text{Thermal})$ , are first negative and then positive for the light mass peak, and opposite, namely first positive and then negative, for the heavy mass peak. Figure 2.5b demonstrates the drops in symmetric fission yields for all resonances. It should be noted that

Figure 2.5b does not show R-values, but rather a ratio of absolute fission yields, one for epithermal energies and the other for thermal energies.

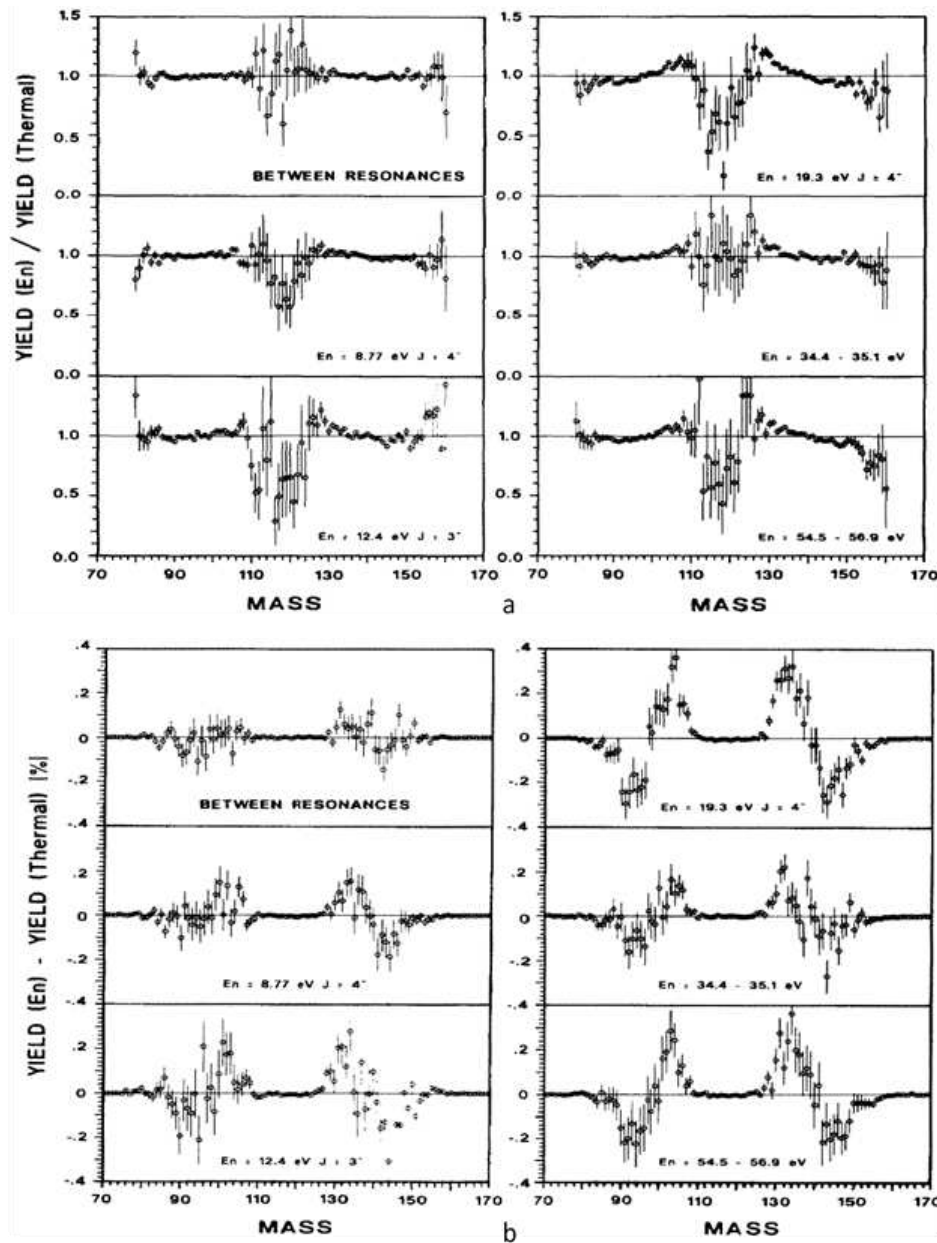


Figure 2.5. Absolute fission fragment yield differences with respect to thermal values (a). Fission fragment yield ratios with respect to thermal values. Note: the values in (b) are not R-values, but rather show a ratio of one pair of absolute yields.

Thus sufficient experimental data exists on fission yield ratios of epithermal neutron energies to form some tentative conclusions. All of them show a similar behavior, namely that the

fluctuation of the ratios or R-values show a resonance like structure, especially for fission products in the valley (symmetric fission), where the ratios or R-values are generally smaller than one. However there is little correlation between the spin values of the fission cross section resonances and the resonance like behavior in the ratio of symmetric to asymmetric fission. Possible explanations include the mass symmetry may indicate a possible correlation with the excess energy at the fission barrier [22], the possibility of multiple chance fission for each spin (i.e second chance fission [15]) or that each fission channel has a characteristic yield distribution [23].

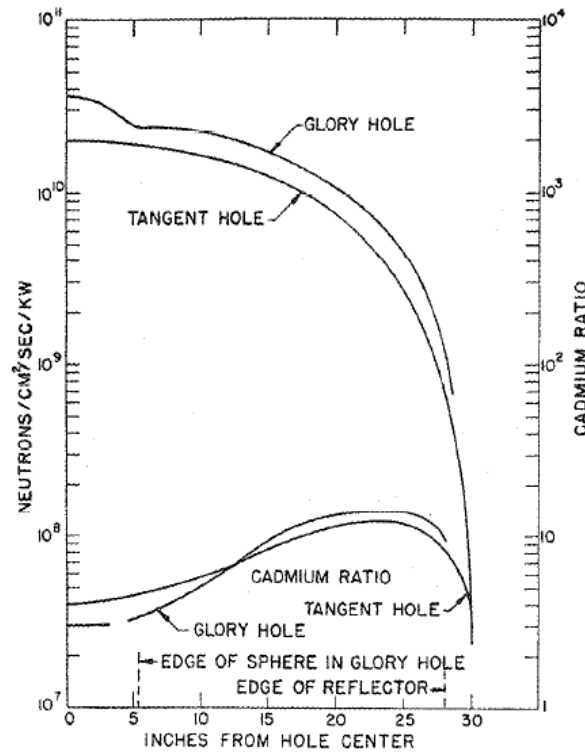


Figure 2.6. SUPU Water Boiler flux and cadmium ratio distributions in the central position (i.e. “glory hole”) and tangent hole.

## 2.4 Water Boiler & Omega West Reactor Thermal Calibrations

Historically, thermal calibration measurements ( $r^*$ -values) were made routinely in two thermal reactors at Los Alamos. The SUPU Water Boiler reactor was the first reactor used for these measurements [24]. The Water Boiler reactor was a homogeneous enriched  $^{235}\text{U}$  liquid-fuel reactor. The 35 kW SUPU Water Boiler was the third Water Boiler reactor incarnation at Los Alamos and operated almost daily from 1951 until its deactivation in 1974. Thermal fission calibrations and thermal  $K_{99}^*$  measurements were made with the use of the thermal columns (i.e.

“glory hole”) in the reactor. As shown in Figure 2.7, the peak neutron flux was  $3.7 \times 10^{10}$  n/cm<sup>2</sup>-s with a cadmium ratio for Au of approximately 2 at the peak and a maximum cadmium ratio of 10 [25]. As will be shown in Chapter 3, these cadmium ratios are available and accessible within sampling positions of the USGS TRIGA reactor.

The Omega West Reactor (OWR) was an 8 MW thermal, light-water moderated, and cooled, heterogeneous, tank-type research reactor operated by the Isotope and Nuclear Chemistry Division of the Los Alamos National Laboratory. The reactor first went critical in 1956 and was decommissioned in 1993. The flux in the thermal column was  $6 \times 10^{11}$  n/cm<sup>2</sup>-s with a cadmium ratio for indium of 2000 [26]. For gold, this ratio is calculated at of 670. Thermal calibration measurements were later taken from this reactor, but were in good agreement with the SUPO Water Boiler reactor [7].

Measurement uncertainties are estimated as the combined standard uncertainty following propagation of error rules. The uncertainties of the individual components, or standard uncertainties, are provided as one standard deviation ( $1\sigma$ ) to simplify incorporating these values in the uncertainty model. The standard uncertainties are estimated by statistical evaluation of standard uncertainty expressed as one sigma values. Statistical estimates are based on the mean and variance of repeated independent measurements, and least square fit to measurement data. Uncertainty for measurement efficiencies were constructed for representative sources covering the range of areal thicknesses.

## 2.5 References Cited

1. Ilas G, Gauld IC (2011). Oak Ridge National Laboratory (ORNL) ; Sponsoring Organization: ORNL work for others
2. Sanders CE (2003) Isotopic analysis of high-burnup PWR spent fuel samples from the Takahama-3 reactor. Washington, DC : Division of Systems Analysis and Regulatory Effectiveness, Office of Nuclear Regulatory Research, U.S. Nuclear Regulatory Commission, Washington, DC
3. Smith HJ, Gauld IC, Mertzyurek U (2013). Oak Ridge National Laboratory (ORNL) ; Sponsoring Organization: ORNL work for others
4. Keksis AL, Chadwick MB, Selby HD, Mac Innes MR, Barr DW, Meade RA, Burns CJ, Wallstrom TC (2011). American Society for Testing and Materials - ASTM International, 100 Barr Harbor Drive, PO Box C700, West Conshohocken, PA, 19428-2959 (United

- States); European Working Group on Reactor Dosimetry - EWGRD, SCK.CEN, Mol (Belgium)
5. Ford GP, Norris AE (1975). Los Alamos Scientific Lab., N.Mex. (USA) ; LA-6129
  6. Ford GP (1960) *Physical Review*, 118, DOI 10.1103/PhysRev.118.1261
  7. Selby HD, Mac Innes MR, Barr DW, Keksis AL, Meade RA, Burns CJ, Chadwick MB, Wallstrom TC (2010) *Nuclear Data Sheets* 111:2891-2922 DOI 10.1016/j.nds.2010.11.002
  8. Möller P, Madland DG, Sierk AJ, Iwamoto A (2001) *Nature* 409:785
  9. Bjornholm S, Lynn JE (1980) *Rev. Mod. Phys.* 52
  10. Arnikaar HJ (1982) *Essentials of nuclear chemistry*. New York: Wiley
  11. Gol, danskii VI (1971) *Fiz. Szemle* 21: No. 11
  12. Wahl AC (2002). Los Alamos National Lab., NM (US) ; Sponsoring Organization: US Department of Energy (US)
  13. Solders A, Gorelov D, Jokinen A, Kolhinen VS, Lantz M, Mattera A, Penttilä H, Pomp S, Rakopoulos V, Rinta-Antila S (2014), pp. 338-341
  14. Mills RW (1995). University of Birmingham
  15. IAEA-TECDOC-1168 (2000). IAEA
  16. Browne CI (1957) *Physical Review* 107:1
  17. Cowan GA, Turkevich A, Browne CI (1961) *Physical Review*, 122, DOI 10.1103/PhysRev.122.1286
  18. Cowan GA, Bayhurst BP, Prestwood RJ (1963) *Physical Review S*, 130 DOI 10.1103/PhysRev.130.2380
  19. Cowan GA, Bayhurst BP, Prestwood RJ, Gilmore JS, Knobeloch GW (1970) *Phys. Rev.*
  20. Cowan GA, Bayhurst BP, Prestwood RJ, Gilmore JS, Knobeloch GW (1966) *Physical Review*, 144 DOI 10.1103/PhysRev.144.979
  21. Hambsch FJ, Knitter HH, Budtzjorgensen C, Theobald JP (1989) *Nuclear Physics A* 491:56-90
  22. Vandenbosch R (1973) *Nuclear fission*. New York: Academic Press
  23. Faler KT, Tromp RL (1962). Phillips Petroleum Co. Atomic Energy Div., Idaho Falls, Idaho
  24. Ford GP, Gilmore JS, Ames DP, Balagna JP, Barnes JW, Comstock AA, Cowan GA, Elkin PB, Hoffman DC, Knobeloch GW, Lang EJ, Melnick MA, Minkinen CO, Pollock BD, Sattizshn JE, Stanley CW, Warren B (1956). Los Alamos Scientific Lab., N. Mex. ; LA-1997
  25. International Conference on the Peaceful Uses of Atomic E (1955) *Proceedings*. New York : United Nations, New York

26. United States. Dept. of Energy. Assistant Secretary for Environment SaH (1989) Technical safety appraisal of the Omega West Reactor, Los Alamos National Laboratory. Washington, D.C. : U.S. Dept. of Energy, Environment, Safety, and Health ; Springfield, Va. : Available from the National Technical Information Service, Washington, D.C. : Springfield, Va.

## CHAPTER 3

### MEASURED NEUTRON FLUX PARAMETERS IN THE USGS TRIGA MARK I REACTOR

A paper published in the Journal of Radioanalytical and Nuclear Chemistry

M.A. Koehl<sup>2</sup>, R.S. Rundberg<sup>3</sup>, J.C. Braley<sup>2,4</sup>

#### 3.1 Abstract

Using the Westcott convention, the Westcott flux,  $\phi_w$ ; modified spectral index,  $r\sqrt{T_n/T_0}$ ; neutron temperature,  $T_n$ ; and gold-based cadmium ratios were determined for various sampling positions in the USGS TRIGA Mark I reactor. Westcott parameters were determined by a bare multi-monitor method. Thermal-neutron temperature measurements were made using lutetium foils. The differential neutron energy spectrum measurement was obtained using the computer iterative code SAND-II-SNL. Measurement of the neutron spectrum has resulted in a better knowledge of the reactor core and will improve predictive radioisotope production calculations necessary for neutron activation analysis and medical isotope production.

#### 3.2 Introduction

The Nuclear Science and Engineering Center at the Colorado school of Mines (CSM) manages the research relationship, space and infrastructure occupied by CSM researchers proximate to the U.S. Geological Survey (USGS) Training, Research, Isotopes, General Atomic (TRIGA) Mark I Reactor. The USGS operates the Geological Survey TRIGA Reactor (GSTR), a 1 MW low-enriched uranium-fueled, pool-type reactor located at the Denver Federal Center in Lakewood, CO which has been in operation since the late 1960s in support of a number of research activities across the Nation. It is the only research reactor of its type in the Department of the Interior and the only research reactor within a 500 km radius of Denver, CO.

---

<sup>1</sup> Reprinted with permission of Springer, J Radioanal Nucl Chem, October 2015, Volume 306, Issue 1, pp 31-38, DOI 10.1007/s10967-015-4058-9

<sup>2</sup> Graduate Student and Assistant Professor, respectively, Department of Chemistry and Geochemistry, Colorado School of Mines, 1500 Illinois Street, Golden, CO 80401

<sup>3</sup> Los Alamos National Laboratory, Los Alamos, NM 87545

<sup>4</sup> Author for correspondence

The GSTR houses a circular core surrounded by a graphite reflector, Fig. 3.1. The core is currently fueled with less than 20%-enriched uranium–zirconium hydride alloy mixture of 8.5 wt% stainless steel clad, 12 wt% stainless steel clad, and 8 wt% aluminum clad fuel rods [1]. The facility is typically operated for 6 hours per day and 5 days per week at 1 MW, although longer irradiations are possible. The three most often used sample positions are the central thimble, lazy susan, and dry tube. The central thimble (CT), a water-filled irradiation position, is located in the center of the core at the point of maximum neutron flux. The lazy susan (LS) is a water tight rotary specimen rack assembly capable of holding forty samples surrounding the reactor core. The entire assembly rests in a well in the graphite reflector. The dry tube (DT) is a vertical irradiation tube located in a rack mounted to the exterior of the reflector.

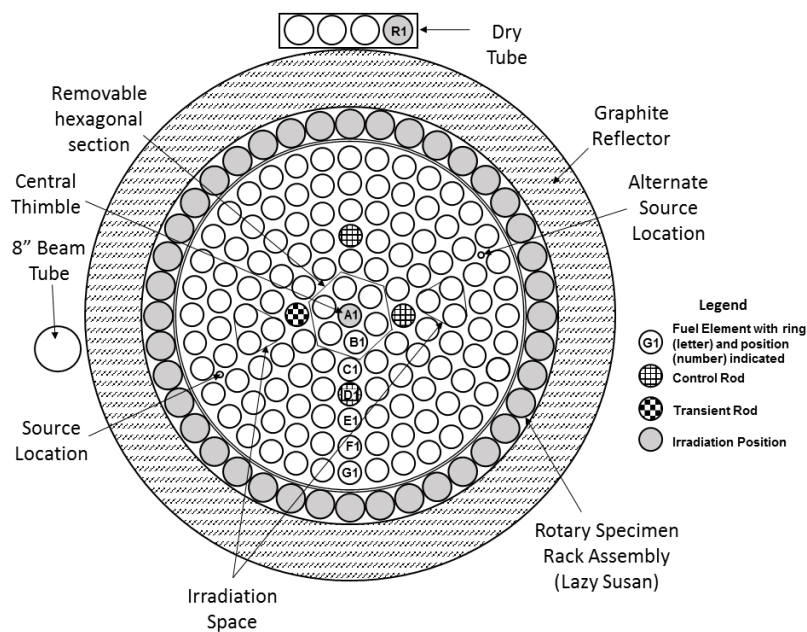


Figure 3.1. Schematic of the U.S. Geological Survey TRIGA Mark I Reactor core showing location of central thimble, lazy susan, and dry tube irradiation positions

Experimental techniques using the reactor, such as neutron activation analysis, characterization of radiation damage to materials, radioisotope production and radiation effects on electronics, rely on accurate neutron spectrum parameters to quantify experimental results or accurately predict radioisotope production. The most recent information on the GSTR core was published subsequent to its initial operation in the 1960s, however the core configuration has changed and the neutron spectrum parameters have changed as well. For these reasons, an updated experimental

characterization of the GSTR reactor using activation foils was completed. The details of the characterization, and comparison of neutron characteristics with other comparable TRIGA reactors, is provided herein.

### 3.3 Experimental

#### 3.3.1 Foil Irradiations

##### *Theory*

Activation foils are one of the most widely used detectors for determining neutron flux. In this method, a suitable stable material is exposed to a neutron flux for a measured period of time. Following irradiation, the material is removed from the neutron field, and measurement is made of the activity induced in it. These foils are normally thin foils or wires and the effect of neutron absorption can be made negligible either through the selection of the foil or by application of a correction factor for self-shielding. The saturated sample activity,  $R_s$ , following irradiation in a reactor is given by Eq. 3.1,

$$R_s = \frac{\lambda N_D M}{SDCmN_A} \quad (3.1)$$

where  $\lambda$  is the decay constant;  $N_D$  is the number of counts under the full energy peak corrected for background and pulse-losses (dead time, random and true coincidence, pulse pile-up, etc.) and converted to disintegrations using detector efficiency, gamma ray intensity and fraction of the sample counted;  $M$  is the atomic mass of the target isotope;  $S$  is the saturation correction,  $S = 1 - e^{-\lambda t_i}$ ;  $t_i$  is the irradiation time;  $C$  is the correction for decay during counting,  $C = (1 - e^{-\lambda t_c})/\lambda t_c$ ,  $t_c$  is the counting time;  $D$  is the decay correction,  $D = e^{-\lambda t_d}$ ;  $t_d$  is the decay time;  $m$  is the mass of the target isotope; and  $N_A$  is Avogadro's constant. This experimentally determined  $R_s$  value is used to evaluate the neutron flux.

The neutron flux in a reactor can be separated into three distinct regions. Fast neutrons produced in a reactor are characterized by an energy distribution according to the Watt spectrum [2]. Moderated or epithermal neutrons are gradually slowed down within the moderator, and develop a distribution proportional to the inverse of the neutron energy. When these neutrons are in equilibrium with the moderator, their energy distribution is characterized by the Maxwell-Boltzmann distribution [2].

Three distinct conventions are used for the characterizing thermal and epithermal neutron fluxes in moderated reactors. The conventions are the Westcott convention, Stoughton and Halperin convention, and the Høgdahl convention [3]. The applicability of the Høgdahl convention is restricted to  $(n,\gamma)$  cross sections that follow the  $1/v$  law in the thermal neutron energy region. The Westcott convention is most often applied when no cadmium filter is used [4] and when the following conditions are satisfied for light water moderation [5]:

$$\frac{\xi\Sigma_s}{\Sigma_a} > 10 \text{ and } \frac{T_n}{T_0} < 1.07 \quad (3.2)$$

where  $\xi\Sigma_s/\Sigma_a$  is the moderating ratio (69 for H<sub>2</sub>O) [6];  $T_n$  is the neutron distribution temperature; and  $T_0$  is the standard temperature of 293.6 K. As will be discussed below, use of the Westcott convention is applicable to characterize the USGS reactor.

### *Methods*

Foils and wires were irradiated in the CT, LS1, and R1, reference Fig. 3.1, sampling positions for times ranging from five minutes, for thermal neutron reactions in the central thimble, to four hours, for fast neutron reactions in the dry tube. Sample preparation consisted of cleaning, sizing, and triple weighing the wires and foils. All samples were irradiated at the point of maximum neutron flux within each sampling position. After irradiation, the induced gamma activities emitted from the activation foils were counted on a Canberra reverse electrode closed ended coaxial high purity germanium (HPGe) detector (model number GR1320) coupled with an EG&G Ortec ADC Spectrum Master 92X multichannel analyzer after an appropriate cooling time to decrease the radiation hazard of the associated foils. A certified NIST traceable Spectrum Techniques <sup>152</sup>Eu source with an uncertainty of  $\pm 5\%$ , was used to determine the efficiency at various distances from the HPGe detector. The saturated activity was calculated using Eq. 3.1.

Foils from a ShieldWerx SWX-1552 Thermal Foils Kit with SWX-531 Cd covers (0.508 mm), Ni (0.762 mm diameter) and 0.67% Au-Al (0.508 mm diameter) wires, and Mg and Al foils from Reactor Experiments were used to determine the differential neutron energy spectrum from the saturated activities. Iron foils were used to determine the fast neutron flux, the 0.67% Au-Al wire was used as a flux monitor for all irradiations, and Lu was used to determine the neutron temperature. Saturated activities input into the SAND-II-SNL code were corrected for thermal and epithermal self-shielding and normalized with the flux monitors to account for variations in

Table 3.1 Characteristics of the Mn, Au, Mo, and Lu activation foils/wire, and their nuclear data

Foil/Wire	Purity (%)	Thickness/ Radius (mm)	Reaction	$\sigma^a$ (barns)	$t_{1/2}^a$ (h)	$E_\gamma^a$ (keV)	$I_\gamma^a$ (%)	$G_{th}^b$	$G_{epi}^b$	$s_0^c$	$g^d$
0.67% Au-Al wire	99.58	0.5080	$^{197}\text{Au}(n,\gamma)^{198}\text{Au}$	98.66	64.7	411.8	95.62	0.9991	0.8801	17.46	1.005
81.3% Mn-Cu foil	99.99	0.0508	$^{55}\text{Mn}(n,\gamma)^{56}\text{Mn}$	13.2	2.57	846.8	98.87	0.9959	0.9973	0.66	1
Mo foil	99.99	0.0762	$^{98}\text{Mo}(n,\gamma)^{99}\text{Mo}$	0.013	67	739.5	12.26	0.9999	0.9776	56.39	1.001
5% Lu-Al foil	99.95	0.1016	$^{176}\text{Lu}(n,\gamma)^{177}\text{Lu}$	2097	161.04	208.4	10.36	0.9973	0.9984	<sup>e</sup>	<sup>e</sup>

<sup>a</sup>Ref. [7]

<sup>b</sup>Calculated from Ref. [9] and Ref. [10]

<sup>c</sup>Calculated from Eq. 3.4. Data for resonance integral,  $I_0$  from Ref. [8]

<sup>d</sup>Ref. [8]

<sup>e</sup>Neutron temperature dependent

the neutron flux within the same sampling position. The Westcott flux and spectral index were derived using the foils and nuclear data [7, 8] listed in Table 3.1.

### 3.3.2 Application of Westcott Convention

In the Westcott convention, the reaction rate is given by  $R_s = n v_0 \widehat{\sigma}_0$  [5], where the effective cross section is given as  $\widehat{\sigma}_0 = \sigma_0 (g + r \sqrt{T_n/T_0} s_0)$ . Accounting for self-shielding of thermal and epithermal neutrons [9, 10], the reaction rate becomes

$$R_s = \varphi_w \sigma_0 \left( G_{th} g + r \sqrt{\frac{T_n}{T_0}} s_0 G_{epi} \right) \quad (3.3)$$

where  $\varphi_w$  is the Westcott 2200 m/s neutron flux;  $\sigma_0$  is the reaction cross-section for 2200 m/s neutrons;  $G_{th}$  and  $G_{epi}$  are self-shielding corrections for thermal and epithermal neutrons, respectively, which can be experimentally determined or calculated [9, 10];  $g$  is a factor which accounts for the departure of the cross section from  $1/v$ -dependence in a Maxwellian thermal neutron spectrum at neutron temperature  $T_n$ ;  $T_0$  is the standard temperature of 293.6 K;  $s_0$  is a quantity that accounts for the departure of the cross-section from  $1/v$ -dependence in the epithermal energy range. It can be calculated by the following equation [5]:

$$s_0 = \frac{2}{\sqrt{\pi}} \frac{\Sigma'}{\sigma_0} = \frac{2}{\sqrt{\pi}} \left( \frac{I_0}{\sigma_0} - 2g \sqrt{\frac{E_0}{E_{Cd}}} \right) \quad (3.4)$$

where  $\Sigma'$  is the resonance integral excess over the  $1/v$  cross section value;  $I_0$  is the resonance integral; and  $E_0$  and  $E_{Cd}$  are the thermal and cadmium cut-off energies, 0.0253 eV and 0.55 eV, respectively.

The spectral index,  $r$ , is approximately the fraction of the total neutron density in the epithermal component. More specifically,  $r = f \sqrt{\pi \mu} / 4$ , where  $f$  is the fraction of the density of epithermal neutrons in the reactor and  $\mu$  is a factor used to normalize the epithermal density distribution [11]. A typical value for  $\mu$  is 5 for well moderated light water reactors [5].

Dividing Eq. 3.3 by  $\sigma_0 G_{th} g$ , yields the following linear equation:

$$\frac{R_s}{\sigma_0 G_{th} g} = \varphi_w + \varphi_w r \sqrt{\frac{T_n}{T_0}} \frac{s_0 G_{epi}}{G_{th} g} \quad (3.5)$$

A plot of  $R_s/\sigma_0 G_{th}g$  vs  $s_0 G_{epi}/G_{th}g$  for multiple foils will result in a straight line with an intercept of  $\varphi_w$  and a slope of  $\varphi_w r \sqrt{T_n/T_0}$ . The modified spectral index,  $r \sqrt{T_n/T_0}$ , can then be calculated by dividing the slope by the intercept [12].

Activation foils are normally chosen so that do not have a widely varying Westcott g-factor, however resonances near the thermal neutron energy range cause a departure of the capture cross section from a  $1/v$ -dependence. The type departure can result in an increasing or decreasing temperature dependence of the Westcott g-factor with the neutron temperature [8]. This temperature dependence can be calculated from the following [5]:

$$g = \frac{\sigma_{Maxwell}}{\sigma_0} = \frac{1}{v_0 \sigma_0} \int_0^\infty \frac{4}{\pi} \frac{v^3}{v_T^3} e^{-\left(\frac{v}{v_T}\right)^2} \sigma(v) dv \quad (3.6)$$

where  $\sigma_{Maxwell}$  is the Maxwell averaged cross section,  $v_0$  is 2200 m/s,  $v$  is the relative velocity of the neutrons, and  $v_T$  is the mean thermal velocity given by [8]:

$$v_T = \sqrt{\frac{2kT_n}{m_{red}}} \quad (3.7)$$

where  $k$  is the Boltzmann constant and  $m_{red}$  is the reduced mass. Due to its sensitivity as an indicator of thermal neutron temperature [13] in the range of 0-400 °C, Lu-176 can be used to determine  $T_n$ . Solving Eq. 3.3 for  $g$  yields

$$g_{Lu} = \frac{R_s}{G_{th} \varphi_w \sigma_0} - r \sqrt{\frac{T_n}{T_0}} \frac{s_0 G_{epi}}{G_{th}} \quad (3.8)$$

and experimental values of  $g_{Lu}$  can be compared to calculated values to determine  $T_n$ .

Once the spectral index and thermal neutron temperatures are known, the conventional 2200 m/s thermal neutron flux,  $\varphi_0$ , and epithermal neutron flux,  $\varphi_e$ , can be calculated from Eq. 3.9 and Eq. 3.10 for comparison to the other conventions [3].

$$\varphi_0 = \left(1 - \frac{4r}{\sqrt{\pi\mu}}\right) \varphi_w \quad (3.9)$$

$$\varphi_e = \frac{2r}{\sqrt{\pi}} \sqrt{\frac{T_n}{T_0}} \varphi_w \quad (3.10)$$

### 3.3.3 SAND-II-SNL Code Operations

The iterative spectrum unfolding code, SAND-II, obtained from the Radiation Safety Information Computational Center (RSICC), has been widely applied to calculate the differential neutron energy spectrum using multiple foils in an energy range from 0.001 eV to 20 MeV [14]. In SAND-II, an initial trial spectrum at each energy value within a 640 energy group structure is multiplied by the neutron reaction cross section of the foil of interest and integrated over all energies to obtain a predicted activity. The calculated and measured activities of the sensors exposed to the neutron flux in each sampling position are then compared. The code subsequently applies an algorithm to alter the trial spectrum to obtain a set of calculated activities with a smaller standard deviation from the measured values in the previous calculation. This iteration continues until the spectrum obtained is within a user defined standard deviation. While the SAND-II-SNL code does not provide a unique solution due to the number of sensors being less than the number of neutron groups, using certain restrictions can limit the range of physically reasonable solutions to an acceptable degree [15]. For these studies, a trial spectrum was determined through a technique of trial adjustment [16]. In this procedure, an initial trial is generated from a flat spectrum. The resulting spectrum is altered by smoothly connecting the points where the sensor set is responsive and subsequently used as the next trial. Iteration is continued in this manner until a minimum standard deviation is reached.

## 3.4 Results

### 3.4.1 Westcott Convention

The neutron flux parameters are shown in Table 3.2. The Westcott flux and spectral index were calculated by plotting Eq. 3.5. The thermal and epithermal flux were calculated from Eq. 3.9 and Eq. 3.10, respectively. The fast neutron flux was based on the saturated activity of  $^{54}\text{Mn}$  formed from the  $^{54}\text{Fe}(n,p)^{54}\text{Mn}$  reaction with neutrons of energy higher than 2.2 MeV [17].

Fig. 3.2 is a plot of Eq. 3.5 for the various sampling positions. The intercept indicates the Westcott flux and the slope is a product of the Westcott flux and the spectral index. Repeated experiments result in an almost identical linear plot for the lazy susan and dry tube positions. The central thimble, located in the center of the core reflects the largest flux and spectral index; variations in the linear plot are due to the positioning of the sample. Cadmium ratios for Au are

given in Table 3.3. Measured saturated activities corrected for infinite dilution are listed in Table 3.4.

Table 3.2 Calculated neutron flux distribution parameters within the GSTR

Sampling Location: (Position of sample:)	Central Thimble (centerline)	Lazy Susan, LS1 (bottom)	Dry Tube, R1 (bottom)
Westcott Flux, $\phi_w$ (n/cm <sup>2</sup> -s)	$1.74 \pm 0.08 \times 10^{13}$	$3.87 \pm 0.19 \times 10^{12}$	$1.47 \pm 0.07 \times 10^{12}$
Spectral Index, $r \sqrt{\frac{T_n}{T_0}}$	$0.069 \pm 0.002$	$0.046 \pm 0.002$	$0.010 \pm 0.001$
$T_n$ (K)	$322 \pm 16$	$281 \pm 14$	$246 \pm 12$
Thermal Flux, $\phi_0$ (n/cm <sup>2</sup> -s)	$1.62 \pm 0.08 \times 10^{13}$	$3.70 \pm 0.18 \times 10^{12}$	$1.45 \pm 0.07 \times 10^{12}$
Epithermal Flux, $\phi_e$ (n/cm <sup>2</sup> -s)	$1.35 \pm 0.07 \times 10^{12}$	$1.99 \pm 0.09 \times 10^{11}$	$1.60 \pm 0.08 \times 10^{10}$
Fast Flux <sup>a</sup> , $\phi_{fast}$ (n/cm <sup>2</sup> -s)	$1.08 \pm 0.05 \times 10^{13}$	$2.4 \pm 0.2 \times 10^{12}$	$8.6 \pm 0.4 \times 10^{11}$

<sup>a</sup>Calculated from  $^{54}\text{Fe}(n,p)^{54}\text{Mn}$  threshold reaction for  $E > 2.2$  MeV.

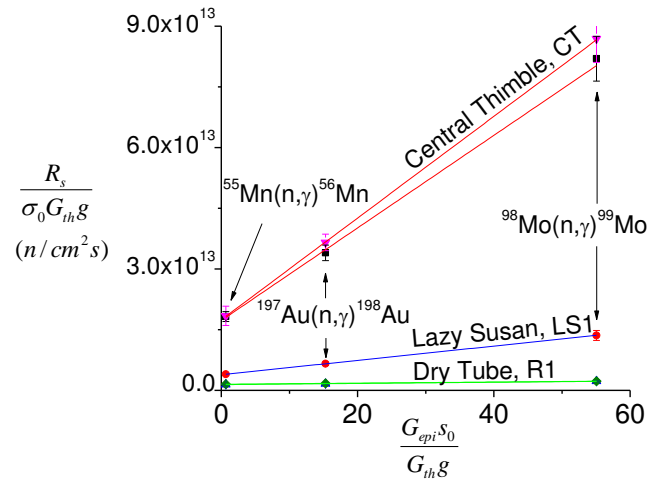


Figure 3.2. A plot of  $s_0 G_{epi} / G_{th} g$  vs  $R_s / \sigma_0 G_{th} g$  for Mn, Au, and Mo foils. The intercept is the Westcott flux,  $\phi_w$ . The modified spectral index,  $r \sqrt{T_n / T_0}$  is calculated by dividing the slope by the intercept

Fig. 3.2 is a plot of Eq. 3.5 for the various sampling positions. The intercept indicates the Westcott flux and the slope is a product of the Westcott flux and the spectral index. Repeated experiments result in an almost identical linear plot for the lazy susan and dry tube positions. The central thimble, located in the center of the core reflects the largest flux and spectral index; variations in the linear plot are due to the positioning of the sample. Cadmium ratios for Au are given in Table 3.3. Measured saturated activities corrected for infinite dilution are listed in Table 3.4.

Table 3.3 Measured vs calculated cadmium ratio for gold in various sampling positions within the GSTR

Sampling Location: (Position of sample:)	Central Thimble (centerline)	Lazy Susan, LS1 (bottom)	Dry Tube, R1 (bottom)
Cadmium Ratio (Au) - Measured	1.98±0.08	2.34±0.07	6.7±0.2
Cadmium Ratio (Au) - Calculated <sup>a</sup>	1.88±0.09	2.36±0.02	7.5±0.9

<sup>a</sup>Calculated from:  $R_{cd} = \frac{G_{th}g+r\sqrt{\frac{T_n}{T_0}}S_0G_{epi}}{r\sqrt{\frac{T_n}{T_0}}} [S + \frac{1}{K}\sqrt{\frac{T_n}{T_0}}]^{-1}$ , where K is a transmission factor for isotropic incidence. For 0.020" thick Cd Covers, K=2.0728 [5].

Neutron temperatures were determined by comparing the measured  $g_{Lu}$  values from Eq. 3.8 with those calculated by Eq. 3.6. Due to the lower than expected neutron temperatures in the lazy susan and dry tube, the initial Westcott g-values for Au-197, Mn-55, and Mo-98, from Table 3.1 were calculated using Eq. 3.6 at the neutron temperatures in Table 3.2 and determined to be within 0.25% of the referenced value across the neutron temperatures reported. Therefore, the values in Table 3.1 were used for all calculations.

### 3.4.2 SAND-II-SNL Code

The spectrum shown in Fig. 3.3 was iteratively calculated by using the trial adjustment technique with measured activities. The standard deviation of measured-to-calculated activities achieved in the central thimble, lazy susan, and dry tube was 11.4%, 4.0% and 7.2%, respectively.

The SAND-II-SNL code was subsequently used to calculate the expected capture activities of infinitely dilute foils in the thermal region. These results are listed in Table 3.5.

Table 3.4 Measured saturated activities for foils in various sampling positions in the GSTR used in the SAND-II-SNL spectrum unfolding code

Foil Reaction <sup>a</sup>	Saturated Activities, $R_s$ (Bq/atom)		
	Central Thimble	Lazy Susan, LS1	Dry Tube, R1
$^{27}\text{Al}(n,a)^{24}\text{Na}$	$7.6\pm 0.7\times 10^{-15}$	$4.7\pm 0.6\times 10^{-16}$	<sup>b</sup>
$^{24}\text{Mg}(n,p)^{24}\text{Na}$	$1.1\pm 0.3\times 10^{-14}$	$8.0\pm 0.8\times 10^{-16}$	<sup>b</sup>
$^{56}\text{Fe}(n,p)^{56}\text{Mn}$	$1.19\pm 0.08\times 10^{-14}$	$1.9\pm 0.1\times 10^{-13}$	$6.7\pm 0.6\times 10^{-14}$
$^{54}\text{Fe}(n,p)^{54}\text{Mn}$	$8.5\pm 0.6\times 10^{-13}$	$9.3\pm 0.6\times 10^{-14}$	$3.2\pm 0.2\times 10^{-14}$
$^{58}\text{Ni}(n,p)^{58}\text{Co}$	$6.7\pm 0.5\times 10^{-13}$	$5.2\pm 0.4\times 10^{-14}$	$2.8\pm 0.2\times 10^{-15}$
$^{115}\text{In}(n,n)^{115\text{m}}\text{In}$	$1.93\pm 0.02\times 10^{-12}$	$1.59\pm 0.03\times 10^{-13}$	$7.7\pm 0.4\times 10^{-15}$
$^{98}\text{Mo}(n,\gamma)^{99}\text{Mo}$	$1.13\pm 0.08\times 10^{-11}$	$1.8\pm 0.1\times 10^{-12}$	$3.0\pm 0.3\times 10^{-13}$
$^{98}\text{Mo}(n,\gamma)^{99}\text{Mo}$ (Cd)	$4.7\pm 0.3\times 10^{-12}$	$1.2\pm 0.1\times 10^{-12}$	$1.5\pm 0.1\times 10^{-13}$
$^{197}\text{Au}(n,\gamma)^{198}\text{Au}$	$3.6\pm 0.2\times 10^{-9}$	$6.5\pm 0.4\times 10^{-10}$	$1.6\pm 0.1\times 10^{-10}$
$^{197}\text{Au}(n,\gamma)^{198}\text{Au}$ (Cd)	$1.9\pm 0.1\times 10^{-9}$	$2.7\pm 0.1\times 10^{-10}$	$2.3\pm 0.2\times 10^{-11}$
$^{59}\text{Co}(n,\gamma)^{60}\text{Co}$	$5.8\pm 0.3\times 10^{-10}$	$1.2\pm 0.1\times 10^{-10}$	$4.5\pm 0.4\times 10^{-11}$
$^{59}\text{Co}(n,\gamma)^{60}\text{Co}$ (Cd)	$2.8\pm 0.2\times 10^{-11}$	$7.3\pm 0.7\times 10^{-12}$	$1.6\pm 0.1\times 10^{-12}$
$^{58}\text{Fe}(n,\gamma)^{59}\text{Fe}$	$1.25\pm 0.05\times 10^{-11}$	$7.7\pm 0.3\times 10^{-13}$	$7.7\pm 0.3\times 10^{-13}$
$^{58}\text{Fe}(n,\gamma)^{59}\text{Fe}$ (Cd)	$1.47\pm 0.8\times 10^{-12}$	$2.5\pm 0.1\times 10^{-13}$	$4.6\pm 0.3\times 10^{-14}$
$^{63}\text{Cu}(n,\gamma)^{64}\text{Cu}$	$7.4\pm 0.4\times 10^{-11}$	$1.32\pm 0.07\times 10^{-11}$	$5.4\pm 0.3\times 10^{-12}$
$^{63}\text{Cu}(n,\gamma)^{64}\text{Cu}$ (Cd)	$4.8\pm 0.2\times 10^{-12}$	$6.2\pm 0.3\times 10^{-13}$	$1.22\pm 0.07\times 10^{-13}$
$^{55}\text{Mn}(n,\gamma)^{56}\text{Mn}$	$2.4\pm 0.3\times 10^{-10}$	$5.3\pm 0.4\times 10^{-11}$	$2.0\pm 0.1\times 10^{-11}$
$^{55}\text{Mn}(n,\gamma)^{56}\text{Mn}$ (Cd)	$1.46\pm 0.01\times 10^{-11}$	$2.2\pm 0.1\times 10^{-12}$	$4.3\pm 0.3\times 10^{-13}$
$^{23}\text{Na}(n,\gamma)^{24}\text{Na}$	$8.3\pm 0.8\times 10^{-12}$	$5.2\pm 0.4\times 10^{-13}$	$6.2\pm 0.6\times 10^{-14}$
$^{23}\text{Na}(n,\gamma)^{24}\text{Na}$ (Cd)	$1.6\pm 0.2\times 10^{-12}$	$4.8\pm 0.4\times 10^{-14}$	$9.9\pm 0.9\times 10^{-15}$
$^{45}\text{Sc}(n,\gamma)^{46}\text{Sc}$	$4.7\pm 0.4\times 10^{-10}$	$7.7\pm 0.6\times 10^{-11}$	$3.3\pm 0.3\times 10^{-11}$
$^{45}\text{Sc}(n,\gamma)^{46}\text{Sc}$ (Cd)	$2.4\pm 0.2\times 10^{-12}$	$2.4\pm 0.1\times 10^{-12}$	$4.2\pm 0.3\times 10^{-13}$

<sup>a</sup>(Cd) indicates the cadmium covered activity

<sup>b</sup>Activities not obtained due to low flux at threshold energies in the try tube

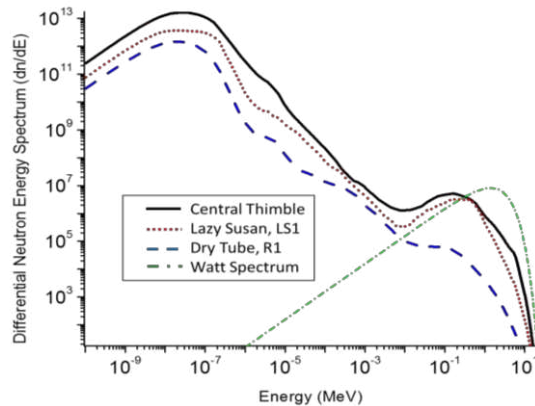


Figure 3.3. SAND-II-SNL differential neutron energy spectrum for various positions within the GSTR

Table 3.5 Saturated thermal activities in various sampling positions within the GSTR calculated with the SAND-II-SNL spectrum unfolding code

Foil Reaction <sup>a</sup>	Saturated Activities, <i>R<sub>s</sub></i> (Bq/atom)		
	Central Thimble	Lazy Susan, LS1	Dry Tube, R1
<sup>98</sup> Mo(n,γ) <sup>99</sup> Mo	9.92x10 <sup>-12</sup>	2.02x10 <sup>-12</sup>	3.07x10 <sup>-13</sup>
<sup>98</sup> Mo(n, γ) <sup>99</sup> Mo (Cd)	4.85x10 <sup>-12</sup>	1.50x10 <sup>-12</sup>	1.50x10 <sup>-13</sup>
<sup>197</sup> Au(n, γ) <sup>198</sup> Au	3.60x10 <sup>-9</sup>	6.50x10 <sup>-10</sup>	1.60x10 <sup>-10</sup>
<sup>197</sup> Au(n, γ) <sup>198</sup> Au (Cd)	2.00x10 <sup>-9</sup>	3.17x10 <sup>-10</sup>	2.38x10 <sup>-11</sup>
<sup>59</sup> Co(n, γ) <sup>60</sup> Co	6.33x10 <sup>-10</sup>	9.49x10 <sup>-11</sup>	4.75x10 <sup>-11</sup>
<sup>59</sup> Co(n, γ) <sup>60</sup> Co (Cd)	2.40x10 <sup>-11</sup>	8.36x10 <sup>-12</sup>	1.54x10 <sup>-12</sup>
<sup>58</sup> Fe(n, γ) <sup>59</sup> Fe	1.07x10 <sup>-11</sup>	9.35x10 <sup>-13</sup>	9.45x10 <sup>-13</sup>
<sup>58</sup> Fe(n, γ) <sup>59</sup> Fe (Cd)	1.48x10 <sup>-12</sup>	3.02x10 <sup>-13</sup>	5.94x10 <sup>-14</sup>
<sup>63</sup> Cu(n, γ) <sup>64</sup> Cu	7.60x10 <sup>-11</sup>	1.12x10 <sup>-11</sup>	5.58x10 <sup>-12</sup>
<sup>63</sup> Cu(n, γ) <sup>64</sup> Cu (Cd)	5.27x10 <sup>-12</sup>	7.48x10 <sup>-13</sup>	8.82x10 <sup>-14</sup>
<sup>55</sup> Mn(n, γ) <sup>56</sup> Mn	2.24x10 <sup>-10</sup>	4.32x10 <sup>-11</sup>	1.67x10 <sup>-11</sup>
<sup>55</sup> Mn(n, γ) <sup>56</sup> Mn (Cd)	1.45x10 <sup>-11</sup>	2.75x10 <sup>-12</sup>	4.90x10 <sup>-13</sup>
<sup>23</sup> Na(n, γ) <sup>24</sup> Na	8.87x10 <sup>-12</sup>	4.28x10 <sup>-13</sup>	6.52x10 <sup>-14</sup>
<sup>23</sup> Na(n, γ) <sup>24</sup> Na (Cd)	1.35x10 <sup>-12</sup>	5.32x10 <sup>-14</sup>	1.04x10 <sup>-14</sup>
<sup>45</sup> Sc(n, γ) <sup>46</sup> Sc	4.55x10 <sup>-10</sup>	6.56x10 <sup>-11</sup>	3.35x10 <sup>-11</sup>
<sup>45</sup> Sc(n, γ) <sup>46</sup> Sc (Cd)	2.53x10 <sup>-11</sup>	2.36x10 <sup>-12</sup>	4.66x10 <sup>-13</sup>

<sup>a</sup>(Cd) indicates the cadmium covered activity

### 3.4.3 Comparison to Similar TRIGA Reactors

Three facilities that are nearly identical to the GSTR core configuration include the Oregon State University (OSU) (MARK II, 1.1 MW), Corvallis; University of Texas, Austin (MARK II, 1.1 MW); and the Malaysian Institute for Nuclear Technology Research (MINT) (MARK II, 1 MW). While each facility has a similar core configuration, fuel composition, fuel burn-up, and irradiation positions vary. The OSU and MINT reactors both use a higher weight percent fuel, 30 wt% and 20 wt%, respectively, in various fuel positions within the reactor [18, 19]. Table 3.6 presents the maximum or average reported flux for thermal, epithermal, and fast neutrons at various irradiation positions within these facilities so as to provide a qualitative comparison of the irradiation positions [18-20].

While different techniques were used to make the neutron flux determinations within each reactor, comparisons of the thermal, epithermal, and Westcott flux can be made. OSU used a spectrum unfolding code, STAY'SL with saturated activities from multiple foils [18]. UT fit the

saturated activities of multiple foils to an idealized neutron spectrum consisting of a Maxwellian, 1/E, and Watt spectrum for the thermal, epithermal, and fast spectrum, respectively [20]. MINT, using the Hogdhal convention, determined the neutron flux based on a bare triple monitor method with  $^{197}\text{Au}$ - $^{94}\text{Zr}$ - $^{97}\text{Zr}$  monitors [19]. Using Eq. 3.9 and Eq. 3.10 with the assumption  $\sqrt{T_n/T_0} \approx 1$ , which is reasonable given the low operating temperature of TRIGA reactors, Table 3.7 provides calculated Westcott flux values, spectral indices, and cadmium ratios of gold in the rotary rack sampling position of the OSU, UT, and MINT TRIGA cores. These calculated values are an approximation and are used to make some comparisons with reactor cores similar to the GSTR.

Table 3.6 Comparison of published neutron flux values at facilities with similar cores to the GSTR

Published Neutron Spectrum Parameters	Central Position	Rotary Rack	Thermal Column
<b>Oregon State University, Corvallis (LEU core)</b>			
Thermal Flux, $\phi_0$ (n/cm <sup>2</sup> -s)	2.89x10 <sup>12</sup> <sup>a</sup>	2.83x10 <sup>12</sup>	3.42x10 <sup>10</sup>
Epithermal Flux, $\phi_e$ (n/cm <sup>2</sup> -s)	1.00x10 <sup>12</sup> <sup>a</sup>	2.46x10 <sup>11</sup>	7.90x10 <sup>8</sup>
Fast Flux <sup>a</sup> , $\phi_{\text{fast}}$ (n/cm <sup>2</sup> -s)	1.51x10 <sup>12</sup> <sup>a</sup>	4.06x10 <sup>11</sup>	1.20x10 <sup>9</sup>
<b>University of Texas, Austin (Mark II)</b>			
Thermal Flux, $\phi_0$ (n/cm <sup>2</sup> -s)	-	2.6±0.02x10 <sup>12</sup>	-
Epithermal Flux, $\phi_e$ (n/cm <sup>2</sup> -s)	-	1.30±0.05x10 <sup>11</sup>	-
Fast Flux <sup>a</sup> , $\phi_{\text{fast}}$ (n/cm <sup>2</sup> -s)	-	-	-
<b>Malaysian Institute for Nuclear Technology Research (Mark II)</b>			
Thermal Flux, $\phi_0$ (n/cm <sup>2</sup> -s)	-	2.72x10 <sup>12</sup>	-
Epithermal Flux, $\phi_e$ (n/cm <sup>2</sup> -s)	-	2.32x10 <sup>11</sup>	-
Fast Flux <sup>a</sup> , $\phi_{\text{fast}}$ (n/cm <sup>2</sup> -s)	-	-	-

<sup>a</sup>Central Position flux is taken from values for the B-1 irradiation position

Table 3.7 Calculated approximate Westcott flux, spectral index, and cadmium ratio (Au) for TRIGA reactors with cores similar to the GSTR. Calculations based on reported thermal and epithermal flux

Irradiation Facility (Lazy Susan / Rotary Rack)	Westcott Flux <sup>a</sup> , $\phi_w$ (n/cm <sup>2</sup> -s)	Spectral Index <sup>b</sup> , $r$	Cadmium Ratio <sup>c</sup> (Au)
Oregon State University <sup>a</sup>	1.32x10 <sup>12</sup>	0.088	1.7
University of Texas	2.72x10 <sup>12</sup>	0.042	2.6
MINT	2.93x10 <sup>12</sup>	0.070	1.9

<sup>a</sup>Calculated from Eq. 3.10 after calculating  $r$ .

<sup>b</sup>Combining Eq. 3.9 and Eq. 3.10,  $r = \frac{5\phi_e\sqrt{\pi}}{2(2\phi_e\sqrt{5}+5\phi_0)}$ , assuming  $\sqrt{T_n/T_0} = 1$ , and  $\mu=5$ .

<sup>c</sup>Calculated similar to Table 3.3.

### 3.5 Discussion

#### 3.5.1 Westcott Convention

The calculated flux shows good agreement with the flux provided by the GSTR operators. The tabulated cadmium ratios based on the spectral index also show good agreement with measured values. In the absence of absorption, leakage, or additional sources, the neutron temperature should come to equilibrium with the moderator temperature. Absorption of low energy neutrons tends to shift this distribution to higher temperatures which is known as absorption hardening. While the experimental results of the neutron temperature within the central thimble sampling position appears to be coupled to the moderator temperature with absorption hardening, the neutron temperature in the lazy susan and dry tube are lower than expected with the neutron temperature within the dry tube position below the freezing point of water. This unexpected result may be due to the proximity of the sampling positions to the graphite reflector resulting in diffusion of low energy neutrons which shift the neutron distribution and results in a lower than expected neutron temperature.

#### 3.5.2 SAND-II-SNL Code

Calculated values for the thermal capture reactions were compared to the experimental values in Table 3.4. These calculated values showed agreement to the experimentally determined activities with the greatest errors of 16%, 25%, and 29% in the central thimble, lazy susan, and dry tube, respectively. The thermal spectrum displays a Maxwell Boltzmann distribution for all

sampling positions. The epithermal spectrum varies as the inverse of the neutron energy with deviations due to resonance cross sections of the structural materials within the core. Fig. 3.3 also shows qualitatively the variance of the fast flux to the Watt spectrum in the central thimble, lazy susan, and dry tube. These variations are due to the various degrees of moderation of the fast neutrons at these sampling positions. The average cross section of a fast reaction is typically calculated from an assumption that the fast flux is distributed in accordance with a Watt spectrum [21]. While the focus of this paper is on the flux parameters of the thermal and epithermal regions, a more detailed measurement of the fast flux should be undertaken prior to quantification of experiments utilizing fast reactions.

### **3.5.3 Comparison to Similar TRIGA Reactors**

Comparisons can be made between the most similar irradiation positions within the OSU, UT, and MINT reactors. For instance, the central comparison of the OSU reactor is in the B-1 position and the rotary rack comparison is the G-14 (G-ring in-core irradiation tube – GRICIT) irradiation position owing to most of the G-ring positions being filled with graphite rods [18]. While these facilities are similar, varying reactors and different positions within one type of reactor can produce different neutron energy distributions, fluxes, and spectrum parameters due to the fuel and materials used to create and moderate fission neutrons.

The core of the UT reactor contains similar fuel to the GSTR, namely 8.5 wt% uranium [20], and is in agreement with the spectral index and cadmium ratio of the lazy susan irradiation position in the GSTR core. MINT and OSU have larger spectral indices and lower cadmium ratios indicating a harder neutron spectrum in the rotary rack sampling position within these reactors. This is likely due to the higher weight percentage of fuel used in the core. Additionally, the thermal flux in the lazy susan irradiation position in the GSTR is higher than in the other three cores. This is due to the fuel burn-up within the GSTR core causing the flux profile to decrease in the central thimble and increase in the lazy susan while keeping the overall power at 1 MW. Published data for the other three cores in the central thimble irradiation position is required to confirm this analysis.

### 3.6 Conclusion

Saturated activity measurements have provided detailed information about the neutron spectral parameters in sampling positions in the GSTR reactor. An analysis, based on the Westcott convention gave a set of spectrum parameters including the Westcott flux, spectral index, neutron temperature which are sufficient to determine the activities for future experiments. The calculated thermal and epithermal flux are given for comparison with other neutron conventions and compared to three similar TRIGA cores. Of the compared cores, the GSTR, due to high fuel burn-up and low weight percent fuel, appears to have the flattest radial flux profile and a relatively thermalized flux in the lazy susan sampling position. The SAND-II-SNL spectrum unfolding code was used to determine the differential neutron energy spectrum in the central thimble, lazy susan, and dry tube irradiation positions.

### 3.7 Acknowledgements

The authors would like to express their sincere thanks to the reactor staff of the GSTR for their support, funding from the Colorado School of Mines, and the NRC Faculty Development Grant program.

### 3.8 References Cited

1. Safety Analysis Report (2009) United States Geological Survey Research Reactor Docket No. 50-274, License No. R-113
2. Lamarsh JR (1961) Introduction to nuclear reactor theory. American Nuclear Society, Ithaca, NY
3. ASTM Standard E261 (2010) DOI 10.1520/E0261-10
4. Williams JG, Gilliam DM (2011) 48:254-262 DOI 10.1088/0026-1394/48/6/S03
5. Westcott CH, Walker WH, Alexander TK (1959). Atomic Energy of Canada Ltd., Chalk River, Ontario
6. J. O. Denschlag (2011) In: Vértes A, Nagy S, Klencsár Z, Lovas RG, Rösch F (eds) Handbook of Nuclear Chemistry. Springer, Berlin, p 2628
7. Chart of Nuclides. <http://www.nndc.bnl.gov/chart/>. Accessed 14 May 2014
8. Pritychenko B, Mughabghab SF (2012) 113:3120-3144 DOI 10.1016/j.nds.2012.11.007
9. Martinho E, Gonçalves IF, Salgado J (2003) 58:371-375 DOI 10.1016/S0969-8043(02)00313-5

10. Martinho E, Salgado J, Goncalves IF (2004) *J. Radioanal. Nucl. Chem.* 261:637-643
11. Benedict M (1981) *Nuclear chemical engineering*. McGraw-Hill, New York
12. Chatani H (2003) Measurement of the Westcott Conventionality Thermal Neutron Flux and Suchlike at Irradiation Facilities of the KUR, JAERI-Conf 2003-06, p 241-246
13. Lomakin S, Romanov V, Bochir V (1968) 24:484-485 DOI 10.1007/BF01312410
14. Hong U, Kang HD, Seo CG, Kang YH (2001) In: Williams JG, Vehar DW, Ruddy FH, Gilliam DM (eds) *Reactor dosimetry: radiation metrology and assessment*. STP 1398, West Conshohocken, PA
15. ASTM Standard E721 (2011) DOI 10.1520/E0721-11
16. Kelly JG (1987) *Neutron Spectrum Adjustment with SANDII Using Arbitrary Trial Functions*. Sandia National Labs, Albuquerque, NM
17. ASTM Standard E263 (2013) DOI 10.1520/E0263-13
18. Schickler RA, Marcum WR, Reese SR (2013) 262:340-349 DOI 10.1016/j.nucengdes.2013.05.004
19. Khoo K, Sarmani S, Abugassa I (2007) 271:419-424 DOI 10.1007/s10967-007-0225-y
20. Graham J, Landsberger S, Ferreira P, Ihlefeld J, Brennecke G (2012) 291:503-507 DOI 10.1007/s10967-011-1270-0
21. Erdtmann G (1976) *Neutron activation tables*. Verlag Chemie, Weinheim, New York

## CHAPTER 4

### EXPERIMENTAL AND MONTE CARLO INVESTIGATION OF MASS ATTENUATION COEFFICIENTS OF FISSION PRODUCT ISOTOPES IN MOLECULAR PRECIPITATES

A paper submitted to Physics Letters B

M.A. Koehl<sup>5</sup>, R.S. Rundberg<sup>6</sup>, J.C. Braley<sup>2,7</sup>

The mass attenuation coefficients for molecular precipitates have been determined through experiment and compared to results using the EGS5 Monte Carlo computer code. Difficulties associated with sufficient production of fission product isotopes in research reactors limits the ability to complete a direct, experimental assessment of mass attenuation coefficients for these isotopes. To overcome these limitations, this study assesses the mass attenuation coefficients of fission product isotopes that can be readily produced by the thermal neutron activation of elements in a reactor. These results are then compared to simulated values calculated from a multipurpose Monte Carlo program, EGS5. EGS5 is then used to calculate the mass attenuation coefficients of additional fission product isotopes not readily produced by thermal neutron activation. The experimental attenuation coefficients of radioisotopes produced through neutron activation agree well with the EGS5 calculated results. This suggests mass attenuation coefficients of molecular precipitates can be approximated using EGS5, especially in the instance of radioisotopes produced predominantly through uranium fission.

#### 4.1 Introduction

The radiochemical study of fission product isotopes is often conducted with gas proportional counters. Procedures for preparation of these samples are found in literature [1-3]. Typically, in the final steps of sample preparation, precipitates are either vacuum filtrated or electrodeposited onto planchets. The filter paper or planchet is then mounted onto a sample holder and positioned near the detector for counting. When preparing replicate samples of the same fission product isotope after irradiation, the initial samples will have the same specific activity. However, due to

---

<sup>5</sup> Graduate Student and Assistant Professor, respectively, Department of Chemistry and Geochemistry, Colorado School of Mines, 1500 Illinois Street, Golden, CO 80401

<sup>6</sup> Los Alamos National Laboratory, Los Alamos, NM 87545

<sup>7</sup> Author for correspondence

slight differences in chemistry and losses in preparation, the final samples will vary in thickness.

The molecule containing the radioactive isotope or the matrix into which it is precipitated can absorb a part of the beta radiation. This effect is known as self-absorption. A correction for the variation in self-absorption due to the sample thickness of the emitted beta radiation must be applied to accurately determine the activity of the sample. In most beta emitters, the self-absorption is significant even in thin layers due to the inactive matrix [4].

The total intensity of the radiation reaching the surface of the sample is given by [4,5]

$$I = \frac{I_0}{\mu} (1 - e^{-\mu x}) \quad (4.1)$$

where  $I$  is the intensity,  $I_0$  is the surface density intensity,  $\mu$  is the mass attenuation coefficient, and  $x$  is the areal thickness. Several authors have given the empirical formulae for the mass attenuation coefficients or have calculated the mass attenuation coefficients through various theories [6-9]. These formulas are approximations since the absorption depends on the distribution of the beta energy [10] as well as the geometry of the detector [7]. In the literature, many reported values exist for mass attenuation coefficient of metal absorbers (e.g. Al, Pb, Cu, and Zn), but few exist for organic compounds or oxides [11]. Therefore it is necessary to prepare samples of varying thickness to determine the mass attenuation coefficient for a given detection system and fit the values to Equation 4.1.

This method works well for activation products such as  $^{99}\text{Mo}$ , which can be easily produced by thermal neutrons in a reactor by the activation of  $^{98}\text{Mo}$  (i.e.  $^{98}\text{Mo}(n,\gamma)^{99}\text{Mo}$ ). The viability of  $^{99}\text{Mo}$  production is driven by the high natural abundance and large thermal cross section of  $^{98}\text{Mo}$ . This technique has been used to estimate efficiency curves for gas proportional counters [12]. Other fission products, such as  $^{97}\text{Zr}$ , are not easily activated in a thermal reactor without isotopic enrichment [13]. Difficulties associated with sufficient production of fission product isotopes in research reactors limits the ability to complete a direct, experimental assessment of mass attenuation coefficients for these isotopes.

To overcome these limitations, this study assesses the mass attenuation coefficients of fission product isotopes that can be readily produced by the thermal neutron activation of elements in a reactor. These results are then compared to simulated values calculated from a multipurpose

Monte Carlo program, EGS5. EGS5 is then used to calculate the mass attenuation coefficients of additional fission product isotopes not readily produced by thermal neutron activation.

## **4.2 Experimental**

The following section will describe the equipment used in this experiment. This includes a gas proportional counting system, source preparation, determination of the gas proportional counter efficiency for various beta emitting particles and, a High Purity Germanium (HPGe) detector,

### **4.2.1 Gas Proportional Counting System**

The detector and lead housing were supplied by Los Alamos National Laboratory (LANL). The body of the gas proportional detector is machined from a solid piece of 6061 aluminum tubing. One end is fitted with a four-hole flange HN female connector with solder cup terminal. Two 1.6 mm (1/16 inch) posts are soldered to the terminal. The collecting electrode loop is 0.05 mm (0.002 inch) diameter stainless steel wire soldered to the posts. The opposite end of the body is counter sunk and covered with a 0.01 cm thick DURAL window held in place by a metal ring. The window diameter is 25 mm. The body of the detector is held in alignment to the slide holder by two 3.18 mm (1/8 inch) steel dowels in each end. The slide holder accommodates 1.6 mm (1/16 inch) thick 6061 aluminum plates measuring 6.35 x 8.26 cm (2.5 x 3.25 inches). The detector is housed inside a 6.35 cm (2.5 inch) thick lead cave which removes nearly all detectable background radiation. A diagram of the gas proportional detector is shown in Figure 4.1. An Ortec 571 amplifier supplies power to an Ortec 109PC preamplifier. Detector bias is supplied by and Ortec 456 high voltage power supply. Tail pulses from the preamplifier are directly routed into an Ortec 406A single channel analyzer with a lower level discriminator (LLD) of 0.02V. Logic pulses are counted by an Ortec 919 ADCAM Multichannel buffer which is connected to computer by an ORTEC Dual-Port Memory to USB Converter. The beta plateau varies 2% over 1800-2000V and operating voltage was determined to be 1900 V. P-10 was used at atmospheric pressure with a flow rate of 50 cc/min CO<sub>2</sub>.

### **4.2.2 Source Preparation**

Standardized solutions were prepared and subsequently irradiated in the Geological Survey TRIGA Reactor (GSTR), a 1 MW low-enriched uranium-fueled, pool-type reactor located at the Denver Federal Center in Lakewood, CO [14]. These solutions were then divided to provide

samples of 5, 10, 15, 20, and 25 mg of the element of interest and precipitated. Precipitates were vacuum filtrated onto 24mm, Grade 42, ashless quantitative filter paper from GE Healthcare. The filtration chimney was made from polyether ether ketone (PEEK) with an inside diameter of 19 mm. Precipitate thickness was measured with a micrometer. Calculated average precipitate densities are shown in Table 4.1. The filter paper with precipitate was mounted on a 1.6 mm thick (14 gauge) 6061 aluminum plate with double sided scotch tape and covered with 3.5  $\mu\text{m}$  thick Mylar film. The density of the filter and double sided tape was averaged from replicate measurement of the thickness and mass.

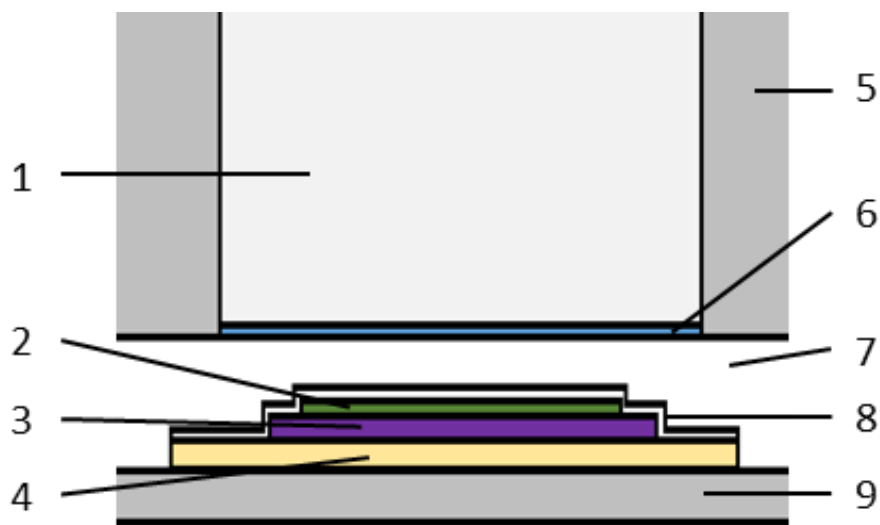


Figure 4.1. Experimental Setup and Monte Carlo Simulation: 1. P-10 gas, 2. Precipitate or electroplated metal, 3. Filter Paper or Stainless Steel planchette, 4. Double-sided Tape, 5. Aluminum, 6. DURAL window, 7. Air, 8. Mylar cover, 9. Aluminum plate.

Silver and cadmium were electroplated onto stainless steel planchettes. Disposable electrodeposition cells were constructed from 20  $\text{cm}^3$  polyethylene liquid scintillation vials similar to other publications [15,16]. The inside diameter of the vials at the neck was 15.4 mm. The anodes were platinum wire loops and the cathodes were 26 gauge type 304 stainless steel planchets laser cut to 3/4 inch diameter.

Table 4.1. Average measured density of precipitates used in this study.

Isotope	Chemical Compound	Compound Density [g/cm <sup>3</sup> ]	Average Measured precipitate Density [g/cm <sup>3</sup> ]
Ag-110, Ag-111	Ag	10.49	-
Cd-115	Cd	8.75	-
Zr-95, Zr-97	ZrO <sub>2</sub>	5.68	0.45 ± 0.07
Cs-134, Cs-136, Cs-137	Cs <sub>2</sub> PtCl <sub>6</sub>	4.19	0.80 ± 0.08
Pd-109, Pd-112	Pd(C <sub>4</sub> H <sub>7</sub> N <sub>2</sub> O <sub>2</sub> ) <sub>2</sub>	1.61	0.18 ± 0.02
Mo-99	MoO <sub>3</sub>	4.69	0.61 ± 0.08
K-42	KClO <sub>4</sub>	2.52	0.78 ± 0.02
Nd-147	Nd <sub>2</sub> O <sub>3</sub>	7.24	0.70 ± 0.09
Sm-143	Sm <sub>2</sub> O <sub>3</sub>	8.35	0.73 ± 0.09

#### 4.2.3 Gas Proportional Counter Efficiency

After irradiation, and counting on the gas proportional counter, the induced gamma activities emitted from the samples were counted on a Canberra reverse electrode closed ended coaxial high purity germanium (HPGe) detector (model number GR1320) coupled with an EG&G Ortec ADC Spectrum Master 92X multichannel analyzer. A certified NIST traceable Spectrum Techniques <sup>152</sup>Eu source with an uncertainty of ±5%, and a NIST traceable Eckert & Ziegler mixed gamma source was used to determine the efficiency at various distances from the HPGe detector. The total activity of the sample was subsequently calculated and the efficiency of the gas proportional counter determined.

#### 4.2.4 EGS5 Monte Carlo Simulation

The Electron Gamma Shower (EGS) code is a general purpose Monte Carlo program for the simulation of electron and photon transport [17]. The current version written in FORTRAN is EGS5. Arbitrary geometries can be created and verified with the particle trajectory and geometry display program, CGView [18]. Energy deposited in the P-10 gas is tallied and counted to determine the efficiency of the simulation. Beta spectrum are derived from International Commission on Radiological Protection Publication (ICRP) 107 [19]. The BinBeta module, written by KF Eckerman from the Radiological Toolbox software developed by Oak Ridge National Laboratory (ORNL) for U. S. Nuclear Regulatory Commission (NRC) was used to produce a beta spectrum Monte Carlo input file for EGS5 with 50 energy bins [20]. In the EGS5

simulation, the composition of the precipitates was calculated by determining the fraction of air within each precipitate using equations 4.2 and 4.3.

$$x_{ppt} = \frac{\rho_{measured} - \rho_{air}}{\rho_{ppt} - \rho_{air}}, \quad (4.2)$$

$$x_{ppt} + x_{air} = 1, \quad (4.3)$$

where  $x_{ppt}$  is the volume fraction of the precipitate,  $x_{air}$  is the volume fraction of air,  $\rho_{measured}$  is the average measured precipitate density in Table 4.1,  $\rho_{air}$  is the density of air in Lakewood, Colorado which is taken to be  $0.96 \times 10^{-3} \text{ g/cm}^3$ ,  $\rho_{ppt}$  is the density of the compound. Since electronic noise is present in the counting system, a lower level discriminator (LLD) is applied to filter out the noise. Pulses from the preamplifier due to the energy deposition of charged particles in the detector volume that are below 0.02V are not counted. To simulate this effect in EGS5, deposited energy in the sensitive area of the detector below 5.1 keV is not counted. This cut off was determined from minimizing the root mean square error of the calculated and measured efficiencies. All simulations were run on a Pentium based laptop running Cygwin with  $10^6$  particles.

#### 4.2.5 Empirical Mass Attenuation Formula

The mass attenuation coefficient of an element is related to the end-point energy of the beta spectrum as in

$$\mu = C_1 E_m^{-C_2} \quad (4.4)$$

where  $C_1$  and  $C_2$  are constants. For a wide range of materials, Thümmel consolidated absorption curves over a wide range of maximum beta energies and proposed the following formula [21]

$$\mu = 15.2 Z^{\frac{4}{3}} \frac{1}{A E_m^{1.485}}, \quad (\text{cm}^2/\text{g}) \quad (4.5)$$

where  $Z$  is the atomic number,  $A$  is the atomic weight, and  $E_m$  is the maximum end point energy of beta particles in MeV. This formula is used to validate both the experimental values and the EGS5 simulated values. The mass attenuation coefficient for any chemical compound or mixture of elements is given by Bragg's Additivity rule

$$\mu_{compound} = \sum w_i \mu_i \quad (4.6)$$

where  $w_i$  and  $\mu_i$  are the weight fraction and mass attenuation coefficient of the  $i^{\text{th}}$  constituent element, respectively. For a chemical compound, the fraction by weight is given by

$$w_i = \frac{A_i a_i}{\sum_j A_j a_j} \quad (4.7)$$

where  $A_i$  is the atomic weight of the  $i^{\text{th}}$  element and  $a_i$  is the number of formula units.

### 4.3 Results

The following section will describe the results of this experiment. This section is divided into two sub-sections which include the gas proportional counter resolution and determination of mass attenuation coefficients.

#### 4.3.1 Detector Resolution

To determine detector resolution losses at high count rates, a  $\text{KClO}_4$  sample containing approximately 10  $\mu\text{Ci}$  of  $^{42}\text{K}$  was prepared. This sample was counted every five minutes for approximately ten half-lives. The decay of  $^{42}\text{K}$  was followed until the activity reached a level at which the half-life of 13.4 hours was observed and the resolution losses were negligible [22]. This occurred after approximately 2.5 days. The deviation of the initial portion of the decay curve at high count rates to that of the expected count rate is given by Equation 4.8 [23]

$$R = \frac{N}{1 + \tau N}, \quad (4.8)$$

where  $R$  is the recorded count rate,  $N$  is the true count rate, and  $\tau$  is the resolving time. This yields a resolving time of  $168.1 \pm 0.5 \mu\text{sec}$  when the recorded rate and true count rate were fitted to Equation 4.8. The measured count rates of all samples is shown vs the EGS5 simulated count rate in Figure 4.2. This yields a resolving time of  $181.6 \pm 0.6 \mu\text{sec}$ .

#### 4.3.2 Mass Attenuation Coefficients

Experimental data was fitted to Equation 4.1 using least square analysis to determine mass attenuation coefficients. EGS5 simulations determined the detector efficiency at various sample thicknesses. Count rates were then calculated assuming a specific activity for all samples. Equation 5 was used in conjunction with Equations 4.6 and 4.7 to determine the empirical mass

attenuation of the compound. Table 4.2 provides a consolidated list mass attenuation coefficients for these measurements and calculations.

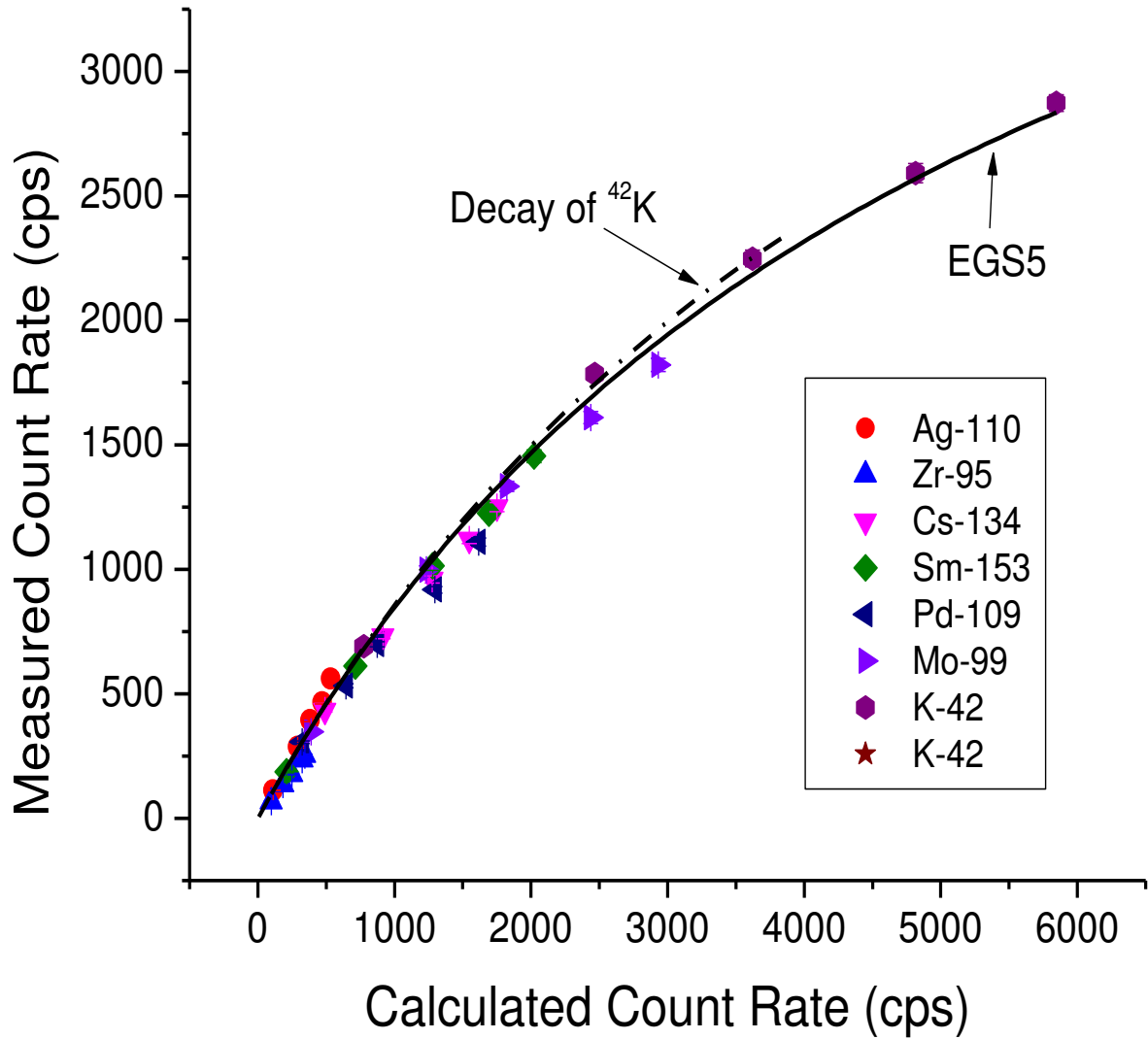


Figure 4.2. Comparison of EGS5 calculated detector resolution vs measured detector resolution from the decay of  $^{42}\text{K}$ .

Table 4.2. Experimental, calculated, and theoretical values of mass attenuation coefficients.

Isotope	End Point Beta Energy [keV]	Average Beta Energy [keV]	Beta Intensity	Mass Attenuation Coefficient $\mu/\rho$ [cm <sup>2</sup> /g]		
				Measured	EGS5	Empirical Formula [21]
Ag-110	530.6	66.8	100.40%	76 ± 4	80 ± 2	60.1
Ag-111	1036.8	350	100.00%		34 ± 1	22.0
Zr-95	1123.6	117	100.00%	70 ± 6	76 ± 2	78.7
Zr-97	1915.7	704	100.10%		8 ± 1	7.5
Cs-134	658.1	157.2	100.01%	45 ± 4	40 ± 2	42.0
Cs-136	681.6	118	101.00%		77 ± 1	39.7
Cs-137	1175.63	187.1	100.00%		42 ± 1	17.7
Sm-153	807.6	224	100.00%	36 ± 6	36 ± 1	32.1
Pd-109	1027.9	360.8	100.01%	28 ± 2	26 ± 1	16.5
Pd-112	244	77	100.00%		46 ± 1	137.7
Mo-99	1214.3	389	100.10%	22 ± 5	25 ± 2	15.0
K-42	3525.4	1430.5	100.00%	5 ± 4	1.7 ± 0.8	2.7
Nd-147	896	232	99.90%		35 ± 2	31.7
Cd-115	1629.7	604.5	99.98%		17. ± 0.5	11.2

Figure 4.3 is a plot of the EGS5 calculated efficiencies of various fission product nuclides verses areal thicknesses. In general, the detector efficiency increases with increase in average beta energy from <sup>112</sup>Pd, <sup>136</sup>Cs, <sup>137</sup>Cs, <sup>147</sup>Nd, and <sup>97</sup>Zr. Since cadmium and silver are electroplated in thin deposits on planchettes rather than precipitated and vacuum filtrated, the efficiency of those two elements is greater.

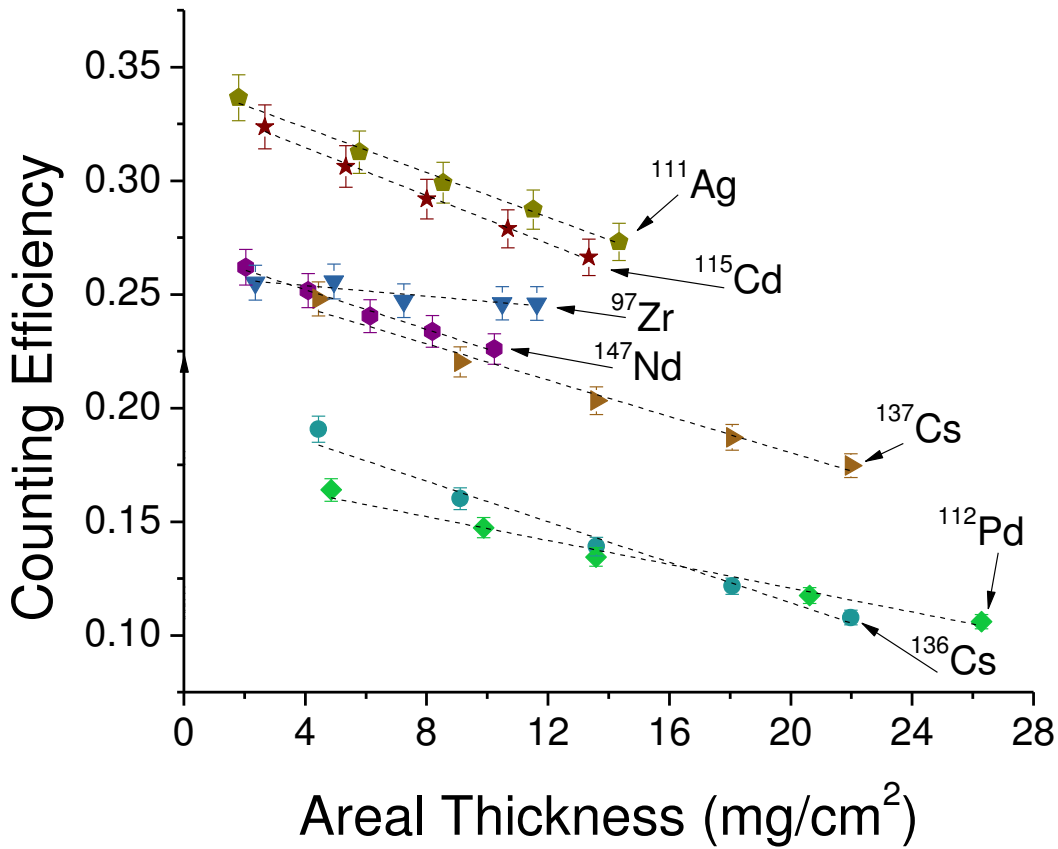


Figure 4.3. EGS5 calculated efficiencies of fission product nuclides over various areal thicknesses.

#### 4.4 Discussion

The following section is a discussion of the results in this experiment. This section is divided into two sub-sections which include the gas proportional counter resolution and determination of mass attenuation coefficients.

##### 4.4.1 Detector Resolution

The EGS5 calculated resolving time is slightly greater than the measured resolving time. This is an important deviation at very high count rates, however with count rates less than 650 cps the difference is less than 1%. Additionally, the effect on calculated mass attenuation coefficients is less than 1.5% at the count rates in this experiment. Therefore the measured resolving time was used for efficiency and mass attenuation calculations.

#### 4.4.2 Mass Attenuation Coefficients

The measured mass attenuation coefficients agree well with the EGS5 calculated results. Both results are slightly higher than the theoretical value which is likely due to the geometry of the sample holder and detector. The  $^{112}\text{Pd}$ , however, has a much lower EGS5 calculated mass attenuation coefficient in this counting system. This may be due to the contribution from two effects. First, the low density of the measured  $\text{Pd}(\text{C}_4\text{H}_7\text{N}_2\text{O}_2)_2$  precipitate allows for a greater range of beta particles within the precipitate. Additionally, the cut-off energy or the minimum beta energy needed to produce a count in the detector is approximately 100 keV [12]. While this reduces the efficiency, this effect also increases the average beta energy from  $^{112}\text{Pd}$  that reaches the sensitive area of the detector. The  $^{137}\text{Cs}$  mass attenuation coefficient from Equation 4.5 is more than half of the EGS5 result. Since the shape of the  $^{137}\text{Cs}$  beta spectrum has a large tail at high energies, the maximum beta energy is 1175.63 keV while the average beta energy is 187.1 keV, Equation 4.5 does not accurately represent the mass attenuation of  $^{137}\text{Cs}$ . The EGS5 calculated results for  $^{137}\text{Cs}$  however agree with other results: 28.4-51.8 [7], 31.0+-0.5 [24], 36.4+-1.7 [11], and 27.33 [25].

There are essentially two methods to determine the mass attenuation coefficient of beta particles: transmission experiments and experiments with constant specific activity as discussed in this paper. In transmission experiments with an incident beam of beta particles, an absorber is placed between the source and detector. The beta particles are attenuated through the absorber in a relationship that is closely represented by Beer's law and the mass attenuation for the absorber is determined. This relationship is only an approximation since beta particles interact with matter differently than electromagnetic waves, have a continuous energy spectrum, and the scattering and backscattering of beta particles changes the energy spectrum and its angular distribution [5]. Nevertheless, resulting empirical relationship for the mass attenuation is given in the form of Equation 4.4 and are accurate for a given experimental setup and compounds. Additionally, the results of experiments using external absorbers to determine the mass attenuation coefficients in compounds have been demonstrated to be different than the mass attenuation coefficients determined by preparing a number of weighted standards of the same specific activity [11]. This effect is more noticeable with beta spectrum of lower average energy [11]. Therefore for isotopes

that emit beta spectrum of low average energy, it is more accurate to prepare various weighted standards or alternately determine the mass attenuation coefficient through a Monte Carlo code.

#### **4.5 Conclusions**

The mass attenuation coefficients of neutron activated isotopes were compared to a Monte Carlo simulation for a wide range of compounds. These coefficients agreed with each other but varied from a calculation based on empirical data. While it is important to directly measure the detector efficiency and mass attenuation curves for a given detector configuration, this manuscript shows that a Monte Carlo simulation can be used to calculate mass attenuation coefficients of isotopes that are not easily produced through activation of thermal neutrons.

#### **4.6 Acknowledgements**

The authors would like to express their sincere thanks to the reactor staff of the GSTR for their support, funding from the Colorado School of Mines, and the NRC Faculty Development Grant program, Grant Number NRC-HQ-11-G-38-0062.

#### **4.7 References Cited**

- 1 J. Kleinberg, Collected radiochemical and geochemical procedures - LA-1721-5th-Ed. Los Alamos National Lab., NM (USA); Sponsoring Organization: DOE/DP, 1990.
- 2 M. Lindner, Radiochemical Purification Procedures for the Elements - UCRL-14258. Lawrence Radiation Lab., Univ. of California, Livermore; Sponsoring Organization: USDOE, 1965.
- 3 E.K. Hyde, Radiochemical Methods for the Isolation of Element 87 (Francium) - UCRL-1578. Radiation Lab., Univ. of Calif., 1951.
- 4 J. Konya, J.z. Kónya, Nuclear and Radiochemistry, Burlington: Elsevier Science, Burlington London; Waltham, MA, 2012.
- 5 P. Massini, Science (New York, N.Y.) 133 (1961) 877.
- 6 R.D. Evans, The atomic nucleus, New York: McGraw-Hill, New York, 1955.
- 7 T. Baltakments, Nuclear Instruments and Methods 82 (1970) 264.
- 8 R. Burek, D. Chocyk, Journal of Radioanalytical and Nuclear Chemistry, Articles 209 (1996) 171.
- 9 O. Gürler, S. Yalçın, Annals of Nuclear Energy 32 (2005) 1918.
- 10 C.Y. Yi, H.S. Han, J.S. Jun, H.S. Chai, Applied Radiation and Isotopes 51 (1999) 217.

- 11 L. Pujol, J.A. Suarez-Navarro, *Applied Radiation and Isotopes* 60 (2004) 693.
- 12 B.P. Bayhurst, R.J. Prestwood, *Nucleonics* 17 (1959) 82.
- 13 C.P. Keim, *Electromagnetic Separation of Stable Isotopes*, *Annu. Rev. Nucl. Sci.*, 1952, p. 263.
- 14 M. Koehl, R. Rundberg, J. Braley, *J Radioanal Nucl Chem* 306 (2015) 31.
- 15 M.H. Lee, C.W. Lee, *Nucl. Instrum. Methods Phys. Res. Sect. A-Accel. Spectrom. Dect. Assoc. Equ* 447 (2000) 593.
- 16 N.A. Talvitie, *Anal. Chem.* 44: No. 2 (1972).
- 17 N.Y. Hirayama H, Bielajew AF, Wilderman SJ, Nelson WR, *STAR* 44 (2006).
- 18 A. Takamura, T. Sugita, Y. Namito, H. Hirayama, *EGS Particle Trajectory and Geometry Display Program in H.H. Namito Y, Ban S (Ed.), Proceedings of the Third International Workshop on EGS, Tsukuba Japan, 2004*, p. 208.
- 19 K.F. Eckerman, A. Endo, *Annals of the ICRP* 38 (2008) 7.
- 20 K.F. Eckerman, A.L. Sjoreen, *Radiological Toolbox User's Guide - NUREG/CR-7166, ORNL/TM-2013/16, Sponsoring Organization: USNRC, 2013.*
- 21 H.W. Thümmel, *Durchgang von Elektronen- und Betastrahlung durch Materieschichten: Streuabsorptionsmodelle*, Akademie-Verlag, 1974.
- 22 E.P. Steinberg, *Counting methods for the assay of radioactive samples*, Argonne, Ill.: Argonne National Laboratory, 1961.
- 23 T.P. Kohman, *Analyt. Chem.* 21 (1949).
- 24 T. Baltakmens, *Nuclear Instruments and Methods* 142 (1977) 535.
- 25 A. Švec, *Applied Radiation and Isotopes* 102 (2015) 63.

## CHAPTER 5

### RELATIVE FISSION PRODUCT YIELDS IN THE USGS TRIGA MARK I REACTOR

A paper to be submitted to Physics Letters B

M.A. Koehl<sup>8</sup>, R.S. Rundberg<sup>9</sup>, J.C. Braley<sup>2,10</sup>

Relative fission product yields have been determined for three sampling positions in the USGS TRIGA Mark I reactor through radiochemical analysis. The relative mass yield distribution for valley nuclides decreases with epithermal neutrons compared to thermal neutrons. Additionally, a proportionality constant which related the measured beta activity of a fission product to the number of fissions that occur in a sample of irradiated uranium was determined for the detector used in this study and used to determine the thermal and epithermal flux. These values agree well with a previous study which used activation foils to determine the flux.

#### 5.1 Introduction

Fission product yield data sets are one of the most important and fundamental compilations of basic information in the nuclear industry. Fission yield data are crucial to the measurement of nuclear fuel burnup, nonproliferation safeguards, reactor design and operation, nuclear physics calculations, decay heat studies, shielding calculations, fuel handling and reprocessing, neutron dosimetry and flux measurements, and environmental studies [1-4]. To characterize fission yields, it is often necessary to determine the number of fissions which occurred in the course of irradiation.

The end of irradiation counting rate ( $A$ ) of a fission product ( $j$ ) of a fissioning isotope ( $f$ ) in a given neutron environment ( $e$ ) for radiochemical studies of precipitates with a carrier solution is given by [5]:

$$A_j^{f,e} = \varepsilon_j \lambda_j Y_j^{f,e} F = \frac{C_j^{f,e}}{D D_I C_Y P} \quad (1)$$

where:  $A$  is the counting rate of nuclide  $j$  in a standardized geometry after irradiation;  $\varepsilon$  is the detector efficiency;  $\lambda$  is the decay constant;  $Y$  is the independent fission yield;  $F$  is the number of

---

<sup>8</sup> Graduate Student and Assistant Professor, respectively, Department of Chemistry and Geochemistry, Colorado School of Mines, 1500 Illinois Street, Golden, CO 80401

<sup>9</sup> Los Alamos National Laboratory, Los Alamos, NM 87545

<sup>10</sup> Author for correspondence

fissions;  $C$  is the measured count rate of the sample normalized to an arbitrary thickness;  $D$  is the correction for decay from the end of irradiation,  $D = 1 - e^{-\lambda_j t_d}$ ;  $t_d$  is the decay time;  $D_I$  is the correction for decay during irradiation,  $D_I = \frac{1 - e^{-\lambda_j t_i}}{\lambda_j t_i}$ ,  $t_i$  is the irradiation time;  $C_Y$  is the correction for chemical yield, and  $P$  is the percent of irradiated fuel. Defining the quantity  $K$  as the inverse product of the efficiency, decay constant and yield gives the following, after rearranging:

$$K_j^{f,e} = \frac{F}{A_j^{f,e}} \quad (2)$$

Thus, the  $K$ -factor is essentially a proportionally constant between the measured saturated counting rate of a reference nuclide to the number of fissions in a sample. Historically, the  $K$ -factor was obtained from the counting rate of  $^{99}\text{Mo}$ , but  $K$ -value assessments need not be specifically referenced to  $^{99}\text{Mo}$  and can be used with other fission products [6]. A specific  $K$ -factor is limited to the detector in which the measurements are made, however the introduction of a mathematical framework based on ratios ( $Q$ -value and  $R$ -value) enables useful data that is detector independent and usable across laboratories [7].  $Q$ -values are ratios of  $K$ -factors and are given in literature [8].

$R$ -values, or relative fission yields, are yields which have been measured relative to some other nuclide or normalized to some value. The basic premise in relative measurements is to reduce the number of absolute measurements - normally to one or possibly a handful. Once the absolute yield of one fission product is accurately known, other absolute yields can be calculated relative to the singular fission product yield.  $R$ -values are defined as a double ratio of fission product count rates [5]:

$$R_j^{f,e} = \frac{A_j^{f,e} / A_{99}^{f,e}}{A_j^* / A_{99}^*} = \frac{Y_j^{f,e} / Y_{99}^{f,e}}{Y_j^* / Y_{99}^*} = \frac{r_j^{f,e}}{r_j^*} \quad (3)$$

where:  $r_j^{f,e}$  is the ratio of measured counting rates of nuclide  $j$  to  $^{99}\text{Mo}$  under the experimental conditions and  $r_j^*$  is the ratio of measured counting rates of nuclide  $j$  to  $^{99}\text{Mo}$  from the thermal irradiation of  $^{235}\text{U}$ .

Three well characterized fission product yields are from a spectrum of thermal neutrons with a mean energy of 0.025 eV, a fast fission neutron spectrum with a mean energy of 2.1 MeV, and monoenergetic 14.1 MeV neutrons from the fusion of deuterium and tritium (i.e.  $D(T,n)^4He$ ) reaction. Figure 1 shows (a) calculated R-values from ENDF-B/VII cumulative fission yields for

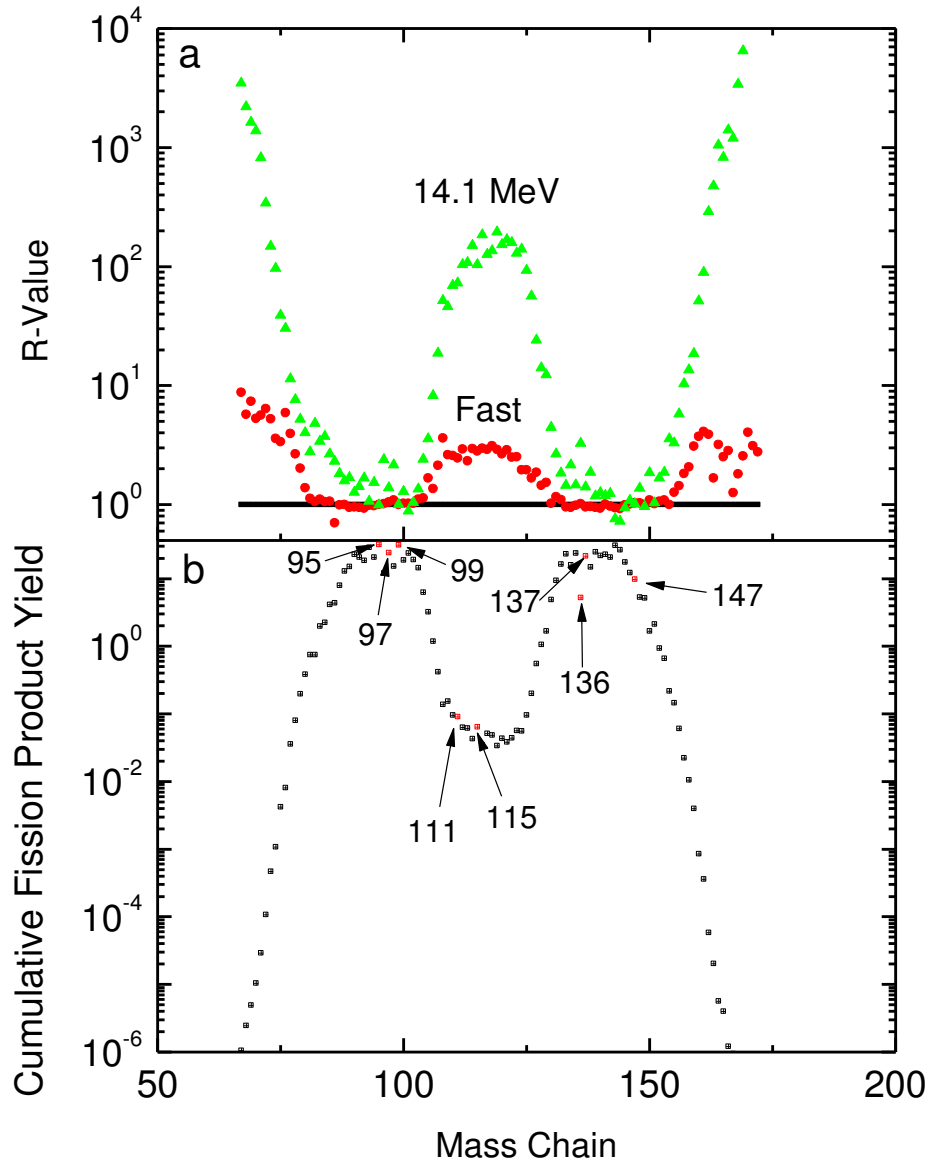


Figure 5.1. (a) Calculated R-values from ENDF-B/VII cumulative fission yields for  $^{235}U$  and (b) the asymmetric mass distribution yields from fission of  $^{235}U$  by thermal neutrons.

$^{235}\text{U}$  and (b) the asymmetric mass distribution yields from fission of  $^{235}\text{U}$  by thermal neutrons. By definition, thermal R-values for  $^{235}\text{U}$  are unity. Highlighted on 1b are the 95, 97, and 99 mass chains representing the light fission fragment; 111 and 115 mass chains representing the valley nuclides; and 136, 137, and 147 mass chains representing the heavy fission fragment. From the three neutron environments, it can be seen that the R-values for neutrons in the valley of the mass distribution curve are extremely sensitive to the neutron environment varying from unity for thermal neutrons to nearly 200 for high energy neutrons.

These R-values have been reported for reactors of various designs but have not been reported in a TRIGA reactor [9]. An aliquot of solution prepared from an irradiated enriched uranium foil was provided by LANL for the K-factor determination. This K-factor was then used to calculate the number of fissions in irradiated samples and thermal or epithermal flux in three sampling positions within the USGS TRIGA Mark I reactor. The cadmium ratio of these sampling positions varied from 2.0 in the Central Thimble to 6.7 in the Dry Tube. Additional separated fission products from each irradiation are used to construct R-values for those sampling positions.

## **5.2 Experimental**

The following section will describe the equipment used in this experiment. This section contains general laboratory practices, the High Performance Liquid Chromatography (HPLC) system used for lanthanide separations, the electroplating set-up, the gas proportional counting system, and preparation of the uranium targets for irradiation in the GSTR.

### **5.2.1 General Laboratory practices**

Ultra-clean laboratory practices were utilized in all steps of this work. All glassware was allowed to soak for a minimum of 1 day each in three successive baths containing Radiac wash, 20% nitric acid, and 18M $\Omega$  deionized water and rinsed with 18M $\Omega$  water before use. All separations were conducted in quadrature. Standardized chemicals of approximately 10 mg/mL were prepared and confirmed through gravimetric analysis. Chemical standardization procedures for prepared solutions were compared against solutions from Inorganic Ventures to determine bias. Table 1 contains the concentrations of the carrier solutions used in this study.

A 10 mL aliquot of irradiated  $^{235}\text{U}$  was provided by LANL for determination of the K-factor for the detector used in this study. LANL analysis determined the mother solution to contain

1.14 x 10<sup>14</sup> fissions. Separation of <sup>99</sup>Mo using the carrier method described below was performed on this sample to determine the K-factor.

Table 5.1. Carrier Standardization.

Element	Standardized Solution	Weighed Form	Concentration [mg/mL]	Precision	Bias
Pd	PdCl <sub>2</sub> in H <sub>2</sub> O	Pd(C <sub>4</sub> H <sub>7</sub> N <sub>2</sub> O <sub>2</sub> ) <sub>2</sub>	9.77	0.15%	0.28%
Ag	AgNO <sub>3</sub>	AgCl	10.93	0.38%	0.59%
Cd	Cd(NO <sub>3</sub> ) <sub>2</sub> • 4H <sub>2</sub> O in H <sub>2</sub> O	CdNH <sub>4</sub> PO <sub>4</sub> • H <sub>2</sub> O	10.28	0.27%	1.11%
Cs	CsCl in H <sub>2</sub> O	Cs <sub>2</sub> PtCl <sub>6</sub>	10.24	0.53%	0.55%
Zr	ZrO(NO <sub>3</sub> ) <sub>2</sub> • 2H <sub>2</sub> O in H <sub>2</sub> O	ZrO <sub>2</sub>	10.18	0.16%	1.01%
Mo	(NH <sub>4</sub> ) <sub>6</sub> Mo <sub>7</sub> O <sub>24</sub> • 4H <sub>2</sub> O in H <sub>2</sub> O	MoO <sub>3</sub>	10.11	0.25%	0.92%
Nd	Nd <sub>2</sub> O <sub>3</sub> in 5% HNO <sub>3</sub>	NdO <sub>3</sub>	10.81	0.31%	0.72%
Sm	Sm <sub>2</sub> O <sub>3</sub> in 5% HNO <sub>3</sub>	SmO <sub>3</sub>	10.30	0.56%	0.08%

Chemical separation methods are derived from various compilations of radiochemical methods. They include national laboratory reports including LA-1721, 5th edition; UCRL-14258; UCRL-1578; and others [10-14]. Generally speaking, an aliquot of irradiated uranium is added to 20 mg of a carrier element in solution. Initial separations involve a purification of the fission products from the bulk uranium. Intermediate separation steps focus on separating fission products from each other. The final step in all chemical separation methods is electrodeposition or a vacuum filtration of precipitates within standardized filtration apparatus onto pre-weighed filter paper to prepare samples for beta counting. Vacuum filtration chimneys were manufactured from PEEK plastic with an inside diameter of 19.05 mm (3/4 inch) to standardize beta counting configurations and ensure systematic errors were ratioed in R-value determination,. The chemical separation methods are briefly described below.

*Cadmium:* Decontamination steps include scavenging with cadmium sulfide (CdS), acid sulfide, and iron hydroxide (Fe(OH)<sub>3</sub>). The cadmium, in 3M HCl, is then placed on an anion

exchange resin (Dowex AG 1-X8) and eluted with 1.5M H<sub>2</sub>SO<sub>4</sub>. Finally, the cadmium is converted to the elemental form by electroplating [15,16].

*Cesium:* Separation begins with a ferric hydroxide scavenge and a precipitation as the silicotungstate. This step gives a decontamination factor of 100 to 200, and is a specific separation of cesium from ammonium, iron, rubidium, and the other alkali metals which may interfere in the determination of cesium as the chloroplatinate. The silicotungstate is dissolved in alkali and is filtered as the chloroplatinate,

*Silver:* Silver is initially separated from other fission products by the specific precipitation of the chloride from nitric acid solution. The silver is then purified by ferric hydroxide scavenging and silver sulfide precipitation, both of which are performed in ammoniacal solution. After repetition of the scavenging-precipitation cycle, the silver is converted to the oxide and finally electroplated.

*Zirconium:* Exchange between carrier and <sup>95</sup>Zr and <sup>97</sup>Zr is affected? by formation of the fluorozirconate complex [ZrF<sub>6</sub>]<sup>2-</sup>. Lanthanide and alkaline-earth activities are removed by lanthanum fluoride scavenging, and zirconium is separated by three barium fluorozirconate Ba[ZrF<sub>6</sub>] precipitations. Zr is recovered from Nd on an anion exchange resin column. Neodymium is adsorbed on the column, which is washed twice. Zirconium is precipitated as the hydroxide (Zr(OH)<sub>4</sub>) and dissolved in HCl. Zirconium is finally precipitated with mandelic acid from hydrochloric acid medium and ignited to the oxide, ZrO<sub>2</sub>.

*Molybdenum:* The separation of molybdenum from fission products is based primarily on its behavior in the +6 oxidation state on an anion exchange resin. Molybdenum (VI) is adsorbed on the resin from hydrochloric acid solutions of concentrations 5M to 9M. Resin washes with a mixture of dilute hydrochloric and hydrofluoric acids and with 3M ammonium hydroxide remove most of the interfering ions. Molybdenum is eluted from the column with 6M ammonium acetate, precipitated with  $\alpha$ -benzoinoxime, and converted by ignition to MoO<sub>3</sub>.

*Lanthanides (Sm and Nd):* After the radiochemical purification of the lanthanides as a group, they are placed on a cation exchange resin containing Dowex AG 50W-X8 and then are gradient-eluted with  $\alpha$ -hydroxyisobutyric acid ( $\alpha$ -HIB) at pH 5.2 to 5.3 under a pressure of 125 to 175 psi as the mobile phase.

### 5.2.2 HPLC System

Lanthanide separations were completed using a Waters 2695 HPLC module externally connected to a 4 outlet manifold assembly. The flow rate for each outlet is controlled by a shut off valve and is maintained at 2.5 mL per minute. Four 6.6 mm by 25 cm liquid chromatography columns are connected in parallel downstream from the shut off valves. Dowex AG 50W-X8 resin, 350 wet mesh, stored in 6M HCl is used as a cation exchange resin. A 2500  $\mu$ L syringe and 2 mL coiled sample loop was used to inject 1 mL samples from a Waters clear glass 12 x 32mm screw neck total recovery vial.

The gradient elution approach was used with alpha-HIBA to separate lanthanides. In this approach, the pH is held constant at between 5.2 and 5.3 and the concentration of alpha-HIBA is increased linearly from 0.05 to 0.3 M. Effluents from the columns are collected in a fraction collector which changes tubes every minute.

### 5.2.3 Electroplating system

Disposable electrodeposition cells were constructed from 20 cm<sup>3</sup> polyethylene liquid scintillation vials similar to other publications [16]. The cathodes were 26 gauge type 304 stainless steel planchets laser cut to  $\frac{3}{4}$  inch diameter. The planchets were prepared by submerging in concentrated HCl overnight, rinsing with 18M $\Omega$  water and covering in 18M $\Omega$  water until ready for use in order to remove the oxidative layer on the stainless steel and activate the planchette. The anode was constructed of 18 gauge platinum wire wound 4 times in a loop. To assemble the cell, the bottom of the liquid scintillation vial was cut off and the planchet was centered on the threaded end of the liquid scintillation vial and wrapped once with Teflon tape. The Teflon tape ensured a liquid tight seal when the cap was applied. The cap is fitted with a  $\frac{1}{4}$  inch nutsert and rubber washer. The inverted vial is then placed in to a 1/4" shaft lock mounted on a plastic base. After the electrolyte is placed in the cell, the anode is inserted and parafilm is placed on the top of the assembly as a liquid barrier. Electrolysis was conducted with a PS-305D 30V/5A DC power supply. DC-DC digital control step down modules were used for fine control of amperage during electrolysis.

#### 5.2.4 Gas Proportional Counting System

The detector and lead housing were supplied by Los Alamos National Laboratory (LANL). The body of the gas proportional detector is machined from a solid piece of 6061 aluminum tubing. One end is fitted with a four-hole flange HN female connector with solder cup terminal. Two 1.6 mm (1/16 inch) posts are soldered to the terminal. The collecting electrode loop is 0.05 mm (0.002 inch) diameter stainless steel wire soldered to the posts. The opposite end of the body is counter sunk and covered with a 0.01 cm thick DURAL window held in place by a metal ring. The window diameter is 25 mm. The body of the detector is held in alignment to the slide holder by two 3.18 mm (1/8 inch) steel dowels in each end. The slide holder accommodates 1.6 mm (1/16 inch) thick 6061 aluminum plates measuring 6.35 x 8.26 cm (2.5 x 3.25 inches). The detector is housed inside a 6.35 cm (2.5 inch) thick lead cave which removes nearly all detectable background radiation. A diagram of the gas proportional detector is shown in Figure 1. An Ortec 571 amplifier supplies power to an Ortec 109PC preamplifier. Detector bias is supplied by an Ortec 456 high voltage power supply. Tail pulses from the preamplifier are directly routed into an Ortec 406A single channel analyzer with a lower level discriminator (LLD) of 0.02V. Logic pulses are counted by an Ortec 919 ADCAM Multichannel buffer which is connected to computer by an ORTEC Dual-Port Memory to USB Converter. The beta plateau varies 2% over 1800-2000V and operating voltage was determined to be 1900 V. P-10 was used at atmospheric pressure with a flow rate of 50 cc/min CO<sub>2</sub>.

Samples were counted multiple times over a period of two weeks. Samples were normalized to 20 mg of the carrier element through corrections of self-absorption constructed through Monte Carlo simulations. Decay corrections of complex decay curves were based on a least squares analysis of the decay curve. The counting rate and standard deviation at the end of the irradiation was averaged between quadruplicate replicates. While all impurities during this experiment were found from analysis of the decay curve, gamma spectroscopy was conducted on the samples as an additional check for impurities.

#### 5.2.5 Preparation of uranium targets

Uranium as UO<sub>2</sub>Cl<sub>2</sub> was obtained from Los Alamos National Laboratory with an enrichment in <sup>235</sup>U of 99.85%. The uranium was purified by dissolution in 20 mL of 8M hydrochloric acid and placing upon a 5 mL Dowex AG 1-X8 column [17]. The column was

washed with 20 mL of 8M HCl and uranium was eluted with 40 mL 1M HCl. The solution was then dried and placed in a furnace at 750 °C for 2 hours [18], converting it to U<sub>3</sub>O<sub>8</sub>. Irradiation targets were made by encapsulating a between 13 mg and 17 mg of the oxide in two layers of aluminum foil and subsequently vacuum sealing in a quartz vial. The quartz vials were placed in an aluminum tube and capped with a Swagelock Tube Fitting. Two samples were irradiated with a cadmium shield to filter out thermal neutrons below 0.5 eV. Table 2 contains the mass, irradiation times, and nuclear data for the targets. Targets were irradiated in the Central Thimble (CT), Lazy Susan (LS1), and Dry Tube (R1) sampling positions in the Geological Survey TRIGA Reactor (GSTR), a 1 MW low-enriched uranium-fueled, pool-type reactor located at the Denver Federal Center in Lakewood, CO [19].

Table 5.2. Characteristics of the U<sub>3</sub>O<sub>8</sub> irradiation targets and nuclear data.

Irradiation Position	Mass U <sub>3</sub> O <sub>8</sub> (mg)	Uranium mass fraction	Irradiation Time (min)	Cross Section (barns)
CT Irradiation Position (Epithermal Neutrons)	17.29	84.8%	60	276
LS Irradiation Position (Epithermal Neutrons)	13.26	84.8%	480	276
LS Irradiation Position (Thermal Neutrons)	13.13	84.8%	5	584.88
DT Irradiation Position (Thermal Neutrons)	13.45	84.8%	30	584.88

### 5.3 Results

The following section will describe the results of this experiment. The results of the determination of the number of fissions in each sample and the relative fission product yields are presented.

### 5.3.1 Determination of the number of fissions

The K-factor for the gas proportional counter calculated from Equation 2 was determined to be  $9.98 \pm 0.15 \times 10^5$  fissions/cpm for the LANL sample. This factor was used to determine the number of fissions in the irradiations in the GSTR. Table 3 lists the number of fissions for each sample. Since the number of fissions,  $F$ , is a product of the fission cross section for thermal or epithermal neutrons,  $\sigma_f$ , the corresponding thermal or epithermal neutron flux,  $\phi$ , the number of atoms, and the irradiation time,  $t_i$ , the flux can be determined from:

$$\phi = \frac{F}{\sigma_f} \frac{M}{mN_A t_i} \quad (4)$$

where  $m$  is the mass of the  $^{235}\text{U}$  in the target,  $N_A$  is Avogadro's constant, and  $M$  is the atomic mass of  $^{235}\text{U}$ . The calculated flux are shown in Table 3 and are compared to previously published values from activation foils.

Table 5.3. Calculated neutron flux based on K-factor method.

Irradiation Position	$^{99}\text{Mo}$ Activity [cpm/mg- $^{235}\text{U}$ ]	Calculated Number of Fissions	Calculated Flux (n/cm <sup>2</sup> s)	Previously Determined Flux [19] (n/cm <sup>2</sup> s)
CT Irradiation Position (Epithermal Flux)	$3.83 \pm 0.02 \times 10^7$	$3.82 \pm 0.06 \times 10^{13}$	$1.33 \pm 0.02 \times 10^{12}$	$1.35 \pm 0.07 \times 10^{12}$
LS Irradiation Position (Epithermal Flux)	$4.89 \pm 0.04 \times 10^7$	$4.88 \pm 0.07 \times 10^{13}$	$2.13 \pm 0.03 \times 10^{11}$	$1.99 \pm 0.09 \times 10^{11}$
LS Irradiation Position (Thermal Flux)	$2.50 \pm 0.02 \times 10^7$	$2.50 \pm 0.04 \times 10^{13}$	$3.79 \pm 0.06 \times 10^{12}$	$3.70 \pm 0.18 \times 10^{12}$
DT Irradiation Position (Thermal Flux)	$4.37 \pm 0.06 \times 10^7$	$4.36 \pm 0.06 \times 10^{13}$	$1.42 \pm 0.03 \times 10^{12}$	$1.45 \pm 0.07 \times 10^{12}$

Table 5.4. Relative fission product yields.

Fission Product	DT Irradiation	LS Irradiation Position – Bare		LS Irradiation Position - Cd		CT Irradiation Position – Cd	
	Position (Cd Ratio = 6.7±0.2)	(Cd Ratio = 2.3±0.1)		Covered (Cd Ratio = 2.3±0.1)		(Cd Ratio = 2.0±0.1)	
	r*-value	r-value	R-Value	r-value	R-Value	r-value	R-Value
<sup>95</sup> Zr	5.38±0.06 x 10 <sup>-2</sup>	5.68±0.13 x 10 <sup>-2</sup>	1.06±0.04	5.47±0.11 x 10 <sup>-2</sup>	1.02±0.02	5.66±0.10 x 10 <sup>-2</sup>	1.05±0.04
<sup>97</sup> Zr	2.28±0.06 x 10 <sup>1</sup>	2.22±0.04 x 10 <sup>1</sup>	0.97±0.03	2.29±0.05 x 10 <sup>1</sup>	1.01±0.03	2.28±0.06 x 10 <sup>1</sup>	1.00±0.04
<sup>115</sup> Cd	8.35±0.11 x 10 <sup>-3</sup>	8.11±0.11 x 10 <sup>-3</sup>	0.97±0.03	7.47±0.08 x 10 <sup>-3</sup>	0.89±0.01	7.34±0.05 x 10 <sup>-3</sup>	0.88±0.03
<sup>111</sup> Ag	3.07±0.05 x 10 <sup>-3</sup>	2.82±0.02 x 10 <sup>-3</sup>	0.92±0.03	2.57±0.04 x 10 <sup>-3</sup>	0.84±0.02	2.57±0.03 x 10 <sup>-3</sup>	0.84±0.03
<sup>136</sup> Cs	9.47±0.23 x 10 <sup>-6</sup>	-	-	9.33±0.21 x 10 <sup>-6</sup>	0.99±0.03	9.53±0.33 x 10 <sup>-6</sup>	1.01±0.05
<sup>137</sup> Cs	3.21±0.05 x 10 <sup>-4</sup>	3.08±0.09 x 10 <sup>-4</sup>	0.96±0.04	3.00±0.09 x 10 <sup>-4</sup>	0.98±0.03	3.28±0.13 x 10 <sup>-4</sup>	1.02±0.05
<sup>147</sup> Nd	3.15±0.09 x 10 <sup>-1</sup>	3.16±0.05 x 10 <sup>-1</sup>	1.00±0.03	3.15±0.09 x 10 <sup>-1</sup>	1.00±0.04	3.17±0.08 x 10 <sup>-1</sup>	1.01±0.04

### 5.3.2 Relative fission product yields

The ratio of measured counting rates of nuclides to the counting rate of  $^{99}\text{Mo}$  are given in Table 4. The neutron spectrum in the Dry Tube is the most thermalized spectrum in the GSTR and is used as the denominator of Equation 3 to construct R-values. R-values for mass chains representing the light and heavy fission fragments of the mass distribution curve (i.e. 95, 97, 136, 137, and 145) show no statistical difference from the expected values for thermal neutrons. R-values for mass chains 111 and 115, however, are less than 1 for irradiations with epithermal neutrons in both cadmium covered and bare irradiations and decrease in the following order: Lazy Susan – bare irradiation, Lazy Susan – cadmium covered irradiation, and Central Thimble – cadmium covered irradiation. Reported errors are calculated from the standard deviation of quadruplicate samples.

### 5.4 Discussion

The K-factor technique requires a fission chamber to accurately determine the number of fissions in the sample [20]. While this method is not directly used in this experiment, the number of fissions of the sample from LANL was determined at that laboratory and used to determine the K-factor for the detector used in this experiment. The K-factor method has been validated at LANL through numerous inter laboratory studies and the number of fissions can be determined with good accuracy [6,21]. Therefore the K-factor determined in this experiment can be traced back to a fission chamber measurement. In this experiment the K-factor method is used to calculate the number of fissions in  $\text{U}_3\text{O}_8$  samples irradiated in the Central Thimble, Lazy Susan, and Dry Tube. When the resulting flux is compared to flux values from previous measurements using activation foild, the results are in agreement with the largest variation of 7% overall.

Since the  $^{99}\text{Mo}$  yield is nearly invariant under the conditions in this study, the R-values are a measure of the relative change of yield of other fission products with neutron energy [9,22-25]. Effects of  $(\gamma, f)$  fission caused by gamma rays from the capture of thermal neutrons in cadmium covered experiments is negligible [9]. The R-values for epithermal neutrons in the Lazy Susan and Central Thimble in the GSTR are in agreement with literature values [9]. Qualitatively, an increase in the R-value represents a fractional increase in the amount of symmetric fission observed in the sample [25]. Conversely, a decrease in the R-value represents an increase of asymmetric fission. R-values for  $^{111}\text{Ag}$  and  $^{115}\text{Cd}$  are the most widely reported

values in literature. The decrease in the  $R_{111}$  and  $R_{115}$  values for the cadmium covered samples suggests that there is an increase in asymmetric fission for epithermal neutrons. This is in agreement with other studies [26]. The decrease in the  $R_{111}$  and  $R_{115}$  values for the bare irradiation in the Lazy Susan suggests that a change in the reactor neutron spectrum as measured by the cadmium ratio (6.7 to 2.3) also has an impact on the overall mass yield distribution.

Figure 2 shows the differential neutron energy spectrum for the Central Thimble, Lazy Susan, and Dry tube compared to the fission cross section of  $^{235}\text{U}$  and R-values that have been reported in literature. Cowen, et al.[27], during the testing era, used time of flight methods to resolve the neutrons incident on a spinning wheel to determine R-values between 19 and 85 eV. In those measurements, the resolution of higher energy neutrons was poor, however below 30 eV, there appears to be a correlation between symmetry and spin [28]. Faler, et al. [25] irradiated foils with monoenergetic neutrons from 0.002 eV and 0.004 eV with carbon-filtered and beryllium-filtered cold neutrons and neutrons between 0.04 and 0.7 eV with a beryllium-crystal neutron spectrometer. The conclusions from that study indicate that while R-values may correlate with spin a more complete answer is that it may also depend on the projection of the total angular momentum on the nuclear symmetry axis. The author is unaware of any studies or reported R-values between 1 eV and 19 eV therefore that region is omitted in Figure 2. Cross sections in 2(b) were calculated from the ENDF-B/VII Reich Moore resonance parameters using NJOY 2012. The total fission cross section of  $^{235}\text{U}$  result from the contributions of resonances with spin parity  $3^-$  and  $4^-$ .

From the work conducted in this study, the reduction in R-value between the bare irradiations in the Dry Tube and the Lazy Susan irradiation positions appears to be due to the resonance at 0.29 eV. Based on the cadmium ratios of those two positions, there are relatively more epithermal neutrons in the Lazy Susan than the Dry Tube, therefore, a lower R-value is expected. Additionally, thermal neutrons were filtered from the cadmium covered samples in the Lazy Susan and Central Thimble sampling positions and a lower R-value is also expected for those samples.

## 5.5 Conclusions

A proportionality constant for the number of fissions that occur in a sample of enriched uranium based on the measured beta activity of the sample has been determined for the detector

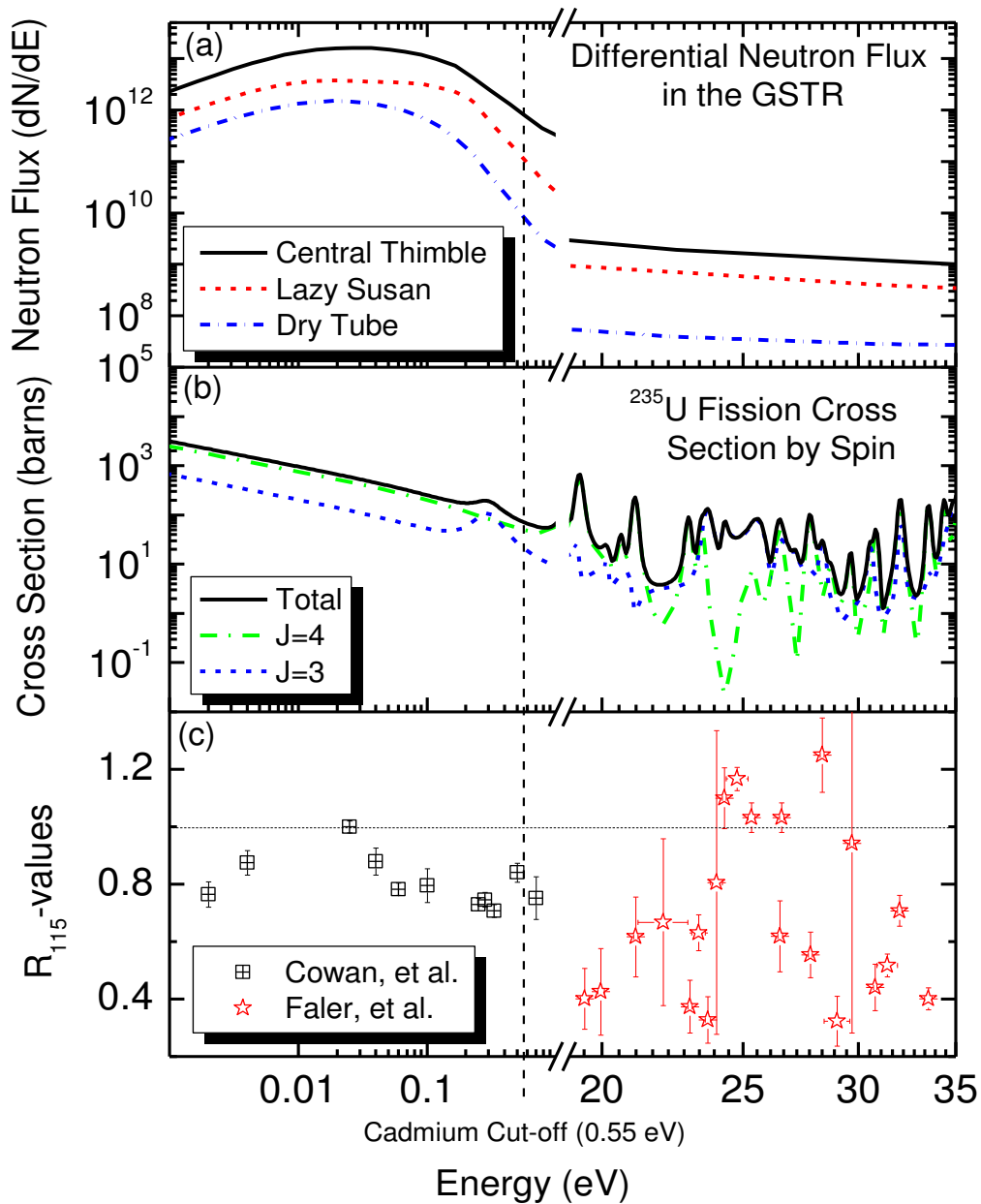


Figure 5.2. Comparison of (a) the differential neutron energy spectrum for sampling positions within the GSTR [19], (b) the  $^{235}\text{U}$  fission cross section from ENDF-B/VII Reich Moore resonance parameters calculated using NJOY 2012, and (c)  $R_{115}$ -values from incident neutrons of 0.002 to 35 eV[25,27]. The thermal  $R_{115}$ -value is designated by a horizontal dashed line and the cadmium cut-off energy of 0.55 eV is designated by a horizontal line.

used in this study. This K-factor was used to determine the thermal and epithermal flux in three irradiation positions in the GSTR and compared to values obtained through the analysis of activated foils. Additionally, relative fission yields have been obtained for the same irradiation positions for mass chains in the peaks and valley of the asymmetric mass distribution of  $^{235}\text{U}$ . The R-values for  $^{111}\text{Ag}$  and  $^{115}\text{Cd}$  show an increase in asymmetric fission from thermal to epithermal neutrons. This effect is also seen between samples with decreasing cadmium ratios.

## 5.6 Acknowledgements

The authors would like to express their sincere thanks to the reactor staff of the GSTR for their support, funding from the Colorado School of Mines, and the NRC Faculty Development Grant program, Grant Number NRC-HQ-11-G-38-0062.

## 5.7 References Cited

- 1 F.L. Lisman, W.J. Maeck, J.E. Rein, Nucl. Sci. Eng. 42: 215-19. (1970).
- 2 M.B. Chadwick, Nuclear Data Sheets 120 (2014) 297.
- 3 M. Robin, J. Bouchard, G. Frejaville, R. Vidal, R. Hageman, Importance of fission product nuclear data in burnup determination. International Atomic Energy Agency, Vienna (Austria), 1974.
- 4 M. Laser, E. Merz, Fission product nuclear data and environmental aspects of the nuclear fuel cycle. International Atomic Energy Agency, Vienna (Austria), 1974.
- 5 H.D. Selby, M.R. Mac Innes, D.W. Barr, A.L. Keksis, R.A. Meade, C.J. Burns, M.B. Chadwick, T.C. Wallstrom, Nuclear Data Sheets 111 (2010) 2891.
- 6 J.L. Yarnell, P.J. Bendt, Calorimetric fission product decay heat measurements for  $^{239}\text{Pu}$ ,  $^{233}\text{U}$ , and  $^{235}\text{U}$  - NUREG/CR-0349; LA-7452-MS. Los Alamos Scientific Lab., NM (USA) ; Sponsoring Organization: Not Available, 1978.
- 7 A.L. Keksis, M.B. Chadwick, H.D. Selby, M.R. Mac Innes, D.W. Barr, R.A. Meade, C.J. Burns, T.C. Wallstrom, Los Alamos National Laboratory Fission Basis. American Society for Testing and Materials - ASTM International, 100 Barr Harbor Drive, PO Box C700, West Conshohocken, PA, 19428-2959 (United States); European Working Group on Reactor Dosimetry - EWGRD, SCK.CEN, Mol (Belgium), 2011.
- 8 G.P. Ford, A.E. Norris, Compilation of yields from neutron- induced fission of  $^{232}\text{Th}$ ,  $^{235}\text{U}$ ,  $^{236}\text{U}$ ,  $^{237}\text{Np}$ ,  $^{238}\text{U}$ , and  $^{239}\text{Pu}$  measured radiochemically at Los Alamos - LA-6129. Los Alamos Scientific Lab., N.Mex. (USA) ; Sponsoring Organization: Not Available, 1975.
- 9 C.I. Browne, Physical Review 107 (1957) 1.

- 10 J. Kleinberg, Collected radiochemical and geochemical procedures - LA-1721-5th-Ed. Los Alamos National Lab., NM (USA) ; Sponsoring Organization: DOE/DP, 1990.
- 11 M. Lindner, RADIOCHEMICAL PURIFICATION PROCEDURES FOR THE ELEMENTS - UCRL-14258. Lawrence Radiation Lab., Univ. of California, Livermore ; Sponsoring Organization: USDOE, 1965.
- 12 E.K. Hyde, RADIOCHEMICAL METHODS FOR THE ISOLATION OF ELEMENT 87 (FRANCIUM) - UCRL-1578. Radiation Lab., Univ. of Calif., 1951.
- 13 J.R. DeVoe, THE RADIOCHEMISTRY OF CADMIUM - NAS-NS-3001. National Research Council. Committee on Nuclear Science; Univ. of Michigan, 1960.
- 14 H.L. Finston, M.T. Kinsley, THE RADIOCHEMISTRY OF CESIUM - NAS-NS-3035. Brookhaven National Lab., 1961.
- 15 M.H. Lee, C.W. Lee, Nucl. Instrum. Methods Phys. Res. Sect. A-Accel. Spectrom. Dect. Assoc. Equ 447 (2000) 593.
- 16 N.A. Talvitie, Anal. Chem. 44: No. 2 (1972).
- 17 U.I. Narayanan, P.B. Mason, J.P. Zebrowski, M. Rocca, I.W. Frank, The Quantitative Ion Exchange Separation of Uranium from Impurities in I.L. Department Of Energy Argonne (Ed.), 1995.
- 18 L.G. Wisnyi, S.W. Pijanowski, U.S.A.E. Commission, C. General Electric, L. Knolls Atomic Power.
- 19 M. Koehl, R. Rundberg, J. Braley, J Radioanal Nucl Chem 306 (2015) 31.
- 20 G.P. Ford, J.S. Gilmore, D.P. Ames, J.P. Balagna, J.W. Barnes, A.A. Comstock, G.A. Cowan, P.B. Elkin, D.C. Hoffman, G.W. Knobeloch, E.J. Lang, M.A. Melnick, C.O. Minkinen, B.D. Pollock, J.E. Sattizshn, C.W. Stanley, B. Warren, MASS YIELDS FROM FISSION BY NEUTRONS BETWEEN THERMAL AND 14.7 MEV - LA-1997. Los Alamos Scientific Lab., N. Mex. ; Sponsoring Organization: USDOE, 1956.
- 21 J.L. Yarnell, P.J. Bendt, Decay heat from products of  $^{235}\text{U}$  thermal fission by fast-response boil-off calorimetry, United States, 1977, p. 37.
- 22 G.A. Cowan, A. Turkevich, C.I. Browne, Physical Review Superseded in part by Phys. Rev. A 122 (1961).
- 23 G.A. Cowan, B.P. Bayhurst, R.J. Prestwood, Physical Review Superseded in part by Phys. Rev. A 130 (1963).
- 24 G.A. Cowan, B.P. Bayhurst, R.J. Prestwood, J.S. Gilmore, G.W. Knobeloch, Physical Review Superseded in part by Phys. Rev. A 144 (1966).
- 25 K.T. Faler, R.L. Tromp, VARIATION IN  $\text{U}^{235}$  MASS YIELDS AT NEUTRON ENERGIES BELOW 0.5 ev - CONF-12-2. Phillips Petroleum Co. Atomic Energy Div., Idaho Falls, Idaho, 1962.

- 26 H.B. Levy, H.G. Hicks, W.E. Nervik, P.C. Stevenson, J.B. Niday, J.C. Armstrong, Jr., Physical Review Superseded in part by Phys. Rev. A, Phys. Rev. B: Solid State, Phys. Rev. C, and Phys. Rev. D 124 (1961).
- 27 G.A. Cowan, B.P. Bayhurst, R.J. Prestwood, J.S. Gilmore, G.W. Knobloch, Phys. Rev. (1970).
- 28 S.F. Mughabghab, Atlas of neutron resonances : resonance parameters and thermal cross sections Z=1-100, Elsevier, Amsterdam, 2006.

## CHAPTER 6

### GENERAL CONCLUSIONS

This project was comprised of three separate stages to determine relative fission product yields in the USGS TRIGA Mark I Reactor (GSTR). Saturated activity measurements of thin activation foils have provided detailed information about the neutron spectral parameters in three sampling positions within the GSTR reactor: Central Thimble, Lazy Susan, and Dry Tube. The Westcott flux, spectral index, and neutron temperature were compared to other similar TRIAGA reactors. The results agree with measurements from other reactors with one notable exception. In the absence of absorption, leakage, or additional sources, the neutron temperature should come to equilibrium with the moderator temperature. Absorption of low energy neutrons tends to shift this distribution to higher temperatures which is known as absorption hardening. While the experimental results of the neutron temperature within the central thimble sampling position appears to be coupled to the moderator temperature with absorption hardening, the neutron temperature in the lazy susan and dry tube are lower than expected with the neutron temperature within the dry tube position below the freezing point of water. This unexpected result may be due to the proximity of the sampling positions to the graphite reflector resulting in diffusion of low energy neutrons which shift the neutron distribution and results in a lower than expected neutron temperature. The SAND-II-SNL spectrum unfolding code which uses experimental activation detector data to determine neutron energy spectra in sampling positions in the GSTR showed good agreement with experimental values.

The second stage in this project focused on the gas proportional counter and the determination of mass attenuation coefficients in the precipitates used in the radiochemical separations procedures. Once the detector resolution was experimentally measured, activity measurements were made of precipitates varying in thickness. This allowed the calculation of mass attenuation coefficients of these precipitates. There are essentially two methods to determine the mass attenuation coefficient of beta particles: transmission experiments and experiments with constant specific activity. In transmission experiments with an incident beam of beta particles, an absorber is placed between the source and detector. The beta particles are attenuated through the absorber in a relationship that is closely represented by Beer's law and the mass attenuation for the absorber

is determined. This relationship is only an approximation since beta particles interact with matter differently than electromagnetic waves, have a continuous energy spectrum, and the scattering and backscattering of beta particles changes the energy spectrum and its angular distribution. In these experiments, a solution of constant specific activity was used to determine the mass attenuation coefficients. While it is important to directly measure the detector efficiency and mass attenuation curves for a given detector configuration, this study showed that a Monte Carlo simulation can be used to calculate mass attenuation coefficients.

The final stage in this project was the measurement of relative fission product yields in the GSTR. First a proportionality constant for the number of fissions that occur in a sample of enriched uranium based on the measured beta activity of the sample was determined for the detector used in this study. This K-factor was used to determine the thermal and epithermal flux in three irradiation positions in the GSTR which were in agreement with values obtained from saturated activity measurements of thin activation foils in the first study. Finally, relative fission yields were calculated for mass chains in the peaks and valley of the asymmetric mass distribution of  $^{235}\text{U}$ . The R-values for  $^{111}\text{Ag}$  and  $^{115}\text{Cd}$  show an increase in asymmetric fission from thermal to epithermal neutrons. This effect is also seen between samples with decreasing cadmium ratios.

While the focus of this research has been on the flux parameters of the thermal and epithermal regions, a more detailed measurement of the fast flux will provide better predictive radioisotope production calculations of experiments utilizing fast reactions. Additional measurements could be made in other sampling positions within the GSTR to better model the flux within the reactor.

Improvements can be made in the experimental setup. An automatic sample changer can improve efficiencies in data collection. Difficulties that arose in the separations of lanthanides could be overcome by elevating the temperature of the columns.

This project could be expanded to measure R-values in various neutron environments between thermal and  $\sim 1.5$  MeV in experimental facilities within the DOE complex. These R-values could be constructed using the thermal measurements from the Dry Tube sampling position and compared to literature values. Additionally, it would be of interest to measure the bare and cadmium covered R-values of other valley nuclides including tin and antimony to confirm if the results complement the  $^{111}\text{Ag}$  and  $^{115}\text{Cd}$  data.

## APPENDIX A

### RADIOCHEMICAL PROCEDURES

This appendix describes the radiochemical separations procedures used in this research

#### A.1 General Instructions Applicable to All Procedures

- Centrifuge all samples at 4,000 RPM for 2 min unless otherwise noted
- Mounting of Samples:

Precipitates are filtered onto one inch Watmann 42 filter paper disks and mounted on Al plates with two-sided Scotch tape. Four drops of rubber cement solution (3 ml rubber cement to 50 ml toluene) are placed on opposing sides of the filter paper which is subsequently covered with Mylar film.

Electroplated samples are mounted on Al plates with two-sided Scotch tape and covered with Mylar film.

- Filter Paper Pulp. The pulp mixture is made by adding six Whatman No. 42 (9-cm) filter papers to 500 ml of H<sub>2</sub>O in a blender and macerating for ~5 min. The pulp mixture is transferred to a container and made slightly acidic with HCl to inhibit mold formation.

#### A.2. Preparation and Standardization of Carrier Solutions

*For all solutions, four standardizations, with results agreeing within 0.5%, are run. All eluate should be clear, colorless liquid. A 47mm filtration assembly is used for standardization.*

##### A.2.1. Cadmium

a. Preparation: Dissolve 27.4 g of Cd(NO<sub>3</sub>)<sub>2</sub>•4H<sub>2</sub>O in H<sub>2</sub>O, make the solution slightly acidic with HCl, and dilute to 1 L with H<sub>2</sub>O.

b. Standardization: Pipette 5.0 ml of the above carrier solution into a 40-mL glass centrifuge tube and evaporate to dryness. Dissolve the residue in 20 mL H<sub>2</sub>O, add 2 mL of 3M NH<sub>4</sub>Cl and bring the solution to a boil. Cool in an ice bath for 30 min and add 4 mL of 1.5M (NH<sub>4</sub>)<sub>2</sub>HPO<sub>4</sub>. Shake well and allow to stand overnight at room temperature. Filter and wash the precipitate with water. Use a small amount of ethanol to drive off excess water. Dry for 40 min at room

temperature and weigh as  $\text{CdNH}_4\text{PO}_4 \cdot \text{H}_2\text{O}$ . (Note: Temperatures in excess of  $100^\circ\text{C}$  will liberate  $\text{NH}_4$ .)

### **A.2.2. Cesium**

a. Preparation: Dissolve 12.7 g of  $\text{CsCl}$  in  $\text{H}_2\text{O}$  and dilute to 1 liter with  $\text{H}_2\text{O}$ .

b. Standardization: Pipet 5 ml of the carrier solution into a 40-ml glass centrifuge tube, add 3 ml 10% chloroplatinic acid, and evaporate to near dryness. Add 5 ml of 15% ethanol and filter. Wash with absolute ethanol. Dry at  $110^\circ\text{C}$  for 15 min, cool, and weigh as  $\text{CsPtCl}_6$ . (Note: Eluate may have yellowish color due to excess chloroplatinic acid.)

### **A.2.3. Silver**

a. Preparation: Dissolve 15.75 g of  $\text{AgNO}_3$ , primary standard grade, in a minimum amount of  $\text{H}_2\text{O}$ , add a few drops of  $\text{HNO}_3$ , and dilute the solution to 1L.

b. Standardization: Pipet 5 mL of carrier solution into a centrifuge tube and add 20 mL 0.2 M  $\text{HCl}$  in excess and leave (preferably overnight) at  $25\text{-}30^\circ\text{C}$  in the dark. Filter and wash with 0.01 M  $\text{HCl}$ . Dry at  $130\text{-}150^\circ\text{C}$ , for 15 min, cool, and weigh as  $\text{AgCl}$ . (Note: Precipitate tends to clump together on the filter and is prone to falling off the filter when dry. Extra caution should be used when moving the filter.)

### **A.2.4. Zirconium**

a. Preparation: Dissolve 30.0 g of  $\text{ZrO}(\text{NO}_3)_2 \cdot 2\text{H}_2\text{O}$  in  $\text{H}_2\text{O}$  and add sufficient concentrated  $\text{HNO}_3$  to make the solution 1M in  $\text{HNO}_3$ . Filter and make the filtrate up to 1 L with 1M  $\text{HNO}_3$ .

b. Standardization: Pipette 5 ml of the solution into a 500-ml beaker, make the solution 2M in  $\text{HCl}$  (2.5 mL 6M  $\text{HCl}$ ), and cool in an ice bath. Prepare the reagent by dissolving 40 g of cupferron in 400 mL of water with stirring. Dilute to 500 mL and filter. (Store for no longer than one week in a refrigerator.) Add 120 mL of this 8% (w/v) cupferron solution to the sample solution and 5 ml filter pulp. Stir vigorously on stir plate at 400 RPM for 5 min. Filter eluate completely before rinsing with 1M  $\text{HCl}$ . Wash the residue five times with the same rinse solution. Transfer the paper and residue to a large (30 ml) weighed porcelain crucible. Press a moistened filter paper on top of the residue and heat on hot plate at  $150^\circ\text{C}$  for 2 h. Place the

crucible in a muffle furnace and heat for 1 hr at 275 °C, driving off water in the hydroxide. Ignite for 30 min at 400°C and then 1 hour at 950°C, cool, and weigh as ZrO<sub>2</sub>.

### **A.2.5. Molybdenum**

a. Preparation: Dissolve 18.4 g of (NH<sub>4</sub>)<sub>6</sub>Mo<sub>7</sub>O<sub>24</sub>•4H<sub>2</sub>O in H<sub>2</sub>O, add 1 ml of 0.5M NaBrO<sub>3</sub>, and dilute to 1 L with 6M HCl.

b. Standardization: Pipette 5.0 ml of the solution into a crucible that has been heated in a muffle furnace at 550°C, cooled, and weighed. Add 0.5 ml of concentrated HNO<sub>3</sub> and 0.5 ml of concentrated HClO<sub>4</sub>. Carefully dry the sample under an infrared lamp, and ensure that no spattering occurs. Ignite in the furnace for 1 h at 500°C, cool, and weigh as MoO<sub>3</sub>.

### **A.2.6. Lanthanides**

a. Preparation: Dissolve 10 g of the desired lanthanide in ~50 ml of 6M HCl. Heat, or add a few drops of concentrated HNO<sub>3</sub> if dissolution is difficult. Filter and dilute to 1 L; adjust the HCl concentration to 2 to 3M. Any pure soluble cerium(III) salt may be used for cerium carrier.

b. Standardization: Pipette 6 ml of carrier solution directly into a weighed porcelain crucible that has been fired for 2 h. Evaporate the solution to dryness. Ignite at 950°C for 2 h, cool, and weigh as Ln<sub>2</sub>O<sub>3</sub>. The lanthanide chloride is converted to the oxide.

## **A.3. Radiochemical Separations**

*For all solutions, four replicates are run.*

### **A.3.1 Cadmium**

#### **a. Introduction**

This procedure is designed for the rapid separation of cadmium from fission products. Decontamination steps include scavenging with cadmium sulfide (CdS), acid sulfide, and iron hydroxide (Fe(OH)<sub>3</sub>). The cadmium, in 3M HCl, is then placed on an anion exchange resin (Dowex AG 1-X8) and eluted with 1.5M H<sub>2</sub>SO<sub>4</sub>. Finally, the cadmium is converted to the elemental form by electroplating. The chemical yield is about 80% and the time required for separations to electroplating in quadruplicate is about 4 hr.

#### **b. Reagents**

Cd carrier: 10 mg Cd/ml, added as  $\text{Cd}(\text{NO}_3)_2 \cdot 4\text{H}_2\text{O}$  in very dilute HCl; standardized

Ag carrier: 10 mg Ag/ml, added as  $\text{AgNO}_3$  in very dilute  $\text{HNO}_3$

Fe carrier: 10 mg Fe/ml, added as  $\text{FeCl}_3 \cdot 6\text{H}_2\text{O}$  in very dilute HCl

Pd carrier: 10 mg Pd/ml, added as  $\text{PdCl}_2$  in  $\text{H}_2\text{O}$

La carrier: 10 mg La/ml, added as  $\text{La}(\text{NO}_3)_3 \cdot 6\text{H}_2\text{O}$  in  $\text{H}_2\text{O}$

HCl: concentrated; *6M*; *3M*; *0.1M*

$\text{H}_2\text{SO}_4$ : 1.5M, concentrated

$\text{NH}_4\text{OH}$ : concentrated

$\text{NH}_4\text{Cl}$ : 3M

$(\text{NH}_4)_2\text{HPO}_4$ : 1.5M

NaCN: 2M

NaOH: *10M*

$\text{H}_2\text{S}$ : gas

Dowex AG 1-X8. 50-100 mesh anion exchange resin, slurry in 6M HCl

Methyl red indicator solution

Phenolphthalein indicator solution: 1% in 90% ethanol

Ethanol: 95%; absolute

c. Prepare

- i. 4 x 125mL Erlnymeyer flasks with funnel and filter paper
- ii. 4 x 5 mL Ag 1-X8 anion exchange columns. Condition columns with 2 x 5 mL washings of 3M HCl.
- iii. 4 x Electrolytic cells

#### d. Procedure

Step 1. Add the sample to 2.0 ml of cadmium carrier (20 mg) in a 40-ml glass centrifuge tube. Add sufficient 6M HCl to make the solution 0.1M with respect to this acid. Bubble in H<sub>2</sub>S for ~3 min, centrifuge, and discard the supernate.

Step 2. To the precipitate add 2 ml of concentrated HCl and boil to expel H<sub>2</sub>S. Dilute to 20 ml with H<sub>2</sub>O add 2 drops of iron carrier, 2 drops of phenolphthalein indicator, and make just barely alkaline by the dropwise addition of concentrated NH<sub>4</sub>OH. Centrifuge, transfer the supernate to a clean centrifuge tube, and discard the precipitate. Add 2 drops of lanthanum carrier, centrifuge, transfer the supernate to a clean centrifuge tube, and discard the precipitate.

Step 3. Add 1 ml of silver carrier, 2 drops of methyl red indicator, and concentrated H<sub>2</sub>SO<sub>4</sub> dropwise until the solution is just barely acid to methyl red indicator. Add 10 drops of 6M HCl and place on a water bath for ~3 min. Centrifuge, transfer the supernate to a clean centrifuge tube, and discard the precipitate.

Step 4. Saturate the supernate with H<sub>2</sub>S, centrifuge, and discard the supernate. (Note: The CdS reaction is reversible. If the concentration of strong acid in the solution is above 0.5M, precipitation is incomplete. Concentrated acids dissolve the precipitate for the same reason.)

Step 5. Dissolve the CdS precipitate in a few drops of concentrated HCl, boil briefly, and add 10 ml of 3M HCl and 3 drops of palladium carrier. While the solution is being heated on a water bath, saturate it with H<sub>2</sub>S. Centrifuge, filter the supernate through filter paper into a 125-ml erlenmeyer flask, and discard the precipitate.

Step 6. Boil the solution to expel H<sub>2</sub>S and then place it on top of a Dowex AG 1-X8, 50 to 100 mesh, anion-exchange resin column (0.8-cm by 5-cm resin bed). Wash the flask with 2 ml of 3M HCl and add the washings to the column. Wash the column with 10 to 15 ml of 0.1M HCl. Discard all effluents. Add 10 ml of 1.5M H<sub>2</sub>SO<sub>4</sub> to the column and when this has passed through, add 20 ml of H<sub>2</sub>O. Collect the eluates in a clean centrifuge tube.

Step 7. Make the solution alkaline with 10M NaOH (~3 mL), centrifuge, discard the supernate, and wash twice with 10 mL of H<sub>2</sub>O.

Step 8. To the precipitate in a 40-ml centrifuge tube add 5 ml of 2M NaCN and stir until solution is effected; heat the solution if necessary. Transfer the solution to a plating cell. Wash the centrifuge tube with 5 ml of 2M NaCN and transfer the washings to the plating cell.

Step 9. Plate the cadmium onto the platinum disk at 25 mA at room temperature for 1 h and 10 min. After the plating is complete, remove the cell, discard the electrolyte, wash the cell with distilled H<sub>2</sub>O, and disassemble it. Wash the cadmium plated platinum disk thoroughly with absolute ethanol, allow to dry at room temperature, weigh, and mount.

### **A.3.2 Cesium**

#### a. Introduction

In the separation of cesium from other fission-product activity, a ferric hydroxide scavenge is followed by a precipitation as the silicotungstate. This step gives a decontamination factor of 100 to 200, and is a specific separation of cesium from ammonium, iron, rubidium, and the other alkali metals which may interfere in the determination of cesium as the chloroplatinate. The silicotungstate is dissolved in alkali and is then filtered as the chloroplatinate, which is dried, weighed, and mounted for counting. The chemical yield is 60-70% and the time required for analysis in quadruplicate is about 8 hr.

#### b. Reagents

Cs carrier: 10 mg Cs/ml, added as CsCl in H<sub>2</sub>O, standardized

Fe carrier: 10 mg Fe/ml, added as Fe(NO<sub>3</sub>)<sub>3</sub>•9H<sub>2</sub>O in very dilute HNO<sub>3</sub>

HCl: 6M; concentrated

NaOH: 10M, 6M

Silicotungstic acid: 0.12M

Ethanol: absolute, squirt bottle

Phenolphthalein indicator solution: 1% in 90% ethanol

Chloroplatanic acid: 10% in H<sub>2</sub>O

### c. Procedure

Step 1. To 2 ml of cesium carrier solution in a 40-ml plastic centrifuge tube, add an aliquot of sample and make up to a volume of 15 ml, the final solution being 6M in HCl. (If the active solution contains HNO<sub>3</sub>, evaporate (with carrier) to dryness and take up with 15 ml of 6M HCl.)

Step 2. Add about 2 g of silicotungstic acid dissolved in 2 ml of H<sub>2</sub>O (1 g/ml) (or 6 mL 0.12M silicotungstic acid). Heat the solution for 10 min, chill the solution for 10 min in an ice bath, and let stand for at least 1 hr (preferably overnight). Centrifuge, discard the supernate, and wash the precipitate twice with 10-ml portions of 6M HCl.

Step 3. Dissolve the Cs precipitate by boiling with 2 ml of H<sub>2</sub>O, adding 3 drops of Fe carrier and adding 2 ml of 6M NaOH (about 0.24 g). Add H<sub>2</sub>O, if necessary, to prevent boiling to dryness. Centrifuge and pour into 10 ml of hot 6M HCl in a 125-ml Erlenmeyer flask and boil. Discard the precipitate. Heat overnight at 90°C (minimum of 2 hours). (Note: It is necessary to heat at this stage to insure complete dissolution of Cs. Silica and tungstic oxide (WO<sub>2</sub>) remain behind.) Centrifuge and transfer the supernate to a 40-ml centrifuge tube. Add 5 ml 6M HCl, gently boil and cool (HCl wash). Centrifuge and transfer the supernate to a 40-ml centrifuge tube.

Step 4. Add 1 mL 10% chloroplatinic acid. Chill for 10 min. Wash precipitate with 5mL 6M HCl.

Step 5. Slurry the precipitate in 5 ml of absolute ethanol and filter on weighed filter paper. Use absolute ethanol to complete transfer and to wash down sides of filter chimney. Dry at 110° for 10 min. Cool for 10 min. weigh, and mount. Count immediately.

### A.3.3 Silver

#### a. Introduction

Silver is initially separated from other fission products by the specific precipitation of the chloride from nitric acid solution. The silver is then purified by ferric hydroxide scavenging and silver sulfide precipitation, both of which are performed in ammoniacal solution. After repetition of the scavenging-precipitation cycle, the silver is converted to the oxide and finally

electroplated prior to counting. The chemical yield exceeds 80% and the time required for analysis in quadruplicate is about 3 hr.

b. Reagents

Ag carrier: primary standard, 10 mg Ag/ml added as  $\text{AgNO}_3$  in very dilute  $\text{HNO}_3$

Fe carrier: 10 mg Fe/ml, added as  $\text{FeCl}_3 \cdot 6\text{H}_2\text{O}$  in very dilute HCl

HCl: concentrated

$\text{HNO}_3$ : concentrated

NaOH: 6M

$\text{NH}_4\text{OH}$ : concentrated

$(\text{NH}_4)_2\text{S}$ : saturated solution

Ethanol: 95%

Phenolphthalein indicator solution: 1% in 90% ethanol

c. Procedure

Step 1. To the sample in a 40-mL glass centrifuge tube, add exactly 2 ml of silver carrier and 5 ml of concentrated  $\text{HNO}_3$  and dilute the solution to 20 mL with  $\text{H}_2\text{O}$ . Heat to boiling and precipitate  $\text{AgCl}$  by the addition of 4 drops of concentrated HCl. Heat until the  $\text{AgCl}$  has coagulated; cool, centrifuge, and discard the supernate.

Step 2. Dissolve the  $\text{AgCl}$  in 2 ml of concentrated  $\text{NH}_4\text{OH}$ , dilute to 20 ml with  $\text{H}_2\text{O}$ , and add 1 ml of iron carrier. Stir, centrifuge, transfer the supernate to a clean 40-ml centrifuge tube, and discard the precipitate.

Step 3. To the solution add 1 ml of saturated  $(\text{NH}_4)_2\text{S}$  solution. Stir vigorously, centrifuge, and discard the supernate.

Step 4. Dissolve the  $\text{Ag}_2\text{S}$  precipitate by heating with 1 ml of concentrated  $\text{HNO}_3$ . (Note: Hot  $\text{HNO}_3$  allows for a rapid dissolution. If the precipitate does not dissolve completely, centrifuge and transfer to another centrifuge tube.) Dilute to 20 ml with  $\text{H}_2\text{O}$  and precipitate

AgCl by the addition of 4 drops of concentrated HCl as in Step 1. Centrifuge and discard the supernate.

Step 5. Repeat Steps 2 and 3 one additional time

Step 6. Dissolve the Ag<sub>2</sub>S by heating with 1 ml of concentrated HNO<sub>3</sub>. Dilute with 20 ml of H<sub>2</sub>O, add two drops of phenolphthalein indicator solution, make the solution alkaline with 6M NaOH (~2.5 mL), and then add 3 drops in excess. Centrifuge the Ag<sub>2</sub>O precipitate and discard the supernate. Wash the precipitate twice with H<sub>2</sub>O.

Step 7. Add 5 ml of 2M NaCN to the precipitate and stir until solution is effected; heat if necessary. Transfer the solution to a plating cell, the cathode of which is a weighed, polished stainless steel disk of 3/4 in. diam. Wash the centrifuge tube with 5 ml 2M NaCN and transfer the washings to the plating cell.

Step 8. Plate the silver on the stainless steel disk at 15 mA at room temperature for 1 h and 10 min. After the plating is complete, remove the cell, discard the electrolyte, wash the cell with H<sub>2</sub>O, and disassemble it. Wash the silver-plated disk thoroughly with absolute ethanol, allow to dry at room temperature, weigh, and mount.

### **A.3.4 Zirconium-95 and Zirconium-97**

#### **a. Introduction**

In the procedure described below, exchange between carrier and <sup>95</sup>Zr and <sup>97</sup>Zr is effected by formation of the fluorozirconate complex [ZrF<sub>6</sub>]<sup>2-</sup>. Lanthanide and alkaline-earth activities are removed by lanthanum fluoride scavenging, and then zirconium is separated by three barium fluorozirconate Ba[ZrF<sub>6</sub>] precipitations. Zr is separated from Nd on an anion exchange resin column. Nd is absorbed on the column which is washed twice. Zirconium is precipitated as the hydroxide (Zr(OH)<sub>4</sub>) and dissolved in HCl. Zirconium is finally precipitated with mandelic acid from hydrochloric acid medium and ignited to the oxide, ZrO<sub>2</sub>, in which form it is weighed and counted. The chemical yield is about 45% and the time required for analysis in quadruplicate is about 7 hr.

#### **b. Reagents**

Zr carrier: 10 mg Zr/ml, added as ZrO(NO<sub>3</sub>)<sub>2</sub>•2H<sub>2</sub>O in 1M HNO<sub>3</sub>; standardized

La carrier: 10 mg La/ml, added as  $\text{La}(\text{NO}_3)_3 \cdot 6\text{H}_2\text{O}$  in  $\text{H}_2\text{O}$

Nb hold-back carrier: Solution of potassium niobate, 10 g per 100 ml of solution.

HCl: 6M; concentrated

$\text{HNO}_3$ : concentrated

$\text{H}_2\text{SO}_4$ : concentrated

HF: concentrated

$\text{H}_3\text{BO}_3$ : saturated aqueous solution

$\text{NH}_4\text{OH}$ : concentrated

$\text{NH}_2\text{OH} \cdot \text{HCl}$ : solid

$\text{Ba}(\text{NO}_3)_2$ : 50 mg Ba/ml

Mandelic acid: 16% aqueous solution

Ethanol: 95%

Dowex AG 1-X8 resin column (in 6M HCl)

Phenolphthalein indicator solution: 1% in 90% ethanol

HCl-HF solution: 9M/0.004M

Filter paper pulp

c. Prepare

- i. Fresh solution of 40 mL mandelic acid
- ii. Weigh out 4 x 600mg of  $\text{NH}_2\text{OH} \cdot \text{HCl}$
- iii. 4 x 5 mL Ag 1-X8 anion exchange columns. Condition columns with 2 x 5 mL washings of 6M HCl followed by 2 x 5 mL washings of 9M/0.004M HCl-HF solution.

d. Procedure

Step 1. Place the sample in a 50-ml plastic centrifuge tube and add 2.0 ml of zirconium carrier. Adjust to 4 to 5M in  $\text{HNO}_3$  and to a volume of  $\sim 12$  ml. Add solid  $\text{NH}_2\text{OH}\cdot\text{HCl}$  so that the solution is 2 to 3% in  $\text{NH}_2\text{OH}$ . Add 3 drops of niobium carrier and make the solution 5M in HF. Heat for 1 hour on a water bath.

Step 2. Add 10 drops (0.5 mL) of lanthanum carrier and centrifuge for a short time (2 min). Add another 10 drops (0.5 mL) of lanthanum carrier (without disturbing) and centrifuge thoroughly (2 min). Decant the supernate into another centrifuge tube and discard the precipitate.

Step 3. Repeat Step 2 two more times.

Step 4. After a total of six  $\text{LaF}_3$  scavengings, add 1 ml of  $\text{Ba}(\text{NO}_3)_2$  solution per 5 ml of the supernate. Let stand for 10 min and centrifuge. Discard the supernate.

Step 5. To the precipitate add 2 ml of saturated  $\text{H}_3\text{BO}_3$  and slurry (with a glass stir rod). Add 2 ml of concentrated  $\text{HNO}_3$  and slurry again. Heat for 15 min. Add 10 to 12 ml of  $\text{H}_2\text{O}$  and mix well. Solution will be clear. If the precipitate does not dissolve completely, centrifuge and decant the supernate into another centrifuge tube.

Step 6. Precipitate  $\text{Ba}[\text{ZrF}_6]$  by the addition of 2 ml of  $\text{Ba}(\text{NO}_3)_2$  solution and 2 ml of concentrated HF. Stir and let sit for 2 min. Centrifuge, decant supernate, and dissolve as in Step 5.

Step 7. Precipitate  $\text{Ba}[\text{ZrF}_6]$  as in Step 6, centrifuge, decant supernate, and dissolve the precipitate in 4 ml of saturated  $\text{H}_3\text{BO}_3$  (mix well prior to addition of HCl), 4 ml of concentrated HCl, and 10 ml of  $\text{H}_2\text{O}$ . Heat until precipitate dissolves. Add 3 drops (100  $\mu\text{L}$ ) of concentrated  $\text{H}_2\text{SO}_4$  diluted with 5 ml of  $\text{H}_2\text{O}$  and let stand for 10 min. (Should see fine white precipitate. It's very important to wait.) Add 1 to 2 drops of  $\text{NH}_4\text{OH}$  and centrifuge. Transfer the supernate to a 40-ml centrifuge tube and discard the  $\text{BaSO}_4$  precipitate.

Step 8. To the supernate, add two drops of phenolphthalein indicator solution and concentrated  $\text{NH}_4\text{OH}$  (8 mL) until the solution is alkaline. Centrifuge down the  $\text{Zr}(\text{OH})_4$  and discard the supernate. Add 5 ml  $\text{H}_2\text{O}$ , centrifuge, and discard supernate. (Good place to stop. May sit overnight.).

Step 9. Dissolve the precipitate in 4 ml of 9M/0.004M HCl-HF solution. Load sample on pre-conditioned columns. (Conditioning steps: Twice, add 4 mL 6M HCl; twice, add 4 ml of 9M/0.004M HCl-HF solution.). Once sample is loaded, record time, wash twice with 5 ml of 9M/0.004M HCl-HF solution. Add 10 mL H<sub>2</sub>O to collected sample. Place in water bath and add a total of 12 mL concentrated NH<sub>4</sub>OH in four batches of 3 mL. (Stir as pipetting – exothermic reaction). Allow to sit for 5 min (Zr(OH)<sub>4</sub> formation). Centrifuge and discard supernate. Dissolve precipitate in 10 mL concentrated HCl. Add 10 ml of 16% mandelic acid. Add 1.5 mL paper pulp solution (ashless filter paper). Heat solution for 1 hour in water bath swirling sample every 15 min.

Step 10. Filter onto 47mm vacuum filter. Transfer the paper and precipitate to a porcelain crucible and heat for 1hr between 250 °C and 275 °C, driving off water in the hydroxide. Ignite for 30 min at 400°C and then 1 hour at 900°C. Powder the ZrO<sub>2</sub> with the fire-polished end of a stirring rod. Add 2 drops of ethanol, slurry, and grind again. Add 10 ml of ethanol, stir, and filter onto a washed, dried, and weighed filter circle. Wash the ZrO<sub>2</sub> with 5 ml of ethanol. Dry at 110°C for 10 to 15 min, cool, weigh, mount, and count.

### **A.3.5. Molybdenum**

#### **a. Introduction**

The separation of molybdenum from fission products is based primarily on its behavior in the +6 oxidation state on an anion exchange resin. Molybdenum (VI) is adsorbed on the resin from hydrochloric acid solutions of concentrations 5 to 9M. Resin washes with a mixture of dilute hydrochloric and hydrofluoric acids and with 3M ammonium hydroxide remove most of the interfering ions. Molybdenum is eluted from the column with 6M ammonium acetate, precipitated with  $\alpha$ -benzoinoxime, and converted by ignition to MoO<sub>3</sub> in which form it is weighed and counted. The chemical yield is about 60% and the time required for analysis in quadruplicate is about 6 hr.

#### **b. Reagents**

Mo carrier: 10 mg Mo/ml (NH<sub>4</sub>)<sub>6</sub>Mo<sub>7</sub>O<sub>24</sub>•4H<sub>2</sub>O solution; standardized

Fe carrier: 10 mg Fe/ml, added as aqueous FeCl<sub>3</sub>•6H<sub>2</sub>O

Cu carrier: 10 mg Cu/ml, added as aqueous  $\text{CuSO}_4 \cdot 5\text{H}_2\text{O}$

$\text{H}_2\text{SO}_4$ : concentrated

$\text{H}_2\text{C}_2\text{O}_4$ : saturated aqueous solution

$\text{NH}_4\text{Cl}$ : 3M

$\text{HNO}_3$ : 1M; concentrated

$\text{HCl}$ : 6M; concentrated

$\text{HCl-HF}$ : 0.1M in  $\text{HCl}$  and 0.05M in  $\text{HF}$

$\text{NH}_4\text{OH}$ : 3M; concentrated

$\text{NH}_4\text{C}_2\text{H}_3\text{O}_2$ : 6M

$\alpha$ -Benzoinoxime: 2% in ethanol (prepare fresh – 40 mL for 4 samples) (Cupron)

$\text{H}_2\text{S}$ : gas

$\text{Br}_2 \cdot \text{H}_2\text{O}$  (75 mL  $\text{H}_2\text{O}$  to 10 mL  $\text{Br}$ ) *refrigerate*

Anion resin: Dowex 1-X8 (50 to 100 mesh; stored in 6M  $\text{HCl}$ )

Ethanol: 95%

Filter paper pulp

c. Prepare

- i. Fresh solution of 40 mL cupron
- ii. 4 x 5 mL Ag 1-X8 anion exchange columns. Condition columns with 2 x 5 mL washings of 6M  $\text{HCl}$ .

d. Procedure

Step 1. (Keep samples warm on water bath. Do not bake out.) Add the sample to 2 ml of molybdenum carrier in a 125-ml erlenmeyer flask. Then add 1 ml of  $\text{Br}_2 \cdot \text{H}_2\text{O}$ , 4 drops of copper carrier, and 1 to 5 ml of concentrated  $\text{H}_2\text{SO}_4$ , depending upon the amount of uranium in the sample (~2 ml of the acid is sufficient for 1 g of uranium). Fume to dryness, add 10 ml of  $\text{H}_2\text{O}$ ,

and warm to dissolve the residue. While the solution is kept warm, saturate with  $\text{H}_2\text{S}$ . Pour the mixture into a 40-ml conical centrifuge tube, centrifuge, and save the supernate for the recovery of uranium.

Step 2. Wash the precipitate by stirring with 5 ml of 3M  $\text{NH}_4\text{Cl}$  and 10 ml of  $\text{H}_2\text{O}$ . Centrifuge and discard the washings. Dissolve the precipitate in 1 ml of concentrated  $\text{HCl}$  and a few drops of concentrated  $\text{HNO}_3$ . Add 10 ml of  $\text{H}_2\text{O}$ , boil to remove excess  $\text{H}_2\text{S}$ , and then add 3 to 4 drops of iron carrier. Precipitate  $\text{Fe}_2\text{O}_3 \cdot x\text{H}_2\text{O}$  by adding 2 to 3 ml of concentrated  $\text{NH}_4\text{OH}$ . Warm to coagulate the precipitate, centrifuge, transfer the supernate to a 125-ml erlenmeyer flask, and discard the precipitate.

Step 3. Take the supernate to half-volume on a hot plate. Add 1 ml of concentrated  $\text{HCl}$  and again take to half-volume. Add 1 ml of concentrated  $\text{HCl}$ , take the solution almost to dryness, and then add 10 ml of 6M  $\text{HCl}$  and 1 ml of  $\text{Br}_2\text{-H}_2\text{O}$ .

Step 4. Heat the solution to boiling, transfer it to a Dowex 1-X8 anion-exchange resin column, and permit it to run through under gravity. Record time. (Note: Using hot reagents on column will result in faster elution.) Wash the sides of column with 25 ml of 6M  $\text{HCl}$  and, when the level of acid reaches the top of the resin, add 10 ml of hot  $\text{HCl-HF}$  solution. When the level of the  $\text{HCl-HF}$  solution reaches the top of the resin, add 5 ml of 3M  $\text{NH}_4\text{OH}$ .

Step 5. As soon as the level of the  $\text{NH}_4\text{OH}$  reaches the top of the resin, all effluents collected to this point are placed in the appropriate waste bottle. Add 15 ml of hot 6M  $\text{NH}_4\text{C}_2\text{H}_3\text{O}_2$  to the resin and permit the solution to pass through; catch the molybdenum eluate in a clean 40-ml centrifuge tube.

Step 6. To the eluate add 2 ml of concentrated  $\text{NH}_4\text{OH}$ , stir, and then add 4 drops of iron carrier. Boil for 1 min while stirring; let sit for 10 min. Centrifuge.

Step 7. Add the supernate to an ice-cold mixture of 6 ml of concentrated  $\text{HNO}_3$ , 1 ml (6 drops) of  $\text{Br}_2\text{-H}_2\text{O}$ , and 1 ml of saturated  $\text{H}_2\text{C}_2\text{O}_4$  in a 40-ml centrifuge tube. Cool in an ice bath for 5 min, add 10 ml of alpha-benzoinoxime solution, and stir vigorously with glass stir bar; let stand for 10 min (fluffy white precipitate). Add 2mL filter paper pulp. Filter onto 47mm vacuum filter and complete the transfer with 1M  $\text{HNO}_3$ .

Step 8. Place the filter paper and contents in a porcelain crucible and ignite to  $\text{MoO}_3$  at  $250^\circ\text{C}$  for 30 min and  $500^\circ\text{C}$  for 1 to 1.5 hours.

Step 9. After ignition, allow the crucible to cool and grind the  $\text{MoO}_3$  to a fine consistency with the end of a stirring rod. Add 2 drops of ethanol and slurry; then add an additional 5 ml of ethanol, stir, and filter onto a washed, dried, and weighed filter circle. Wash with ethanol and dry at  $110^\circ\text{C}$  for ~10 min. Cool, weigh, and mount.

### **A.3.6. Separation of the Lanthanides by HPLC**

#### a. Introduction

After the radiochemical purification of the lanthanides as a group, they are placed on a cation exchange resin of very fine particle size (Dowex AG 50W-X8) and then are gradient-eluted using high performance liquid chromatography with  $\alpha$ -hydroxyisobutyric acid ( $\alpha$ -HIB) at pH 5.2 to 5.3 under a pressure of 125 to 175 psi as the mobile phase. The acid is run through the exchange columns at a rate of 3 ml/min, and the collection system changes tubes every minute. The very small particle size of the resin permits a rapid separation of the elements. In the event that only one or two of the lanthanides are to be separated, the appropriate concentrations of  $\alpha$ -HIB can be used to elute those elements from the column. The chemical yield is about 50% and the time required for analysis in quadruplicate is about 16 hr.

#### b. Reagents

##### *Lanthanide Group Purification*

Ln carrier(s) (Lanthanum, cerium, praseodymium, neodymium, samarium, europium, gadolinium, terbium, thulium, ytterbium, lutetium, and yttrium): 10 mg Ln/ml, added as  $\text{Ln}(\text{NO}_3)_3 \cdot 6\text{H}_2\text{O}$  in  $\text{H}_2\text{O}$

$\text{HClO}_4$ : concentrated

$\text{HCl}$ : concentrated; 6M

$\text{HNO}_3$ : concentrated

$\text{H}_3\text{BO}_3$ : saturated

$\text{HF}$ : concentrated

NH<sub>4</sub>OH: concentrated

NH<sub>2</sub>OH•HCl: 5M aqueous solution

Ethanol: 95%

Zirconium carrier: 10 mg zirconium/ml, added as ZrO(NO<sub>3</sub>)<sub>2</sub>•2H<sub>2</sub>O in 1M HNO<sub>3</sub>

Tellurium carrier: 10 mg tellurium/ml, added as Na<sub>2</sub>TeO<sub>3</sub> in H<sub>2</sub>O

Anion exchange column

### *HPLC*

Cation-exchange resin: Dowex AG 50W-X8 in H<sub>2</sub>O

Alpha-hydroxyisobutyric acid (alpha-HIB): 5M filtered through a 0.45 μm PFTE filter

Alpha-HIB solution: 200mL/L of 5M alpha-HIB and 60 ml/L concentrated NH<sub>4</sub>OH (500 mL of 5M alpha-HIB, 150 mL concentrated NH<sub>4</sub>OH, bring up to 2.5 L)

H<sub>2</sub>C<sub>2</sub>O<sub>4</sub>: saturated aqueous solution

8-quinolinol (8-hydroxyquinoline) solution: 6% by weight in absolute ethanol; stored in a dark bottle

8-quinolinol reagent: a mixture of one part by volume of 8-quinolinol solution, one part of absolute ethanol, two parts of concentrated NH<sub>4</sub>OH, and four parts H<sub>2</sub>O; made up just before use.

8-quinolinol reagent I: a solution of 0.5 g of 8-quinolinol (8-hydroxyquinoline) and ~100 mg of phenolphthalein in 100 ml of ethanol

8-quinolinol reagent II: a mixture of 10 ml of 8-quinolinol reagent I and 5 ml of concentrated NH<sub>4</sub>OH diluted to 200 ml with H<sub>2</sub>O

Filter pulp

Ethanol: absolute

c. Prepare

i. 4 x 5 mL AG 1-X8 anion exchange columns. Condition columns with 2 x 5 mL washings of concentrated HCl.

ii. 4 x 5 mL AG 50W-X8 cation exchange columns (Omnifit 6.6mm X 25cm). Condition columns with H<sub>2</sub>O.

#### d. Lanthanide Group Purification

In this procedure all precipitates are digested on a water bath. They may be centrifuged while the solutions are still hot.

Step 1. Into a 125-ml erlenmeyer flask, pipette 2 mL of desired carrier and the active sample, 4 ml of concentrated HClO<sub>4</sub>, and 1 ml of concentrated HNO<sub>3</sub>; fume to near dryness. Add 3 ml of concentrated HNO<sub>3</sub> and enough H<sub>2</sub>O to transfer the solution to a 40-ml plastic centrifuge tube. Add H<sub>2</sub>O to bring the volume to ~15 ml, then add 2 to 5 ml of concentrated HF, digest on a water bath for 30 min, and centrifuge for 15 min. Decant the supernate and wash the precipitate with ~20 ml of H<sub>2</sub>O that contains a few drops of concentrated HF. Centrifuge and discard the supernate.

Step 2. Slurry the precipitate with 2 ml of saturated H<sub>3</sub>BO<sub>3</sub>; add 2 ml of concentrated HNO<sub>3</sub>. Heat to dissolve precipitate, then add 10 ml of H<sub>2</sub>O, and 2 drops of zirconium carrier. Heat to dissolve any precipitate. Add 2 to 5 ml of concentrated HF, heat on a water bath for a few minutes, and centrifuge. Wash the precipitate with H<sub>2</sub>O that contains a few drops of HF. Centrifuge and discard the supernate.

Step 3. Slurry the precipitate with 2 ml of saturated H<sub>3</sub>BO<sub>3</sub>, add 2 ml of concentrated HNO<sub>3</sub>, and heat on a water bath, if necessary, to dissolve the precipitate. Add 15 ml of H<sub>2</sub>O.

Step 4. Add 8 ml of concentrated NH<sub>4</sub>OH, heat for 1 min on a water bath, digest, and centrifuge. Discard the supernate. (The anion-exchange resin column may be prepared at this time.) Wash the precipitate with 15 ml of H<sub>2</sub>O to which a few drops of concentrated NH<sub>4</sub>OH has been added. Centrifuge and discard the supernate.

Step 5. Dissolve the hydroxide precipitate in 4 ml of concentrated HCl and 1 drop of concentrated HNO<sub>3</sub>, and add 2 drops each of zirconium and tellurium carriers. Heat the sample for only 30 s on a water bath (to promote tellurium exchange but not to reduce the HCl

concentration). Pass the solution through an anion-exchange resin column and collect the eluate in a 125-ml erlenmeyer flask. Rinse the column with a 4-ml and a 6-ml 6M HCl rinse solution, and collect the rinsings in the flask.

Step 6. Boil out excess HCl by heating the flask over a flame and reduce the volume to 4 to 5 ml. Transfer the solution to a long, tapered centrifuge tube with 15 ml of H<sub>2</sub>O. Add 8 ml of concentrated NH<sub>4</sub>OH and 3 drops of 5M NH<sub>2</sub>OH.HCl. Heat on a water bath for ~1 min, digest, centrifuge, and discard the supernate. Twice wash the precipitate with 15 ml of H<sub>2</sub>O that contains a few drops of NH<sub>4</sub>OH.

Step 7. Dissolve the precipitate in 10-20 drops of concentrated HCl and evaporate to dryness. Again dissolve the dried precipitate in 1-2 drops of concentrated HCl and add 1 ml of H<sub>2</sub>O. Transfer solution to Waters “total recovery” HPLC vial with a fine-tipped pipette being careful not to pipette any residue from the bottom of the sample tube. Ensure total volume in HPLC vial is ~1mL.

#### e. HPLC Separation

*0.45µm filtered 1M alpha-HIB solution (pH 5.2-5.3) and 18MΩ H<sub>2</sub>O are used in the mobile phase (solvents).*

*Ensure all Solvent Reservoirs are filled with Fresh Solvent*

Step 1. Load samples onto columns.

Step 2. Ensure two fraction collector racks are placed in the fraction collector

Step 3. Operate the HPLC gradient from 5% to 30% alpha-HIBA over 288 vials with a flow rate of 2.5 to 3 mL per minute. Fraction collector tubes advance every minute.

Step 4. When the fraction collector method is complete, remove racks and continue to Treatment of Eluted Elements.

The approximate tubes at which the lanthanides are eluted are as follows:

lutetium 25 to 40

thulium 50 to 70

yttrium 108 to 133

terbium 133 to 153

europium 173 to 188

neodymium 193 to 208

Add a few drops of precipitating agent—8-quinolinol reagent or saturated  $\text{H}_2\text{C}_2\text{O}_4$  solution—to the collection tubes of every third row. When elution of an element is detected, add the appropriate precipitating agent to the first and last few tubes of the elution band. When elution of the element is complete, combine the tubes containing the heaviest precipitates into a separate, labeled 40-ml glass centrifuge for the oxalates or a 125-ml Erlenmeyer flask for the 8-quinolates. Label carefully.

#### f. Treatment of Eluted Elements

Any lanthanide element that is heavier than yttrium (in terms of its properties, yttrium would occupy a position between dysprosium and holmium in the lanthanide sequence) precipitates more quantitatively as the 8-quinolate than as the oxalate. Every element preceding yttrium in the sequence can best be precipitated with saturated  $\text{H}_2\text{C}_2\text{O}_4$  solution.

For the light lanthanides and yttrium, add a few drops of saturated  $\text{H}_2\text{C}_2\text{O}_4$  to each fraction to precipitate and locate the individual lanthanides. Promethium is located by measuring the activity in the tubes between samarium and neodymium. Combine the individual lanthanide fractions in centrifuge tubes. To the promethium fraction, add 2 ml of neodymium carrier. Add 5 ml of saturated  $\text{H}_2\text{C}_2\text{O}_4$  acid to the centrifuge tubes and digest the oxalates for 15 min on a water bath. Centrifuge, suspend the oxalates in ~5 ml of  $\text{H}_2\text{O}$ , and filter on a 2.5-cm filter circle. Ignite the oxalates in a porcelain crucible for ~1 h at  $950^\circ\text{C}$ .

For the heavy lanthanides, combine the fractions that contain an individual element in a 250-ml beaker. Add 1.5 ml of 8-quinolinol and concentrated  $\text{NH}_4\text{OH}$  to make each fraction alkaline to phenolphthalein. Add ~2 ml of filter pulp and digest the mixture in a water bath for 15 to 30 min. Cool to room temperature and filter on a 4.5-cm circle of paper. Wash with water. Ignite for 1.5 h at  $950^\circ\text{C}$ .

After ignition, allow the crucible to cool and grind the oxides to a fine consistency with the end of a stirring rod. Add 2 drops of ethanol and slurry; then add an additional 5 ml of ethanol, stir, and filter onto a washed, dried, and weighed filter circle. Wash with ethanol and dry at 110°C for ~10 min. Cool, weigh, and mount.

## APPENDIX B

### EGS5 SIMULATION

The Electron Gamma Shower (EGS) code is a general purpose Monte Carlo program for the simulation of electron and photon transport. In this simulation a shell script was created to run the EGS5 Fortran code. The geometry for the modeled detector is adjusted from the detector sensitive area and isotope thickness listed in the shell script.

Input files for beta spectrum are derived from International Commission on Radiological Protection Publication (ICRP) 107. The BinBeta module, written by KF Eckerman from the Radiological Toolbox software developed by Oak Ridge National Laboratory (ORNL) for U. S. Nuclear Regulatory Commission (NRC) was used to produce a beta spectrum Monte Carlo input file for EGS5 with 50 energy bins.

This appendix consists of a shell script, EGS5 code, geometry file (BC.Data File), material input file (Example BC.Inp File), and an example spectrum file from the BinBeta program.

## Example Shell Script

```
#!/bin/sh
# set -x
#
export THICKNESS
export EGSNCASES
export SENARH
export DURALTHICK
export MEDARR5
export ISOTOPE
#
EGSNCASES=1000000
DURALTHICK=0.00100
ISOTOPE=Ag-110m
FOLDER=Ag
MEDARR5=AG
compile=1
#
for SENARH in 2.5
do
for THICKNESS in 0.00017 0.00055 0.00081 0.00110 0.00137
do
echo Sensitive Area = $SENARH # Height of Sensitive Area in Detector
echo Precipitate Thickness = $THICKNESS # Precipitate Thickness
echo DURAL Thickness = $DURALTHICK # Thickness of DURAL window
if [ $compile -eq 1 ]
then
./egs5run_mod
compile=0
else
./run5again_mod
fi
done
done
#
echo " "
echo "===== "
echo "mass_attenuation script has ended"
echo "===== "
```

## EGS5 Fortran Code

```

|*****|
|*** P-10 gas proportional counter Model          *
|*** EGS5.0 USER CODE - 10 Dec 2015/2200        *
|*****|
|*****|
! This code is run under the mass_attenuation shell script *
! Beta_Counter.data file required (cg-input file) for geometry *
! Beta_Counter.inp file required for PEGS5 material inputs *
! IRCP 107 file from Radiological Toolbox (filename=$IsotopeOUT.txt) *
! created with 50 energy bins required for beta spectrum (Unit = 2) *
! Cg-data can be checked by CGview. *
! Use Ranlux random number generator. *
|*****|
|*****|
!23456789|123456789|123456789|123456789|123456789|123456789|123456789|12

!-----
!----- main code -----
implicit none
include 'include/egs5_h.f'          ! Main EGS "header" file
include 'include/egs5_bounds.f'
include 'include/egs5_brempr.f'
include 'include/egs5_edge.f'
include 'include/egs5_media.f'
include 'include/egs5_misc.f'
include 'include/egs5_stack.f'     !!! inserted
include 'include/egs5_thresh.f'
include 'include/egs5_uphiot.f'
include 'include/egs5_useful.f'
include 'include/egs5_usersc.f'
include 'include/egs5_userxt.f'
include 'include/randomm.f'
include 'auxcommons/aux_h.f'      ! Auxiliary-code "header" file
include 'auxcommons/edata.f'
include 'auxcommons/etaly1.f'
include 'auxcommons/instuf.f'
include 'auxcommons/lines.f'
include 'auxcommons/nfac.f'
include 'auxcommons/watch.f'
include 'auxcommons/geom_common.f' ! geom-common file
integer mxbin,ne
parameter (mxbin = 1024)
common/totals/depe,deltae,spec(3,mxbin),maxpict,ne,iarg2
real*8 depe,deltae,spec,specs(3,mxbin),spec2s(3,mxbin)
common/betspec/                  ! Beta Spectrum
* esbinlo(MXEBIN),esbinhi(MXEBIN),escdf(MXEBIN),nsebin
real*8 esbinlo,esbinhi,escdf,totdepe
common/pptgeo/                  ! Radius and z-plane of ppt
* rppt,pptz
real*8 rppt,pptz

```

```

integer nsebin,iarg2
real*8  totke,rnnow,etot,esumt,wtin,espdf(MXEBIN),specph(3,mxbin)
real*8  elow,eup,avsp(3),sigsp(3),rdet,tdet,dvol,emaxhisto
real*8  wtsum,pefs,pef2s,tefs,tef2s,adoses,adose2s,tefslld,
*      tef2slld,avtellld,sigtellld
real*8  phs(mxbin),ph2s(mxbin),avpe,avph,avte,avdose,dweight
real*8  sigpe,sigph,sigte,sigdose,spec2ph(3,mxbin)
real*8  radiusmylar,thickdural,thickmylar,radiusp10,thickppt,
*      thickfilter,radiusfilter,thickplanchette,radiusplanchette
real*8  saheight,saz,daheight,etotin(MXEBIN),deltaein,ekeinmax
real  tarray(2),tt,tt0,tt1,cputime,etime
integer maxpict,lnlib
integer i,icases,idin,ie,ifti,ifto,ii,iiz,imed,ireg,isam,
*      izn,nlist,j,k,n,ner,ntype,idum
character*24 medarr(MXMED),medar5
character*132 skip
character*20 isoname,betfile
character*9  thickpptstr,thick,egsnccasesstr,senareastr,dural
character*2  electroplate
real*8  lld                ! Cut off for Lower Level Discriminator
character*9  LLDstr

! -----
! Write in geometry of filter or SS backing
! and ppt thickness to the cg file
! -----
open(4,FILE='egs5job.inp',ACCESS='direct',FORM='formatted',
* RECL=77)

!  thickppt = 0.05709    ! PPT thickness (Writes in F7.5 format)
call getenv('THICKNESS', thickpptstr) ! Read in variable from .sh script
read(thickpptstr,*)thickppt

!  saheight = 2.5      ! Height of sensitive area along z-axis
call getenv('SENARH', senareastr) ! Read in variable from .sh script
read(senareastr,*)saheight

!  thickdural = 0.00100    ! DURAL Thickness [cm]
call getenv('DURALTHICK', dural) ! Read in variable from .sh script
read(dural,*)thickdural

call getenv('MEDARR5', electroplate) ! Medium of electroplate (if Ag or Cd)

if (electroplate.eq.'AG'.or.electroplate.eq.'CD')then
!  thickplanchette = 0.04572
thickplanchette = 0.03300
radiusplanchette = 0.9525
write(4,101,rec=19) thickplanchette,radiusplanchette,CHAR(13), ! Filter thickness and radius
*  CHAR(10)
rppt = 0.7720          ! Electroplate radius
pptz = thickplanchette + 0.168    ! z-axis coord of ppt and mylar for SS planchette
medarr(7)='SS_304      ' ! PEGS5 medium name for zone 7
else

```

```

    thickfilter = 0.03850
    radiusfilter = 1.2000
    write(4,101,rec=19) thickfilter,radiusfilter,CHAR(13),CHAR(10) ! SS thickness and radius
    medarr(7)='Filter_Paper' ! PEGS5 medium name for zone 7
    rppt = 0.9525 ! Filtration chimney radius
    pptz = thickfilter + 0.168 ! z-axis coord of ppt and mylar for filter
    write(4,104,rec=7) '9',pptz,CHAR(13),CHAR(10) ! Write coordinates for ppt
end if

! saz = saheight + 0.274 ! z-coord for sensitive area
daheight = 5.252 - saheight ! Height of dead area
radiusp10= 1.25 ! P-10 detector radius [cm]
thickmylar = 0.00035 + thickppt ! Thickness of mylar + ppt
! thickmylar = 0.00035 ! Thickness of mylar
radiusmylar = rppt + 0.00035

write(4,104,rec=1) '1',pptz,CHAR(13),CHAR(10) ! Write coordinates for ppt
write(4,104,rec=7) '9',pptz,CHAR(13),CHAR(10) ! Write coordinates for mylar
write(4,101,rec=2) thickppt,rppt,CHAR(13),CHAR(10) ! PPT thickness and radius
write(4,102,rec=4) thickdural,radiusp10,CHAR(13),CHAR(10) ! DURAL thickness and radius
write(4,102,rec=6) saheight,radiusp10,CHAR(13),CHAR(10) ! Sensitive Area height and radius
write(4,103,rec=8) thickmylar,radiusmylar,CHAR(13),CHAR(10) ! Mylar thickness and radius

101 format(16X,F7.5,7X,F6.4,39X,2A)
102 format(16X,F7.5,9X,F4.2,39X,2A)
103 format(16X,F7.5,6X,F7.5,39X,2A)
104 format(2X,'RCC',4X,A,2(12X,'0'),7X,F6.4,2(12X,'0'),2A)
close(4)

!-----
! Units 7-26 are used in pegs and closed. It is better not
! to use as output file. If they are used, they must be opened
! after getcg etc. Unit for pict must be 39.
!-----

! (1) Open files
call getenv('ISOTOPE', isoname) ! Read in variable from .sh script
Inlib = Inblnk(isoname)
betfile=isoname(1:Inlib)..'out.txt'
open(2,FILE=betfile,STATUS='old') !!! Beta spectrum from ICRP 107
open( 6,FILE='egs5job.out',STATUS='unknown') ! General output
open( 4,FILE='egs5job.inp',STATUS='old' ) ! CG input
open(39,FILE='egs5job.pic',STATUS='unknown') ! CG output
open(90,FILE='spc.dat' ,STATUS='unknown') ! spc-gamma output
open(91,FILE='de.dat' ,STATUS='unknown') ! dE output (**day-4)

! (2) Initialization
call counters_out(0)
call block_set

!ooo (3) User setting parameters-1
! ncases = 10000 ! number of calculations
call getenv('EGSNCASES', egscasesstr) ! Read in variable from .sh script

```

```

read(egsnccasesstr,*)ncases
maxpict = 200          ! number of incident radiations in CGview
ilines = 0
nwrite = 10
nlines = 10
iwatch = 0

!  chard(1) = 0.001          ! set characteristic dimensions
!  chard(2) = 0.01
!  chard(3) = 0.0002
!  chard(4) = 0.1
!  chard(5) = 0.00035
!  chard(6) = 0.02
!  chard(7) = 0.01
!  chard(8) = 0.1
!  chard(9) = 0.1
!  estepr(2) = 0.001D0      ! estepe multiplier
!  k1Hscl(2) = 0.001       ! Region dependent step size scaling factor
!  k1Lscl(2) = 0.001       ! Region dependent step size scaling factor
!  ecut(9) = 10
!  pcut(9) = 10

!ooo (4) User setting parameters-2 (link PEGS5-material to EGS5 med)

nmed=8
medarr(1)='Air_MCNP      '
medarr(2)='P-10_MCNP    '
medarr(3)='DURAL_Window  '
medarr(4)='Aluminum_6061 '
call getenv('MEDARR5',medar5) ! Medium of electroplate (if Ag or Cd)
medarr(5)= medar5
!  medarr(5)='KClO4      '
!  medarr(5)='KClO4_dense '
!  medarr(5)='ZrO2_dense  '
medarr(6)='Tape_Double_Sided '
!  medarr(7)='Filter_Paper ' ! Determined in geometry section
medarr(8)='Mylar        '

!ooo (5) Initialize tally parameters
ne      = 1024          ! number of energy-steps for output histogram (max mxbin)
emaxhisto = 100.0D-3    ! max energy of the output histogram (MeV)
deltae   = emaxhisto /real(ne)

!!ooo (6) Initialize tally
do j=1,ne
  do ntype=1,3
    spec  (ntype,j) = 0.D0
    specph (ntype,j) = 0.D0
    spec2ph(ntype,j) = 0.D0
  end do
end do

!ooo (7) Initialize Energy-deposit tally

```

```

ncount = 0
wtsum = 0.D0
depe = 0.D0
! pefs = 0.D0
! pef2s = 0.D0
totdepe = 0.D0
totke = 0.D0
tefs = 0.D0
tef2s = 0.D0
tefslld = 0.D0
tef2slld = 0.D0
iarg2 = 0
do j=1,ne
  phs(j) = 0.D0
  ph2s(j) = 0.D0
end do

! (8) Some treatments
call geneout(1)
call media0(medarr) ! set media
call geneout(2)
call pegs5
npreci=3 ! PICT data mode for CGView in free format
call cgcontrol(1,4,39)

!ooo (9) User setting parameters-3 (EGS options)
do i=1,nreg-1 ! Set option except vacuum region
  if(med(i).ne.0) then
    iphter(i) = 0 ! Switches for PE-angle sampling
    iedgfl(i) = 0 ! K & L-edge fluorescence
    iauger(i) = 0 ! K & L-Auger
    iraylr(i) = 0 ! Rayleigh scattering
    lpolar(i) = 0 ! Linearly-polarized photon scattering
    incohr(i) = 0 ! S/Z rejection
    iprofr(i) = 0 ! Doppler broadening
    impacr(i) = 0 ! Electron impact ionization
    if(i.eq.1.or.i.eq.2.or.i.eq.3.or.i.eq.4.or.i.eq.8)then ! 1.Precipitate, 2.DURAL, 3.P-10, 4.Air, 8.Mylar
      iraylr(i) = 1 ! Rayleigh scattering
      incohr(i) = 1 ! S/Z rejection
      iprofr(i) = 1 ! Doppler broadening
      impacr(i) = 1 ! Electron impact ionization
      iauger(i) = 1 ! K & L-Auger
    end if
  end if
end do

! (10) Some treatments
call rfluxinit0
emaxe = 0.D0 ! Autoset ecuts when emaxe=0
call hatch0
call geneout(3)
call geneout(4)
call cgcontrol(4,idum,idum)

```

```

call cgcontrol(5,idum,idum)
if(iwatch.gt.0) call swatch(-99,iwatch)

! (11) Read in Beta Spectrum from Rad_Toolkit (binbeta.exe) file
do i=1,65
  read(2,*) skip      ! Skip these lines
end do
nsebin=50      ! BinBeta output file made with 50 energy bins
do i=1,nsebin
  read(2,*) esbinlo(i),esbinhi(i),espdf(i),escdf(i)
end do
write(6,125)
125  FORMAT(/,'Beta Spectrum',/)
write(6,*)'Beta File = ',betfile
write(6,*)'Number of bins: ',nsebin
write(6,*)' E1  E2  PDF  CDF'
write(6,126) (esbinlo(i),
* esbinhi(i),espdf(i),escdf(i),i=1,nsebin)
126  format(3(F7.5,1X),F7.5)
iqin=-1      ! Incident charge - electrons
ekeinmax=esbinhi(nsebin)      ! Maximum Kinetic energy
deltaein=ekeinmax / 50      ! Energy bin for tracking source spectrum
write(6,270)
270  FORMAT(/,' Energy/Coordinates/Direction cosines/etc.',/,
* 6X,'e',14X,'x',14X,'y',14X,'z',
* 14X,'u',14X,'v',14X,'w',11X,'iq',3X,'ir',1X,'iarg',/)

call getenv('LLDES', LLDstr)! Read in variable from .sh script
read(LLDstr,*)lld      ! Read in LLD in keV

!~~~~~
!~~~~ (11) MAIN LOOP ~~~~~ MAIN LOOP
!~~~~~
do i=1,ncases

  call source(wtin)      ! source generating here
  irin = 0      ! set 0 for Autoset
  call cgcontrol(2,idum,idum) ! Autoset irin
  etot = ekein + iabs(iqin)*RM
  totke = totke + ekein      ! Keep running sum of KE

! Keep track of source spectrum
  ie=ekein/deltaein + 1
  if (ie .gt. 50) ie = 50
  etotin(ie)=etotin(ie) + wtin

! Print first NWRITE or NLINES, whichever comes first
  if (ncount .le. nwrite .and. ilines .le. nlines) then
    ilines = ilines + 1
    write(6,280)etot,xin,yin,zin,uin,vin,win,iqin,irin,idin,ncount
280  FORMAT(7G15.7,4I5)
  end if

```

```

!   Compare maximum energy of material data and incident energy
if(etot+(1-iabs(iqin))*RM.gt.emaxe) then
  write(6,fmt="( ' Stopped in MAIN.',
1  ' (Incident kinetic energy + RM) > min(UE,UP+RM).')")
  stop
end if

!   =====
!   call shower (iqin,etot,xin,yin,zin,uin,vin,win,irin,wtin) ! Main calc
!   =====

!ooo (13) Energy-deposition tally
if(depe .gt. 0.D0) then
  totdepe = totdepe + depe
  ie      = depe/deltae + 1
  if (ie .gt. ne) ie = ne
  phs(ie) = phs(ie) + wtin
  ph2s(ie) = ph2s(ie) + wtin*wtin
  tefs     = tefs     + wtin
  tef2s    = tef2s    + wtin*wtin

  if(depe.gt.lld*1.0E-3)then    ! LLD in MeV
    tefslld = tefslld + wtin
    tef2slld = tef2slld + wtin*wtin
  end if

!ooo (14) Pulse height tally
do ntype=1,3
  do ie=1,ne
    specph(ntype,ie) = specph (ntype,ie) + spec(ntype,ie)
    spec2ph(ntype,ie) = spec2ph(ntype,ie) +
*      spec(ntype,ie) * spec(ntype,ie)
    spec(ntype,ie) = 0.D0
  end do
end do
depe = 0.D0
end if

ncount = ncount + 1
if(iwatch.gt.0) call swatch(-1,iwatch)

end do
!~~~~~
!~~~~~ MAIN LOOP END
!~~~~~

tt=etime(tarray)
tt1=tarray(1)
cputime=tt1-tt0
write(6,300) cputime
300 format(/,' Elapsed Time (sec)=' ,G15.5)

write(6,310) ncount,ncases

```

```

310 FORMAT(/, Ncount='I10,' (actual cases run)',/,
*      ' Ncases='I10,' (number of cases requested)',/)

! (14) Some treatments after calculation
if(iwatch.gt.0) call swatch(-88,iwatch)
call plotxyz(99,0,0,0.D0,0.D0,0.D0,0.D0,0,0.D0,0.D0)
call cgcontrol(6,idum,idum)
call counters_out(1)

!ooo (15) output tallies
! Pulse Height Distribution
write(90,*)"Energy Deposition Tally"
write(90,*)"x:E (keV)"
write(90,*)"y:Probability per particle"
write(90,*)"p:ylog nofr noms"
write(90,*)"h:x n y1 (photon),lh0b d1 y2 (electron),lh0r d2
$      y3 (positron),lh0rrr d3"
do ie = 1,ne
  elow  = deltae*(ie-1)*1.0D3
  eup   = deltae*ie*1.0D3
  avsp(1) = specph(1,ie)/real(ncount) ! gamma spectrum
  spec2ph(1,ie)= spec2ph(1,ie)/real(ncount)
  sigsp(1) = dsqrt((spec2ph(1,ie)-avsp(1)*avsp(1))/real(ncount))
  avsp(2) = specph(2,ie) /real(ncount) ! e- spectrum
  spec2ph(2,ie)= spec2ph(2,ie)/real(ncount)
  sigsp(2) = dsqrt((spec2ph(2,ie)-avsp(2)*avsp(2))/real(ncount))
  avsp(3) = specph(3,ie) /real(ncount) ! e+ spectrum
  spec2ph(3,ie)= spec2ph(3,ie)/real(ncount)
  sigsp(3) = dsqrt((spec2ph(3,ie)-avsp(3)*avsp(3))/real(ncount))

  write(90, '(2f10.3,6(1pe12.5))')
$  elow,eup,avsp(1),sigsp(1),avsp(2),sigsp(2),avsp(3),sigsp(3)
end do

close(unit=1)

write(6,*)'~~~~~'

! Total efficiency
avte = tefs /real(ncount)
tef2s = tef2s/real(ncount)
sigte = dsqrt((tef2s-avte*avte)/real(ncount))
avte = avte *100.0
sigte = sigte*100.0
write(6, '(A,G11.4,A,G9.2,A)')
* ' Total efficiency =', avte,'+-',sigte,' %'
write(6,*)

! Total efficiency with LLD
avtellld = tefslld /real(ncount)
tef2slld = tef2slld/real(ncount)
sigtellld = dsqrt((tef2slld-avtellld*avtellld)/real(ncount))
avtellld = avtellld *100.0

```

```

sigtelld = sigtelld*100.0
write(6,'(A,G11.4,A,G9.2,A)')
* ' Total efficiency with LLD =', avtelld,'+-',sigtelld,' %'
write(6,*)

write(6,'(A,G11.4)') Total energy in system [MeV] = ',totke
write(6,*)
write(6,'(A,G11.4,2X,G9.2,A)') Total deposited energy [MeV] = ',
*      totdepe,totdepe/totke*100.0,'%'
write(6,*)
write(6,*)'~~~~~'

! Deposited energy after each step
write(6,*)
write(6,*)Total number ausgab(iarg=2) calls = ',iarg2

open(unit=1,file='dE_spectrum.csv',form='formatted',
* status='unknown',access='append')
write(1,*)Deposited Energy Tally'
write(1,*)ncases, ppt thickness [cm], total efficiency, sigma,
* sensitive area height [cm], DURAL thickness'
write(1,*)ncases,',',thickppt,',',avte,',',sigte,
* ',',saheight,',',thickdural
write(1,*)'E-lo [keV]',',',E-high [keV]',',',PDF',',',sigma'
! Total energy deposition tally per particle
write(91,*)"Energy Deposition Tally"
write(91,*)'x:E (keV)'
write(91,*)'y:PDF'
write(91,*)'p:ylog nofr noms'
write(91,*)'h:x n y,lh0cc d'
do ie = 1,ne
  elow  = deltae*(ie-1)*1.0D03
  eup   = deltae*ie*1.0D03
  avph  = phs(ie) / real(ncount)
  ph2s(ie) = ph2s(ie) / real(ncount)
  sigph = dsqrt((ph2s(ie)-avph*avph)/real(ncount))
  write(91,',(2f10.3,g12.5,g12.5))elow,eup,avph,sigph
  write(1,*) elow,',',eup,',',avph,',',sigph
end do
close(unit=1)

open(unit=1,file='mass_att.dat',form='formatted',
* status='unknown',access='append')
write(1,*)ncases,',',thickppt,',',avte,',',sigte,',',avtelld,',',
* sigtelld,',',saheight,',',thickdural,',',lld,',',isoname
close(unit=1)

! Source spectrum
write(6,*)
write(6,*)'Source Spectrum'
write(6,'(A,G11.4)')End point energy = ',ekeinmax
write(6,*)'Upper Energy      PDF'
write(6,415) (deltaein*ie,etoin(ie)/ncount,ie=1,50)

```

415 FORMAT(G10.5,' MeV--',1X,G12.5)

```
write(6,*)'~~~~~'  
write(6,*)  EGS5 sucessfully finished!  '  
write(6,*)'~~~~~'  
end
```

```
!-----subroutine source-----  
!ooo (16) Source description  
subroutine source(wtin)  
implicit none  
include 'include/egs5_h.f'      ! Main EGS "header" file  
include 'auxcommons/aux_h.f'   ! Auxiliary-code "header" file  
include 'auxcommons/instuf.f'  
include 'include/randomm.f'  
include 'include/egs5_stack.f'  
common/betspec/                ! Beta Spectrum  
* esbinlo(MXEBIN),esbinhi(MXEBIN),escdf(MXEBIN),nsebin  
real*8 esbinlo,esbinhi,escdf,rnnow  
common/pptgeo/                 ! Radius and z-plane of ppt  
* rppt,pptz  
real*8 rppt,pptz  
integer nsebin,i  
real*8 pi,wtin,phi,thet,rr0,xi0,yi0,zi0,zimin,thickppt  
parameter (pi=3.14159265358979d0)  
character*9 thickpptstr  
  
wtin = 1.0      ! Incident particle weight  
iqin = -1      ! Incident particle charge  
  
! Determine energy from beta spectrum  
call randomset(rnnow)  
do i=2,nsebin  
  if(rnnow.le.escdf(i)) go to 1000  
end do  
1000 ekein=esbinhi(i)-(esbinhi(i)-esbinlo(i)) * (escdf(i)-rnnow)  
* / (escdf(i)-escdf(i-1))  
  
! Determine position within precipitate  
1100 call randomset(rnnow)  
xi0=2.0*rnnow-1.0  
call randomset(rnnow)  
yi0=2.0*rnnow-1.0  
rr0=sqrt(xi0*xi0+yi0*yi0)  
if (rr0.gt.1.0) go to 1100  
call randomset(rnnow)  
zi0=rnnow  
! rppt = 0.9525      ! Filtration chimney radius  
  
xin=xi0*rppt      ! Source position  
yin=yi0*rppt  
! zimin=0.2065      ! z-plane for start of ppt  
zimin=pptz        ! z-plane for start of ppt
```

```

call getenv('THICKNESS', thickpstr) ! Read in variable from .sh script
read(thickpstr,*)thickpstr
zin = zimin + zi0 * thickpstr

! Isotropic Source - Direction
call randomset(rnnow)
phi = rnnow*pi
call randomset(rnnow)
thet = (2*rnnow - 1)*pi
uin = sin(phi)*cos(thet)
vin = sin(phi)*sin(thet)
win = cos(phi)

! Verify the normalization of source direction cosines
if(abs(uin*uin+vin*vin+win*win-1.0).gt.1.e-6) then
  write(6,fmt='( Following source direction cosines are not',
1  ' normalized.',3e12.5)')uin,vin,win
  stop
end if
end

!-----end subroutine source-----

!-----ausgab.f-----
!-----
!23456789|123456789|123456789|123456789|123456789|123456789|123456789|12
!-----
! Required subroutine for use with the EGS5 Code System
!-----
! A AUSGAB to:
!
! 1) Score total energy deposition and energy deposition with LLD
! 2) Score pulse height deposition of each particle inside detector
! 3) Print out particle transport information
! 4) call plotxyz if ncount<=maxpict
!-----

subroutine ausgab(iarg)

implicit none
include 'include/egs5_h.f' ! Main EGS "header" file
include 'include/egs5_epcont.f' ! COMMONs required by EGS5 code
include 'include/egs5_misc.f'
include 'include/egs5_stack.f'
include 'include/egs5_useful.f'
include 'auxcommons/aux_h.f' ! Auxiliary-code "header" file
include 'auxcommons/etaly1.f' ! Auxiliary-code COMMONs
include 'auxcommons/lines.f'
include 'auxcommons/ntaly1.f'
include 'auxcommons/watch.f'
integer mxbin,ne
parameter (mxbin = 1024)
common/totals/depe,deltae,spec(3,mxbin),maxpict,ne,iarg2
real*8 depe,deltae,spec,edepwt

```

```

integer iarg,maxpict,ie,iql,irl,ntype,iarg2

irl = ir(np)
iql = iq(np)

!ooo set deposit energy
  edepwt = edep*wt(np)

  if (iarg .lt. 5) then ! Keep track of energy deposition (for conservation purposes)
    esum(iql+2,irl,iarg+1) = esum(iql+2,irl,iarg+1) + edepwt
    nsum(iql+2,irl,iarg+1) = nsum(iql+2,irl,iarg+1) + 1
  end if

  if (iwatch .gt. 0) call swatch(iarg,iwatch)
  if(iarg.ge.5) return

!-----
!ooo Tally (for single-irl ver.) -----
!-----
  if ( irl.eq.3 ) then

!ooo Energy Deposition
  depe = depe + edepwt

!ooo Pulse Height Deposition Tally
  if ( iql.eq.0 ) then      ! photon
    ntype = 1
  elseif ( iql.eq.-1 ) then ! electron
    ntype = 2
  else                      ! positron
    ntype = 3
  endif
  do ie=1,mxbin
    if(edepwt.le.ie*deltae) go to 2000
    if(ie.eq.mxbin) go to 2000
  end do
2000 spec(ntype,ie) = spec(ntype,ie) + edep

  if(iarg.eq.2) iarg2 = iarg2 + 1
  endif

!-----
!----- Tally end -----
!-----

  if (ncount.le.maxpict) then
    call plotxyz(iarg,np,iq(np),x(np),y(np),z(np),e(np),ir(np),
*      wt(np),time(np))
  end if

  return
  end

!-----last line of ausgab.f-----
!-----howfar.f-----
! Version: 070627-1600

```

! Reference: T. Torii and T. Sugita, "Development of PRESTA-CG  
! Incorporating Combinatorial Geometry in EGS4/PRESTA", JNC TN1410 2002-201,  
! Japan Nuclear Cycle Development Institute (2002).  
! Improved version is provided by T. Sugita. 7/27/2004

!-----  
! Required (geometry) subroutine for use with the EGS5 Code System  
!-----

! This is a CG-HOWFAR.  
!-----

```

subroutine howfar
implicit none
include 'include/egs5_h.f'      ! Main EGS "header" file
include 'include/egs5_epcont.f' ! COMMONs required by EGS5 code
include 'include/egs5_stack.f'
include 'auxcommons/geom_common.f' ! geom-common file
integer i,j,jjj,ir_np,nozone,jty,kno
integer irnear,irnext,irlold,irlfg,itvlf,ihitcg
double precision xidd,yidd,zidd,x_np,y_np,z_np,u_np,v_np,w_np
double precision tval,tval0,tval00,tval10,tvalmn,delhow
double precision atvaltmp
integer iq_np

ir_np = ir(np)
iq_np = iq(np) + 2

if(ir_np.le.0) then
  write(6,*) 'Stopped in howfar with ir(np) <=0'
  stop
end if

if(ir_np.gt.izonin) then
  write(6,*) 'Stopped in howfar with ir(np) > izonin'
  stop
end if

if(ir_np.EQ.izonin) then
  idisc=1
  return
end if

tval=1.d+30
itvalm=0

c  body check
u_np=u(np)
v_np=v(np)
w_np=w(np)
x_np=x(np)
y_np=y(np)
z_np=z(np)

do i=1,nbbody(ir_np)
  nozone=ABS(nbzone(i,ir_np))

```

```

jty=itblty(nozone)
kno=itblno(nozone)
c rpp check
  if(jty.eq.ityknd(1)) then
    if(kno.le.0.or.kno.gt.irppin) go to 190
    call rppcg1(kno,x_np,y_np,z_np,u_np,v_np,w_np)
c sph check
  elseif(jty.eq.ityknd(2)) then
    if(kno.le.0.or.kno.gt.isphin) go to 190
    call sphcg1(kno,x_np,y_np,z_np,u_np,v_np,w_np)
c rcc check
  elseif(jty.eq.ityknd(3)) then
    if(kno.le.0.or.kno.gt.irccin) go to 190
    call rcccg1(kno,x_np,y_np,z_np,u_np,v_np,w_np)
c trc check
  elseif(jty.eq.ityknd(4)) then
    if(kno.le.0.or.kno.gt.itrcin) go to 190
    call trccg1(kno,x_np,y_np,z_np,u_np,v_np,w_np)
c tor check
  elseif(jty.eq.ityknd(5)) then
    if(kno.le.0.or.kno.gt.itorin) go to 190
    call torcg1(kno,x_np,y_np,z_np,u_np,v_np,w_np)
c rec check
  elseif(jty.eq.ityknd(6)) then
    if(kno.le.0.or.kno.gt.irecin) go to 190
    call reccg1(kno,x_np,y_np,z_np,u_np,v_np,w_np)
c ell check
  elseif(jty.eq.ityknd(7)) then
    if(kno.le.0.or.kno.gt.iellin) go to 190
    call ellcg1(kno,x_np,y_np,z_np,u_np,v_np,w_np)
c wed check
  elseif(jty.eq.ityknd(8)) then
    if(kno.le.0.or.kno.gt.iwedin) go to 190
    call wedcg1(kno,x_np,y_np,z_np,u_np,v_np,w_np)
c box check
  elseif(jty.eq.ityknd(9)) then
    if(kno.le.0.or.kno.gt.iboxin) go to 190
    call boxcg1(kno,x_np,y_np,z_np,u_np,v_np,w_np)
c arb check
  elseif(jty.eq.ityknd(10)) then
    if(kno.le.0.or.kno.gt.iarbin) go to 190
    call arbcg1(kno,x_np,y_np,z_np,u_np,v_np,w_np)
c hex check
  elseif(jty.eq.ityknd(11)) then
    if(kno.le.0.or.kno.gt.ihexin) go to 190
    call hexcg1(kno,x_np,y_np,z_np,u_np,v_np,w_np)
c haf check
  elseif(jty.eq.ityknd(12)) then
    if(kno.le.0.or.kno.gt.ihafin) go to 190
    call hafcg1(kno,x_np,y_np,z_np,u_np,v_np,w_np)
c tec check
  elseif(jty.eq.ityknd(13)) then
    if(kno.le.0.or.kno.gt.itecin) go to 190

```

```

    call teccg1(kno,x_np,y_np,z_np,u_np,v_np,w_np)
c   gel check
    elseif(jty.eq.ityknd(14)) then
        if(kno.le.0.or.kno.gt.igelin) go to 190
        call gelcg1(kno,x_np,y_np,z_np,u_np,v_np,w_np)
c
c**** add new geometry in here
c
    end if
190 continue
    end do
c
    irnear=ir_np
    if(itvalm.eq.0) then
        tval0=cgeps1
        xidd=x_np+tval0*u_np
        yidd=y_np+tval0*v_np
        zidd=z_np+tval0*w_np
310 continue
        if(x_np.ne.xidd.or.y_np.ne.yidd.or.z_np.ne.zidd) goto 320
        tval0=tval0*10.d0
        xidd=x_np+tval0*u_np
        yidd=y_np+tval0*v_np
        zidd=z_np+tval0*w_np
        go to 310
320 continue
c   write(*,*) 'srzone:1'
    call srzone(xidd,yidd,zidd,iq_np,ir_np,irnext)
c
    if(irnext.ne.ir_np) then
        tval=0.0d0
        irnear=irnext
    else
        tval00=0.0d0
        tval10=10.0d0*tval0
        irlold=ir_np
        irlfg=0
330 continue
        if(irlfg.eq.1) go to 340
        tval00=tval00+tval10
        if(tval00.gt.1.0d+06) then
            write(6,9000) iq(np),ir(np),x(np),y(np),z(np),
&                u(np),v(np),w(np),tval00
9000 format(' TVAL00 ERROR : iq,ir,x,y,z,u,v,w,tval=',
&        2I3,1P7E12.5)
            stop
        end if
        xidd=x_np+tval00*u_np
        yidd=y_np+tval00*v_np
        zidd=z_np+tval00*w_np
        call szold(xidd,yidd,zidd,irlold,irlfg)
        go to 330
340 continue

```

```

c
  tval=tval00
  do j=1,10
    xidd=x_np+tval00*u_np
    yidd=y_np+tval00*v_np
    zidd=z_np+tval00*w_np
c
    write(*,*) 'srzone:2'
    call srzone(xidd,yidd,zidd,iq_np,irlold,irnext)
    if(irnext.ne.irlold) then
      tval=tval00
      irnear=irnext
    end if
    tval00=tval00-tval0
  end do
  if(ir_np.eq.irnear) then
    write(0,*) 'ir(np),tval=',ir_np,tval
  end if
end if
else
  do j=1,itvalm-1
    do i=j+1,itvalm
      if(atval(i).lt.atval(j)) then
        atvaltmp=atval(i)
        atval(i)=atval(j)
        atval(j)=atvaltmp
      endif
    enddo
  enddo
  itvlf=0
  tvalmn=tval
  do jjj=1,itvalm
    if(tvalmn.gt.atval(jjj)) then
      tvalmn=atval(jjj)
    end if
    delhow=cgeps2
    tval0=atval(jjj)+delhow
    xidd=x_np+tval0*u_np
    yidd=y_np+tval0*v_np
    zidd=z_np+tval0*w_np
410  continue
    if(x_np.ne.xidd.or.y_np.ne.yidd.or.z_np.ne.zidd) go to 420
    delhow=delhow*10.d0
    tval0=atval(jjj)+delhow
    xidd=x_np+tval0*u_np
    yidd=y_np+tval0*v_np
    zidd=z_np+tval0*w_np
    go to 410
420  continue
c
  write(*,*) 'srzone:3'
  call srzone(xidd,yidd,zidd,iq_np,ir_np,irnext)
  if((irnext.ne.ir_np.or.atval(jjj).ge.1.).and.
&   tval.gt.atval(jjj)) THEN
    tval=atval(jjj)

```

```

        irnear=irnext
        itvlfq=1
        goto 425
    end if
end do
425 continue
    if(itvlfq.eq.0) then
        tval0=cgmnst
        xidd=x_np+tval0*u_np
        yidd=y_np+tval0*v_np
        zidd=z_np+tval0*w_np
430 continue
        if(x_np.ne.xidd.or.y_np.ne.yidd.or.z_np.ne.zidd) go to 440
        tval0=tval0*10.d0
        xidd=x_np+tval0*u_np
        yidd=y_np+tval0*v_np
        zidd=z_np+tval0*w_np
        go to 430
440 continue
        if(tvalmn.gt.tval0) then
            tval=tvalmn
        else
            tval=tval0
        end if
    end if
end if
    ihitcg=0
    if(tval.le.ustep) then
        ustep=tval
        ihitcg=1
    end if
    if(ihitcg.eq.1) THEN
        if(irnear.eq.0) THEN
            write(6,9200) iq(np),ir(np),x(np),y(np),z(np),
            &          u(np),v(np),w(np),tval
9200 format(' TVAL ERROR : iq,ir,x,y,z,u,v,w,tval=',2I3,1P7E12.5)
            idisc=1
            itverr=itverr+1
            if(itverr.ge.100) then
                stop
            end if
            return
        end if
        irnew=irnear
        if(irnew.ne.ir_np) then
            call rstnxt(iq_np,ir_np,irnew)
        endif
    end if
    return
end

```

!-----last line of subroutine howfar-----

```

subroutine geneout(iout)
implicit none
!-----
! iout and general outputs
! 1 Media information (general output)
! 2 Character dimensions (general output)
! 3 Media information (general output)
! 4 X-ray information (general output)
!-----
integer iout,i,j,ii,iiz,izn,ner
include 'include/egs5_h.f'
include 'include/egs5_bounds.f'
include 'include/egs5_brempr.f'
include 'include/egs5_edge.f'
include 'include/egs5_media.f'
include 'include/egs5_misc.f'
include 'include/egs5_thresh.f'
include 'include/egs5_uphiot.f'
include 'include/egs5_useful.f'
include 'include/egs5_usersc.f'
include 'include/egs5_userxt.f'
include 'include/randomm.f'
include 'auxcommons/aux_h.f'
include 'auxcommons/edata.f'
include 'auxcommons/etaly1.f'
include 'auxcommons/instuf.f'
include 'auxcommons/lines.f'
include 'auxcommons/nfac.f'
include 'auxcommons/watch.f'
include 'auxcommons/geom_common.f' ! geom-common file

if( iout.eq.1 )then
  if(nmed.gt.MXMED) then
    write(6,'(A,I4,A,I4,A/A)')
*    ' nmed ('nmed,') larger than MXMED ('MXMED,)',
*    ' MXMED in iclude/egs5_h.f must be increased.'
    stop
  end if

elseif( iout.eq.2)then
  write(6,fmt="(chard =,5e12.5)") (chard(j),j=1,nmed)
  write(6,'(A/)') 'PEGS5-call comes next'

elseif( iout.eq.3 )then
  write(6,'(/A)') ' Quantities associated with each MEDIA:'
  do j=1,nmed
    write(6,'(/1X,24A1)') (media(i,j),i=1,24)
    write(6,'(5X,A,G15.7,A,G15.7,A)')
*    ' rho=',rhom(j),' g/cu.cm   rlc=',rlcm(j),' cm'
    write(6,'(5X,A,G15.7,A,G15.7,A)')
*    ' ae=',ae(j),' MeV   ue=',ue(j),' MeV'
    write(6,'(5X,A,G15.7,A,G15.7,A/)')
*    ' ap=',ap(j),' MeV   up=',up(j),' MeV'
  end do
end if

```

```

end do

elseif( iout.eq.4 )then
  do i=1,nreg
    if (med(i) .eq. 0) then
      write(6,'(A,I3,A)') ' medium(',i,')=vacuum'
    else
      write(6,'(A,I3,A,24A1,A,G10.5,A,G10.5,A)')
*      ' medium in region(',i,')=',(media(ii,med(i)),ii=1,24),
*      'ecut=',ecut(i),' MeV, pcut=',pcut(i),' MeV'

      if (iedgfl(i) .ne. 0) then ! Output X-ray energy
        ner = nne(med(i))
        do iiz=1,ner
          izn = zelem(med(i),iiz) ! Atomic number of this element
          write(6,'(A,I3)') ' X-ray information for Z=',izn
          write(6,'(A/4G15.5/4G15.5/2G15.5)')
*          ' K-X-ray energy in keV',(ekx(ii,izn),ii=1,10)
          write(6,'(A/4G15.5/4G15.5)')
*          ' L-1 X-ray in keV',(elx1(ii,izn),ii=1,8)
          write(6,'(A/4G15.5/G15.5)')
*          ' L-2 X-ray in keV',(elx2(ii,izn),ii=1,5)
          write(6,'(A/4G15.5/3G15.5)')
*          ' L-3 X-ray in keV',(elx3(ii,izn),ii=1,7)
        end do
      end if
    end if
  end do
endif
end

```

```

subroutine cgcontrol(icnt,i1,i2)
implicit none

```

```

!-----
! icnt and treatment
! 1 call geomgt and write dummy geom
! 2
! 3
! 4 region and medium information (CG output)
!-----

```

```

integer i,j,icnt,ifti,ifto,i1,i2
include 'include/egs5_h.f'
include 'include/egs5_bounds.f'
include 'include/egs5_brempr.f'
include 'include/egs5_edge.f'
include 'include/egs5_media.f'
include 'include/egs5_misc.f'
include 'include/egs5_thresh.f'
include 'include/egs5_uphiot.f'
include 'include/egs5_useful.f'
include 'include/egs5_usersc.f'
include 'include/egs5_userxt.f'
include 'include/randomm.f'

```

```

include 'auxcommons/aux_h.f'
include 'auxcommons/edata.f'
include 'auxcommons/etaly1.f'
include 'auxcommons/instuf.f'
include 'auxcommons/lines.f'
include 'auxcommons/nfac.f'
include 'auxcommons/watch.f'
include 'auxcommons/geom_common.f' ! geom-common file

if( icnt.eq.1 )then
  ifti = i1
  ifto = i2
  write(6,fmt="(' CG data)")
  call geomgt(ifti,6) ! Read in CG data
  write(6,fmt="(' End of CG data',/)")

  if(npreci.eq.3) write(ifto,fmt="('CSTA-FREE-TIME)")
  if(npreci.eq.2) write(ifto,fmt="('CSTA-TIME)")

  rewind ifti
  call geomgt(ifti,ifto) ! Dummy call to write geom info for ifto
  write(ifto,'(A)') 'CEND'

  nreg = izonin
  read(4,*) (med(i),i=1,nreg)

elseif( icnt.eq.2 )then

  if(irin.le.0.or.irin.gt.nreg) then
    call srzone(xin,yin,zin,iqin+2,0,irin)
    if(irin.le.0.or.irin.ge.nreg) then
      write(6,'(A,I5)') ' Stopped in MAIN. irin = ',irin
      stop
    end if
    call rstnxt(iqin+2,0,irin)
  end if

elseif( icnt.eq.4 )then

  write(39,fmt="('MSTA)")
  write(39,fmt="(i4)") nreg
  write(39,fmt="(15i4)") (med(i),i=1,nreg)
  write(39,fmt="('MEND)")

elseif( icnt.eq.5 )then
  write(39,fmt="(0 1)")

elseif( icnt.eq.6 )then
  write(39,'(A)') '9' ! Set end of batch for CG View
endif
end

subroutine media0(medarr)

```

```

implicit none
include 'include/egs5_h.f'
include 'include/egs5_media.f'
character*24 medarr(MXMED)
integer i,j
do j=1,nmed
  do i=1,24
    media(i,j)=medarr(j)(i:i)
  end do
end do
end

```

```

subroutine rluxinit0
include 'include/randomm.f'
luxlev = 1
inseed = 1
write(6,'(/A,I12,5X,A)') ' inseed=',inseed,
*   '(seed for generating unique sequences of Ranlux)'
call rluxinit ! Initialize the Ranlux random-number generator
end

```

```

subroutine hatch0
include 'include/egs5_h.f'
include 'include/egs5_misc.f'
write(6,'(/A)') ' Call hatch to get cross-section data'
open(UNIT=KMPI,FILE='pgs5job.pegs5dat',STATUS='old')
open(UNIT=KMPO,FILE='egs5job.dummy',STATUS='unknown')
call hatch
close(UNIT=KMPI)
close(UNIT=KMPO)
end

```

**BC.Data File**

```

RCC 1 0 0 0.2065 0 0
      0.01105 0.9525
RCC 3 0 0 0.274 0 0
      0.00100 1.25
RCC 2 0 0 0.274 0 0
      2.10000 1.25
RCC 9 0 0 0.2065 0 0
      0.00035 0.95285
SPH 4 0 0 0 20
RCC 10 0 0 0.774 0 0
      5.526 1.75
RPP 5 -3.175 3.175 -4.125 4.125 0.274
      0.774
RPP 6 -3.175 3.175 -4.125 4.125 0
      0.16
RPP 7 -2.5 2.5 -2.5 2.5 0.16
      0.168
RCC 8 0 0 0.168 0 0
      0.0385 1.2
END
Z0001 +1
Z0002 +3
Z0003 +2 -3
Z0004 +4 -10 -5 -6 -1 -7 -8
      -9
Z0005 +10 -2 OR +5 -2 -3 OR +6
Z0006 +7
Z0007 +8
Z0008 +9 -1
Z0009 -4
END
5 3 2 1 4 6 7 8 0

```

### Example BC.Inp File

```
MIXT
&INP NE=6,RHO=0.18,RHOZ=0.035173,0.031757,0.004662,0.689506,0.227338,0.011553,
  IAPRIM=1,IRAYL=1,IBOUND=1,INCOH=1,ICPROF=-3,IMPACT=1,
  EFRACL=0.01,EFRACH=0.01 &END
PdDMG
PD C H N O AR
ENER
&INP AE=0.512,AP=0.0010,UE=4.1,UP=3.6 /END
PWLF
&INP /END
DECK
&INP /END
MIXT
&INP NE=4,RHO=0.61,RHOZ=0.086569,0.245183,0.656936,0.011311,
  IAPRIM=1,IRAYL=1,IBOUND=1,INCOH=1,ICPROF=-3,IMPACT=1,
  EFRACL=0.01,EFRACH=0.01 &END
MoO3
MO O N AR
ENER
&INP AE=0.512,AP=0.0010,UE=4.1,UP=3.6 /END
PWLF
&INP /END
DECK
&INP /END
MIXT
&INP NE=5,RHO=0.78,RHOZ=0.303099,0.521508,0.00898,0.087273,0.07914,
  IAPRIM=1,IRAYL=1,IBOUND=1,INCOH=1,ICPROF=-3,IMPACT=1,
  EFRACL=0.01,EFRACH=0.01 &END
KClO4
O N AR K CL
ENER
&INP AE=0.512,AP=0.0010,UE=4.1,UP=3.6 /END
PWLF
&INP /END
DECK
&INP /END
MIXT
&INP NE=4,RHO=0.7,RHOZ=0.07486,0.224202,0.689073,0.011865,
  IAPRIM=1,IRAYL=1,IBOUND=1,INCOH=1,ICPROF=-3,IMPACT=1,
  EFRACL=0.01,EFRACH=0.01 &END
Nd2O3
ND O N AR
ENER
&INP AE=0.512,AP=0.0010,UE=4.1,UP=3.6 /END
PWLF
&INP /END
DECK
&INP /END
MIXT
&INP NE=8,RHO=7.999,RHOZ=0.18,0.1, 0.0008,0.02,0.01,0.00045,0.0003,0.68845,
```

```

    IAPRIM=1,IRAYL=1,IBOUND=1,INCOH=1,ICPROF=-3,IMPACT=1,
    EFRACL=0.01,EFRACH=0.01 &END
SS_304
CR NI C MN SI P S FE
ENER
&INP AE=0.512,AP=0.0010,UE=4.1,UP=3.6 /END
PWLF
&INP /END
DECK
&INP /END
MIXT
&INP NE=3,RHO=1.38,RHOZ=0.041959,0.625017,0.33302,
    IAPRIM=1,IRAYL=1,IBOUND=1,INCOH=1,ICPROF=-3,IMPACT=1,
    EFRACL=0.01,EFRACH=0.01 &END
Mylar
H C O
ENER
&INP AE=0.512,AP=0.0010,UE=4.1,UP=3.6 /END
PWLF
&INP /END
DECK
&INP /END
MIXT
&INP NE=3,RHO=1.49,RHOZ=0.061708,0.4445,0.4934 /END
Filter_Paper
H C O
ENER
&INP AE=0.512,AP=0.0010,UE=4.1,UP=3.6 /END
PWLF
&INP /END
DECK
&INP /END
MIXT
&INP NE=3,RHO=1.7,RHOZ=0.020793,0.247793,0.731431 /END
Tape_Double_Sided
H C CL
ENER
&INP AE=0.512,AP=0.0010,UE=4.1,UP=3.6 /END
PWLF
&INP /END
DECK
&INP /END
MIXT
&INP NE=5,RHO=2.7,RHOZ=0.01,0.97875,0.006,0.0025,0.00275,
    IMPACT=0,IRAYL=1 /END
Aluminum_6061
MG AL SI CR CU
ENER
&INP AE=0.512,AP=0.0010,UE=4.1,UP=3.6 /END
PWLF
&INP /END
DECK
&INP /END

```

```

MIXT
&INP NE=3,RHO=2.8,RHOZ=0.95,0.04,0.01,
  IAPRIM=1,IRAYL=1,IBOUND=1,INCOH=1,ICPROF=-3,IMPACT=1,
  EFRACL=0.01,EFRACH=0.01 &END
DURAL_Window
AL CU MG
ENER
&INP AE=0.512,AP=0.0010,UE=4.1,UP=3.6 /END
PWLF
&INP /END
DECK
&INP /END
MIXT
&INP NE=3,RHO=0.96E-03,GASP=1.0,RHOZ=0.23143,0.75575,0.01282,
  IAPRIM=1,IRAYL=1,IBOUND=1,INCOH=1,ICPROF=-3,IMPACT=1,
  EFRACL=0.01,EFRACH=0.01 &END
Air_MCNP
O N AR
ENER
&INP AE=0.512,AP=0.0010,UE=4.1,UP=3.6 /END
PWLF
&INP /END
DECK
&INP /END
MIXT
&INP NE=3,RHO=1.56E-03,GASP=0.82,RHOZ=0.286,0.071,0.643,
  IAPRIM=1,IRAYL=1,IBOUND=1,INCOH=1,ICPROF=-3,IMPACT=1,
  EFRACL=0.01,EFRACH=0.01 &END
P-10_MCNP
H C AR
ENER
&INP AE=0.51114,AP=0.0010,UE=4.1,UP=3.6 /END
PWLF
&INP /END
DECK
&INP /END

```

## Example Spectrum File

Ag-110M Decay Mode: B-IT T1/2 = 249.76 d

Below is the beta spectrum normalized and binned for sampling in Monte Carlo calculations. Distributions for bins uniform in energy and uniform in probability are tabulated. P(E1, E2) is probability of a beta with energy between E1 and E2 and P(0, E2) is the probability of a particle of energy < E2.

Beta yield (/nt) = 9.864E-01  
Energy (MeV/nt) = 6.917E-02  
Mean energy (MeV) = 7.013E-02  
End point (MeV) = 1.467E+00

Spectrum normalized to emission of a single beta particle.

50 Bins Uniform in Energy

E1	E2	P(E1,E2)	P(0,E2)
0.00000	0.02935	0.51645	5.1645E-01
0.02935	0.05869	0.21031	7.2676E-01
0.05869	0.08804	0.05140	7.7816E-01
0.08804	0.11739	0.03005	8.0820E-01
0.11739	0.14674	0.02837	8.3657E-01
0.14674	0.17608	0.02656	8.6313E-01
0.17608	0.20543	0.02448	8.8761E-01
0.20543	0.23478	0.02216	9.0977E-01
0.23478	0.26412	0.01965	9.2942E-01
0.26412	0.29347	0.01700	9.4642E-01
0.29347	0.32282	0.01429	9.6070E-01
0.32282	0.35216	0.01158	9.7229E-01
0.35216	0.38151	0.00897	9.8125E-01
0.38151	0.41086	0.00652	9.8777E-01
0.41086	0.44020	0.00434	9.9211E-01
0.44020	0.46955	0.00254	9.9465E-01
0.46955	0.49890	0.00116	9.9581E-01
0.49890	0.52825	0.00054	9.9634E-01
0.52825	0.55759	0.00032	9.9666E-01
0.55759	0.58694	0.00028	9.9694E-01
0.58694	0.61629	0.00026	9.9720E-01
0.61629	0.64563	0.00024	9.9744E-01
0.64563	0.67498	0.00022	9.9766E-01
0.67498	0.70433	0.00020	9.9786E-01
0.70433	0.73368	0.00018	9.9804E-01
0.73368	0.76302	0.00017	9.9821E-01
0.76302	0.79237	0.00015	9.9836E-01
0.79237	0.82172	0.00015	9.9851E-01
0.82172	0.85106	0.00014	9.9865E-01
0.85106	0.88041	0.00013	9.9878E-01
0.88041	0.90976	0.00013	9.9891E-01
0.90976	0.93910	0.00012	9.9903E-01
0.93910	0.96845	0.00012	9.9915E-01
0.96845	0.99780	0.00011	9.9926E-01

0.99780	1.02714	0.00010	9.9936E-01
1.02714	1.05649	0.00010	9.9945E-01
1.05649	1.08584	0.00009	9.9954E-01
1.08584	1.11519	0.00008	9.9962E-01
1.11519	1.14453	0.00007	9.9970E-01
1.14453	1.17388	0.00006	9.9976E-01
1.17388	1.20323	0.00006	9.9982E-01
1.20323	1.23257	0.00005	9.9987E-01
1.23257	1.26192	0.00004	9.9991E-01
1.26192	1.29127	0.00003	9.9994E-01
1.29127	1.32062	0.00002	9.9996E-01
1.32062	1.34996	0.00002	9.9998E-01
1.34996	1.37931	0.00001	9.9999E-01
1.37931	1.40866	0.00001	1.0000E+00
1.40866	1.43800	0.00000	1.0000E+00
1.43800	1.46735	0.00000	1.0000E+00

#### 50 Bins Uniform in Probability

E1	E2	P(E1,E2)	P(0,E2)
0.00000	0.00083	0.02000	2.0000E-02
0.00083	0.00168	0.02000	4.0000E-02
0.00168	0.00254	0.02000	6.0000E-02
0.00254	0.00342	0.02000	8.0000E-02
0.00342	0.00431	0.02000	1.0000E-01
0.00431	0.00523	0.02000	1.2000E-01
0.00523	0.00616	0.02000	1.4000E-01
0.00616	0.00712	0.02000	1.6000E-01
0.00712	0.00809	0.02000	1.8000E-01
0.00809	0.00909	0.02000	2.0000E-01
0.00909	0.01011	0.02000	2.2000E-01
0.01011	0.01115	0.02000	2.4000E-01
0.01115	0.01222	0.02000	2.6000E-01
0.01222	0.01332	0.02000	2.8000E-01
0.01332	0.01444	0.02000	3.0000E-01
0.01444	0.01560	0.01999	3.1999E-01
0.01560	0.01679	0.02003	3.4002E-01
0.01679	0.01802	0.01998	3.6000E-01
0.01802	0.01928	0.02000	3.8000E-01
0.01928	0.02060	0.02000	4.0000E-01
0.02060	0.02195	0.02000	4.2000E-01
0.02195	0.02336	0.02000	4.4000E-01
0.02336	0.02483	0.02000	4.6000E-01
0.02483	0.02636	0.02000	4.8000E-01
0.02636	0.02797	0.02000	5.0000E-01
0.02797	0.02965	0.02000	5.2000E-01
0.02965	0.03143	0.01996	5.3996E-01
0.03143	0.03332	0.02010	5.6006E-01
0.03332	0.03533	0.01995	5.8001E-01
0.03533	0.03748	0.01997	5.9998E-01
0.03748	0.03982	0.02001	6.1999E-01
0.03982	0.04239	0.02003	6.4002E-01
0.04239	0.04523	0.01998	6.6000E-01
0.04523	0.04846	0.02000	6.8000E-01

0.04846	0.05224	0.02000	7.0000E-01
0.05224	0.05685	0.02000	7.2000E-01
0.05685	0.06296	0.02001	7.4001E-01
0.06296	0.07257	0.02001	7.6002E-01
0.07257	0.08980	0.01998	7.8000E-01
0.08980	0.10921	0.02000	8.0000E-01
0.10921	0.12938	0.02000	8.2000E-01
0.12938	0.15041	0.02000	8.4000E-01
0.15041	0.17251	0.02000	8.6000E-01
0.17251	0.19601	0.01999	8.8000E-01
0.19601	0.22144	0.02000	9.0000E-01
0.22144	0.24957	0.02000	9.2000E-01
0.24957	0.28183	0.02000	9.4000E-01
0.28183	0.32126	0.02001	9.6001E-01
0.32126	0.37662	0.01992	9.7993E-01
0.37662	1.46735	0.02007	1.0000E+00